

**The Power Balance of Beams and Plates using the Dynamic
Stiffness Method**

W.S. Park, D.J. Thompson and N.S. Ferguson

ISVR Technical Memorandum 846

October 1999



SCIENTIFIC PUBLICATIONS BY THE ISVR

Technical Reports are published to promote timely dissemination of research results by ISVR personnel. This medium permits more detailed presentation than is usually acceptable for scientific journals. Responsibility for both the content and any opinions expressed rests entirely with the author(s).

Technical Memoranda are produced to enable the early or preliminary release of information by ISVR personnel where such release is deemed to be appropriate. Information contained in these memoranda may be incomplete, or form part of a continuing programme; this should be borne in mind when using or quoting from these documents.

Contract Reports are produced to record the results of scientific work carried out for sponsors, under contract. The ISVR treats these reports as confidential to sponsors and does not make them available for general circulation. Individual sponsors may, however, authorize subsequent release of the material.

COPYRIGHT NOTICE

(c) ISVR University of Southampton All rights reserved.

ISVR authorises you to view and download the Materials at this Web site ("Site") only for your personal, non-commercial use. This authorization is not a transfer of title in the Materials and copies of the Materials and is subject to the following restrictions: 1) you must retain, on all copies of the Materials downloaded, all copyright and other proprietary notices contained in the Materials; 2) you may not modify the Materials in any way or reproduce or publicly display, perform, or distribute or otherwise use them for any public or commercial purpose; and 3) you must not transfer the Materials to any other person unless you give them notice of, and they agree to accept, the obligations arising under these terms and conditions of use. You agree to abide by all additional restrictions displayed on the Site as it may be updated from time to time. This Site, including all Materials, is protected by worldwide copyright laws and treaty provisions. You agree to comply with all copyright laws worldwide in your use of this Site and to prevent any unauthorised copying of the Materials.

UNIVERSITY OF SOUTHAMPTON
INSTITUTE OF SOUND AND VIBRATION RESEARCH
DYNAMICS GROUP

**The Power Balance of Beams and Plates using
the Dynamic Stiffness Method**

by

W.S. Park, D.J. Thompson and N.S. Ferguson

ISVR Technical Memorandum No. 846

October 1999

Authorized for issue by
Dr. M.J. Brennan
Group Chairman

© Institute of Sound & Vibration Research

CONTENTS

SUMMARY	i
1. INTRODUCTION	1
2. SINGLE BEAM INVESTIGATIONS	3
2.1 Equations of motion	3
2.1.1 Flexure	3
2.1.2 Extension	4
2.1.3 Torsion	5
2.2 Dynamic stiffness matrix	6
2.2.1 Flexure	6
2.2.2 Extension	8
2.2.3 Torsion	9
2.2.4 Dynamic stiffness matrix for a beam	9
2.3 Inclusion of damping	10
2.4 Natural frequencies and forced response	11
2.5 Strain energies and power	12
2.5.1 Strain energy for flexure	12
2.5.2 Strain energy for extension	12
2.5.3 Strain energy for torsion	12
2.5.4 Power	13
2.6 Simulations for a single beam	14
2.6.1 Model	15
2.6.2 Natural frequencies	15
2.6.3 Forced response	20
2.6.4 Power balance	20
3. COUPLED BEAM INVESTIGATIONS	24
3.1 Dynamic Stiffness matrix	24
3.2 Simulations for two perpendicular beams	25
3.2.1 Model	25
3.2.2 Natural frequencies	25
3.2.3 Forced response	26
3.2.4 Power balance	26

4. SINGLE PLATE INVESTIGATIONS	33
4.1 Equations of motion	33
4.1.1 Flexure	33
4.1.2 Extension/shear	35
4.2 Dynamic stiffness matrix	37
4.2.1 Flexure	37
4.2.2 Extension/shear	38
4.2.3 Dynamic stiffness matrix for a single plate	40
4.2.4 The removal of the matrix singularity	40
4.3 Concentrated force	41
4.4 Strain energies and power	42
4.4.1 Strain energy for flexure	42
4.4.2 Strain energy for extension	42
4.4.3 Power	43
4.5 Simulations for a single plate	43
4.5.1 Model	43
4.5.2 Natural frequencies	43
4.5.3 Dispersion relationships	45
5. COUPLED PLATE INVESTIGATIONS	47
5.1 Dynamic Stiffness matrix	47
5.2 Simulations for two coplanar plates	48
5.2.1 Model	48
5.2.2 Natural frequencies	48
5.2.3 Forced response	51
5.3 Simulations for two perpendicular plates	55
5.3.1 Model	55
5.3.2 Power balance	55
6. CONCLUSIONS	62
7. REFERENCES	63
 APPENDICES	
A. List of Symbols	65
B. Dynamic Stiffness and Transformation Matrices	67

B.1 Dynamic Stiffness Matrix for a single beam 1	67
B.2 Dynamic Stiffness Matrix for a single beam 2	68
B.3 Dynamic Stiffness Matrix for two perpendicular beams	69
B.4 Transformation Matrix T_b for two perpendicular beams	70
B.5 Dynamic Stiffness Matrix for a coupled plate system	71
B.6 Transformation Matrix T_p for a coupled plate system	72

C. MATLAB Program

C.1 Beam

C.2 Plate

SUMMARY

The power balance between the input power and the dissipated power for beams and plates has been investigated by using the dynamic stiffness method. In this report the dynamic stiffness matrices are provided for the simple structures, i.e. a single beam, a single plate, coupled beams and coupled plates joined at an arbitrary angle. Computer simulations, using MATLAB, have been performed to illustrate the method.

For a given excitation and boundary condition, the natural frequencies, the forced response, the strain energy and the power can be obtained; a numerical integration is required to obtain the strain energy. The dissipated power obtained from the strain energy agrees well with the input power for all the frequency range considered. If the kinetic energy is used to estimate the dissipated power, this is underestimated below resonant peaks and overestimated above these peaks.

The accuracy of the strain energy calculation depends on the step size along the length used in the integration, compared to the smallest wavelength considered. A step size of 20 mm for the beams and 9 mm for the plates has been used, that is about $1/7$ and $1/6$ of the smallest wavelength for the beam and plate, respectively. This gave good agreement within the range of acceptable error. If a concentrated force is applied to the plate structure, the number of Fourier components required for convergence of the solution can be derived from the cut-on frequency of each mode. By including Fourier components above half of the respective cut-on frequency good agreement is found.

1. INTRODUCTION

Engineering structures consisting of beams, plates and shells are used in the design of automotive structures. Recent trends are towards making vehicles more comfortable and also lighter, due to environmental and economic considerations. In the process of minimising the weight of a car, the fuel economy can be improved and the production cost can be reduced. Simultaneously, a good design should produce a quiet and comfortable environment as well as the various performance requirements for the car. Unfortunately, these two objectives, economy and low noise and vibration, are conflicting. Reducing the noise and vibration levels on existing constructions is often very difficult, if not impossible, and will often involve high expenditure and an increase in weight. Therefore during the design process the prediction of the dynamic response of a structure is a necessary consideration so that potential problems, such as excessive vibration levels, resonance problems, failure due to acoustic fatigue and noise problems, can be avoided.

There are a number of methods available for determining the dynamic response of a structure. These range from analytical methods to numerical methods and from the low frequency to the high frequency regions. Three characteristics of the dynamic response that are important for selecting a proper method are (i) whether global modes or localised modes are important, (ii) sensitivity to structural details and (iii) modal overlap. However, each method has its specific advantages, disadvantages and limitations. ESDU [1] provides good guidelines on how to choose an appropriate method for prediction of the dynamic response of a structure subjected to some kind of excitation.

The dynamic stiffness method is a method that can be used to approach the high frequency analysis to which the conventional finite element method cannot be applied. For certain continuous elements it is possible to derive the dynamic properties of a structural component exactly using the dynamic stiffness matrix. The dynamic stiffness matrix is a function of frequency and contains mass information. The equations of motion can be solved to yield the dynamic response of the structure in any selected frequency range. Langley [2-4] developed the free and forced vibrations of a row of rectangular panels, the power flow of beams and frameworks and the vibration analysis of stiffened shell structures. This method can be viewed as

providing an exact solution for the response of an idealised structure, whereas the main restriction for this method is that for plate structures each system must be simply supported on two opposite edges which must be parallel.

This report presents the theory of the dynamic stiffness method for beams and plates, with particular emphasis on the power balance (input power and dissipated power). Computer simulations, using MATLAB, are included to illustrate the method. A list of symbols is given in Appendix A.

2. SINGLE BEAM INVESTIGATIONS

In practice, beams are very simple and useful components of structures. In this study, a beam is considered as an Euler-Bernoulli beam for simplicity. Some assumptions for a uniform beam are:

- The effects of rotary inertia and transverse shear deformation are neglected (valid for slender beams).
- The material of the beam is elastic, homogeneous and isotropic.
- The cross-section of the beam does not vary along its length.
- Forces due to gravity will be neglected.

2.1 Equations of motion

2.1.1 Flexure

For a beam of uniform cross-section, the differential equation governing the flexural vibrations may be written as [5]

$$EI \frac{\partial^4 w}{\partial x^4} + \rho A \frac{\partial^2 w}{\partial t^2} = p(x, t). \quad (2.1)$$

where E is Young's modulus, I is the relevant second moment of area of the cross-section, ρ is the density of the material of the beam, A is its cross-sectional area, w is a vertical displacement and $p(x, t)$ is a force distribution at any section x at time t . For free vibrations, $w(x, t)$ can be written as a harmonic function of time, i.e.

$$w(x, t) = W(x) e^{j\omega t} \quad (2.2)$$

where ω is the circular frequency.

Substituting equation (2.2) into equation (2.1) and letting $p(x, t) = 0$, then

$$\frac{d^4 W}{dx^4} - \frac{\rho A \omega^2}{EI} W = 0. \quad (2.3)$$

The general solution of equation (2.3) can be written as

$$W(x) = B_1 \sin(k_f x) + B_2 \cos(k_f x) + B_3 \sinh(k_f x) + B_4 \cosh(k_f x) \quad (2.4)$$

where k_f is the flexural wavenumber, $k_f = (\rho A \omega^2 / EI)^{1/4}$.

The four constants B_i are determined from the boundary conditions. The standard boundary conditions for a uniform beam are as follows:

- simply supported or pinned, for which the displacement is zero and the bending moment is zero;

$$W = 0 \text{ and } EI(d^2W/dx^2) = 0. \quad (2.5)$$

- fixed or clamped, for which the displacement and slope are zero;

$$W = 0 \text{ and } dW/dx = 0. \quad (2.6)$$

- free, for which the bending moment and shear force are zero;

$$EI(d^2W/dx^2) = 0 \text{ and } EI(d^3W/dx^3) = 0. \quad (2.7)$$

- combinations of these boundary conditions.

For some particular boundary conditions, the natural frequencies and mode shapes for the first few modes have been presented in references [5, 6].

2.1.2 Extension

For extensional vibrations it is assumed that cross-sections, which are initially plane and perpendicular to the axis of the beam, remain plane and perpendicular to that axis and that normal stress in the axial direction is the only component of stress. From the stress-strain relationship and the dynamic equilibrium of an element of the beam, the equation of motion of the extensional free vibrations of beams is given by [5]

$$EA \frac{\partial^2 u}{\partial x^2} - \rho A \frac{\partial^2 u}{\partial t^2} = 0. \quad (2.8)$$

$$\text{i.e.} \quad c_e^2 \frac{\partial^2 u}{\partial x^2} - \frac{\partial^2 u}{\partial t^2} = 0. \quad (2.9)$$

where E is Young's modulus, ρ is the density of the material of the beam, A is its cross-sectional area, u is an extensional displacement and c_e is the velocity of propagation of extensional waves, $c_e = (E/\rho)^{1/2}$.

For free vibrations it is assumed that the extensional displacement is a harmonic function of time, i.e.

$$u(x, t) = U(x)e^{j\omega t}. \quad (2.10)$$

Substituting equation (2.10) into equation (2.9), then

$$c_e^2 \frac{\partial^2 U}{\partial x^2} - \omega^2 U = 0. \quad (2.11)$$

The solution has the form

$$U(x) = B_5 \sin(k_e x) + B_6 \cos(k_e x) \quad (2.12)$$

where k_e is the extensional wavenumber, $k_e = \frac{\omega}{c_e}$. The two constants, B_5 and B_6 , are determined from the boundary conditions and the solutions for some particular boundary conditions have been presented in reference [5].

2.1.3 Torsion

The equation of motion for the torsional vibrations of beams is derived using the same concept as the extensional vibrations. From the torque-twist relationship and the dynamic equilibrium of an element of the beam, the equation of motion of the torsional free vibrations of beams is given by [5]

$$GJ \frac{\partial^2 \theta}{\partial x^2} - \rho J \frac{\partial^2 \theta}{\partial t^2} = 0 \quad (2.13)$$

$$\text{i.e.} \quad c_t^2 \frac{\partial^2 \theta}{\partial x^2} - \frac{\partial^2 \theta}{\partial t^2} = 0 \quad (2.14)$$

where G is the shear modulus, ρ is the density of the material of the beam, J is the polar second moment of area, θ is a torsional displacement and c_t is the velocity of propagation of torsional waves, $c_t = (G/\rho)^{1/2}$. For non-circular cross-sections, a shape factor κ needs to be considered and c_t is redefined as $c_t = (\kappa G/\rho)^{1/2}$.

For free vibrations it is assumed that the torsional displacement is a harmonic function of time,

$$\text{i.e.} \quad \theta(x, t) = \Theta(x) e^{j\omega t}. \quad (2.15)$$

Substituting equation (2.15) into equation (2.14), then

$$c_t^2 \frac{\partial^2 \Theta}{\partial x^2} - \omega^2 \Theta = 0. \quad (2.16)$$

The solution has the form

$$\Theta(x) = B_7 \sin(k_t x) + B_8 \cos(k_t x) \quad (2.17)$$

where k_t is the torsional wavenumber, $k_t = \frac{\omega}{c_t}$. The two constants, B_7 and B_8 , are determined from the boundary conditions.

2.2 Dynamic stiffness matrix

Consider a beam of length l , located between $x = 0$ and $x = l$ (See Figure 2.1).

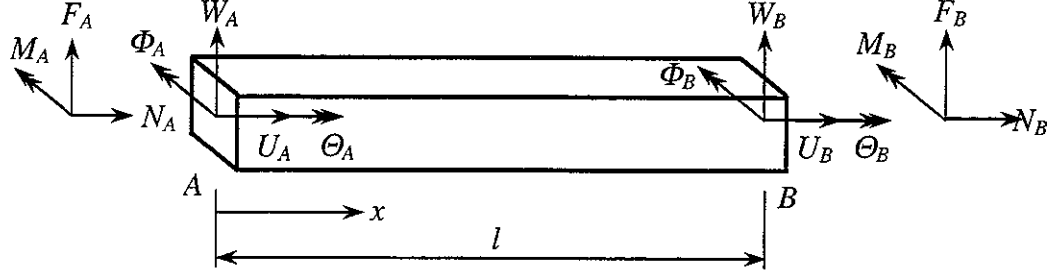


Figure 2.1. Single beam

2.2.1 Flexure

The four constants B_i of equation (2.4) can be determined from the displacements and slopes at each end;

$$\text{at } x = 0; \quad W_A = B_2 + B_4, \quad (2.18)$$

$$\Phi_A = \left(\frac{dW}{dx} \right)_{x=0} = k_f (B_1 + B_3), \quad (2.19)$$

and

$$\text{at } x = l; \quad W_B = B_1 \sin(k_f l) + B_2 \cos(k_f l) + B_3 \sinh(k_f l) + B_4 \cosh(k_f l), \quad (2.20)$$

$$\Phi_B = \left(\frac{dW}{dx} \right)_{x=l} = k_f \{ B_1 \cos(k_f l) - B_2 \sin(k_f l) + B_3 \cosh(k_f l) + B_4 \sinh(k_f l) \}. \quad (2.21)$$

Rearranging equations (2.18), (2.19), (2.20) and (2.21) in matrix form, then the displacement vector for the flexural vibration,

$$\mathbf{u}_f = \mathbf{D}_1 \mathbf{b}_f \quad (2.22)$$

where

$$\mathbf{u}_f^T = [W_A \quad \Phi_A \quad W_B \quad \Phi_B], \quad (2.23)$$

$$\mathbf{b}_f^T = [B_1 \quad B_2 \quad B_3 \quad B_4], \quad (2.24)$$

and

$$\mathbf{D}_1 = \begin{bmatrix} 0 & 1 & 0 & 1 \\ k_f & 0 & k_f & 0 \\ \sin k_f l & \cos k_f l & \sinh k_f l & \cosh k_f l \\ k_f \cos k_f l & -k_f \sin k_f l & k_f \cosh k_f l & k_f \sinh k_f l \end{bmatrix}. \quad (2.25)$$

The shear forces and bending moments at each end are given in terms of displacements by

$$F_A = EI \left(\frac{d^3 W}{dx^3} \right)_{x=0} = EI k_f^3 (-B_1 + B_3) \quad (2.26)$$

$$M_A = -EI \left(\frac{d^2 W}{dx^2} \right)_{x=0} = -EI k_f^2 (-B_2 + B_4) \quad (2.27)$$

$$F_B = -EI \left(\frac{d^3 W}{dx^3} \right)_{x=l} = -EI k_f^3 (-B_1 \cos k_f l + B_2 \sin k_f l + B_3 \cosh k_f l + B_4 \sinh k_f l) \quad (2.28)$$

$$M_B = EI \left(\frac{d^2 W}{dx^2} \right)_{x=l} = EI k_f^2 (-B_1 \sin k_f l - B_2 \cos k_f l + B_3 \sinh k_f l + B_4 \cosh k_f l). \quad (2.29)$$

Equations (2.26), (2.27), (2.28) and (2.29) can be written in matrix form

$$\mathbf{F}_f = \mathbf{D}_2 \mathbf{b}_f \quad (2.30)$$

where the force vector

$$\mathbf{F}_f^T = [F_A \quad M_A \quad F_B \quad M_B] \quad (2.31)$$

and

$$\mathbf{D}_2 = EI k_f^2 \begin{bmatrix} -k_f & 0 & k_f & 0 \\ 0 & 1 & 0 & -1 \\ k_f \cos k_f l & -k_f \sin k_f l & -k_f \cosh k_f l & -k_f \sinh k_f l \\ -\sin k_f l & -\cos k_f l & \sinh k_f l & \cosh k_f l \end{bmatrix}. \quad (2.32)$$

Premultiplying equation (2.22) by \mathbf{D}_1^{-1} gives, $\mathbf{b}_f = \mathbf{D}_1^{-1} \mathbf{u}_f$ and substituting this into equation (2.30),

$$\mathbf{F}_f = \mathbf{D}_2 \mathbf{D}_1^{-1} \mathbf{u}_f = \mathbf{K}_f \mathbf{u}_f \quad (2.33)$$

where \mathbf{K}_f is the dynamic stiffness matrix for the flexural vibrations of a beam,

$$\mathbf{K}_f = \mathbf{D}_2 \mathbf{D}_1^{-1}. \quad (2.34)$$

Note that the beam has two principal axes of flexure. The same equations apply for both directions with different values of I and k_f .

2.2.2 Extension

The two constants B_i of equation (2.12) can be determined from the axial displacements at each end;

$$\text{at } x = 0; \quad U_A = B_6 \quad (2.35)$$

and

$$\text{at } x = l; \quad U_B = B_5 \sin(k_e l) + B_6 \cos(k_e l) \quad (2.36)$$

where k_e is the extensional wavenumber, $k_e = \frac{\omega}{c_e}$.

Rearranging equations (2.35) and (2.36) in matrix form, then the displacement vector for the extensional vibration,

$$\mathbf{u}_e = \mathbf{D}_3 \mathbf{b}_e \quad (2.37)$$

where

$$\mathbf{u}_e^T = [U_A \ U_B], \quad \mathbf{b}_e^T = [B_5 \ B_6] \quad (2.38), (2.39)$$

and

$$\mathbf{D}_3 = \begin{bmatrix} 0 & 1 \\ \sin(k_e l) & \cos(k_e l) \end{bmatrix}. \quad (2.40)$$

From the force-displacement relations at the ends,

$$N_A = -EA \left(\frac{dU}{dx} \right)_{x=0} = -EAB_5 k_e \quad (2.41)$$

and

$$N_B = EA \left(\frac{dU}{dx} \right)_{x=l} = EAk_e \{B_5 \cos(k_e l) - B_6 \sin(k_e l)\}. \quad (2.42)$$

The above equations can be written as

$$\mathbf{F}_e = \mathbf{D}_4 \mathbf{b}_e \quad (2.43)$$

where the applying force vector

$$\mathbf{F}_e^T = [N_A \ N_B] \quad (2.44)$$

and

$$\mathbf{D}_4 = EAk_e \begin{bmatrix} -1 & 0 \\ \cos(k_e l) & -\sin(k_e l) \end{bmatrix}. \quad (2.45)$$

Premultiplying equation (2.37) by \mathbf{D}_3^{-1} gives, $\mathbf{b}_e = \mathbf{D}_3^{-1}\mathbf{u}_e$ and substituting this into equation (2.43),

$$\mathbf{F}_e = \mathbf{D}_4\mathbf{D}_3^{-1}\mathbf{u}_e = \mathbf{K}_e\mathbf{u}_e \quad (2.46)$$

where \mathbf{K}_e is the dynamic stiffness matrix for the extensional vibrations of a beam,

$$\mathbf{K}_e = \mathbf{D}_4\mathbf{D}_3^{-1} = E A k_e \begin{bmatrix} \cot(k_e l) & -\operatorname{cosec}(k_e l) \\ -\operatorname{cosec}(k_e l) & \cot(k_e l) \end{bmatrix}. \quad (2.47)$$

2.2.3 Torsion

The dynamic stiffness matrix for the torsional vibrations may be derived by the same procedure as the extensional vibrations. Applying the boundary conditions at each end,

$$\mathbf{F}_t = \mathbf{K}_t\mathbf{u}_t \quad (2.48)$$

where \mathbf{K}_t is the dynamic stiffness matrix,

$$\mathbf{K}_t = G J k_t \begin{bmatrix} \cot(k_t l) & -\operatorname{cosec}(k_t l) \\ -\operatorname{cosec}(k_t l) & \cot(k_t l) \end{bmatrix} \quad (2.49)$$

and \mathbf{u}_t is the displacement vector for the torsional vibrations of a beam,

$$\mathbf{u}_t^T = [\Theta_A \quad \Theta_B]. \quad (2.50)$$

2.2.4 Dynamic stiffness matrix for a beam

Each end point of a beam has six degrees of freedom, three translational degrees of freedom (u, v, w) and three rotational degrees of freedom (θ, ϕ, ψ) in the Cartesian coordinate system (x, y, z), respectively. The dynamic stiffness matrix for flexure, extension and torsion may be combined in a 12×12 matrix

$$\mathbf{K}_b = \begin{bmatrix} \mathbf{K}_{fz} & 0 & 0 & 0 \\ 0 & \mathbf{K}_{fy} & 0 & 0 \\ 0 & 0 & \mathbf{K}_e & 0 \\ 0 & 0 & 0 & \mathbf{K}_t \end{bmatrix} \quad (2.51)$$

where \mathbf{K}_{fz} and \mathbf{K}_{fy} are the dynamic stiffness matrices for flexure in the vertical and lateral direction, \mathbf{K}_e is the dynamic stiffness matrix for extension and \mathbf{K}_t is the dynamic stiffness matrix for torsion, respectively.

The complete dynamic stiffness matrix for a single beam is presented in Appendix B.1 and B.2. The dynamic stiffness matrix \mathbf{K}_b can be reduced by applying the boundary conditions at the end points, $x = 0$ and $x = l$.

The wavespeed and wavenumber for flexural, extensional and torsional wave are summarised in Table 2.1.

Table 2.1 The wavespeed and wavenumber for flexural, extensional and torsional wave of a beam.

	Flexural wave	Extensional wave	Torsional wave
Wavespeed	$c_f = (EI/\rho A)^{1/4} \omega^{1/2}$	$c_e = (E/\rho)^{1/2}$	$c_t = (G/\rho)^{1/2}$
Wavenumber	$k_f = (\rho A \omega^2 / EI)^{1/4}$	$k_e = \frac{\omega}{c_e} = \omega (\rho / E)^{1/2}$	$k_t = \frac{\omega}{c_t} = \omega (\rho / G)^{1/2}$

2.3 Inclusion of damping

For an elastic beam the stress σ_x and the strain ε_x in the longitudinal direction are related by Hooke's law, i.e.

$$\sigma_x = E \varepsilon_x. \quad (2.52)$$

For hysteretic damping, the stress-strain relationship of a viscoelastic material excited harmonically is given by [5]

$$\sigma_x = E \left(\varepsilon_x + \frac{\eta}{\omega} \frac{\partial \varepsilon_x}{\partial t} \right) \quad (2.53)$$

in which η is the hysteretic damping constant or the loss factor and ω is the excitation frequency. With the steady-state response to harmonic excitation, all physical quantities can be represented in complex notation with a time dependence $\exp(j\omega t)$. Thus

$$\partial \varepsilon_x / \partial t = j\omega \varepsilon_x \text{ and } \sigma_x = E (1 + j\eta) \varepsilon_x. \quad (2.54), (2.55)$$

Similar expressions can be used for other types of motion. In Table 2.1 the material properties and wave to be replaced for the damped system are given.

Table 2.2. The properties related to the hysteretic damping.

Property	Undamped	Damped	Small Damping
Young's modulus	E	$E(1+j\eta)$	$E(1+j\eta)$
Shear modulus	G	$G(1+j\eta)$	$G(1+j\eta)$
The flexural wavenumber	k_f	$k_f(1+j\eta)^{-1/4}$	$k_f(1-j\eta/4)$
The extensional wavenumber	k_e	$k_e(1+j\eta)^{-1/2}$	$k_e(1-j\eta/2)$
The torsional wavenumber	k_t	$k_t(1+j\eta)^{-1/2}$	$k_t(1-j\eta/2)$

2.4 Natural frequencies and forced response

In general, the equation of motion for a beam system can be given as

$$\mathbf{F} = \mathbf{K}\mathbf{u} \quad (2.56)$$

where \mathbf{F} is a force vector containing forces and moments acting at the ends of the beam, \mathbf{K} is the dynamic stiffness matrix considered the hysteretic damping and \mathbf{u} is the displacement vector of the beam system containing displacements and rotations at the ends of the beam. In dynamics problems, the dynamic stiffness matrix depends upon frequency and the stiffness and mass of the system.

For free vibration the external excitation force is zero and the natural frequencies are determined from

$$\det(\mathbf{K}) = 0 \quad (2.57)$$

where \mathbf{K} is the dynamic stiffness matrix for the beam reduced as appropriate according to the boundary conditions at the end points, $x = 0$ and $x = l$.

The response to known harmonic excitation \mathbf{F} can also be evaluated in closed form using the inverse of the dynamic stiffness matrix or receptance matrix \mathbf{K}^{-1} :

$$\mathbf{u} = \mathbf{K}^{-1}\mathbf{F}. \quad (2.58)$$

Having determined the responses \mathbf{u} at the end points of the beam at each frequency, the responses along the beam axis can be determined. These depend upon the types of vibration.

- Flexure;

$$W(x) = B_1 \sin(k'_f x) + B_2 \cos(k'_f x) + B_3 \sinh(k'_f x) + B_4 \cosh(k'_f x) \quad (2.59)$$

where $k'_f = \{\rho A \omega^2 / EI(1 + j\eta)\}^{1/4}$, η is the hysteretic damping constant and $B_1 -$

B_4 are given by equation (2.22).

- Extension;

$$U(x) = B_5 \sin(k'_e x) + B_6 \cos(k'_e x) \quad (2.60)$$

where $k'_e = \omega \{E(1 + j\eta)/\rho\}^{-1/2}$ and $B_5 - B_6$ are given by equation (2.37).

- Torsion;

$$\theta(x) = B_7 \sin(k'_t x) + B_8 \cos(k'_t x) \quad (2.61)$$

where $k'_t = \omega \{G(1 + j\eta)/\rho\}^{-1/2}$.

As the dynamic stiffness matrix of a single beam or a coupled beam system is a set of complicated functions of frequency, the dynamic response may be obtained for an arbitrary frequency range by a separate calculation for each frequency.

2.5 Strain energies and power

2.5.1 Strain energy for flexure

The total strain energy of a beam in flexure is given by [7]

$$U_f = \int_0^l \frac{M^2}{2EI} dx = \frac{1}{2} EI \int_0^l \left(\frac{d^2 w}{dx^2} \right)^2 dx \approx \frac{EI}{2n} \sum_{i=1}^n \left(\frac{d^2 w_i}{dx^2} \right)^2 \quad (2.62)$$

where M is the bending moment, E is the Young's modulus, I is the second moment of area of the cross-section, w is a vertical displacement and n is the total number of integration points from $\frac{\Delta x}{2}$ to $(l - \frac{\Delta x}{2})$.

2.5.2 Strain energy for extension

The total strain energy of a beam in extension is given by [7]

$$U_e = \frac{1}{2} EA \int_0^l \left(\frac{du}{dx} \right)^2 dx \approx \frac{EAl}{2n} \sum_{i=1}^n \left(\frac{du_i}{dx} \right)^2 \quad (2.63)$$

where A is the cross-sectional area and u is an extensional displacement.

2.5.3 Strain energy for torsion

The total strain energy of a beam in torsion is given by [7]

$$U_t = \frac{1}{2} GJ \int_0^l \left(\frac{d\theta}{dx} \right)^2 dx \approx \frac{GJl}{2n} \sum_{i=1}^n \left(\frac{d\theta_i}{dx} \right)^2 \quad (2.64)$$

where G is the shear modulus, J is the polar second moment of area and θ is a torsional displacement.

In practice, the integration of equations (2.62), (2.63) and (2.64) may be performed numerically by summing over the step length Δx along the length of the beam as indicated. The discrete summation is an approximation to the continuous integral.

2.5.4 Power

The time averaged power input P_{in} produced by a harmonic force \mathbf{F} is given by

$$P_{in} = \text{Re}\{Y\} \tilde{F}^2 = \text{Re}\{Z\} \tilde{v}^2 = \frac{1}{2} \text{Re}(\mathbf{F}^* \mathbf{v}) \quad [\text{Watt (W) or Nm/sec}] \quad (2.65)$$

where Y is input mobility, Z is input impedance, \tilde{F} is r.m.s. force amplitude, \tilde{v} is r.m.s. velocity amplitude at the excitation point and \mathbf{F}^* is the complex conjugate of the applied force amplitude \mathbf{F} .

The Statistical Energy Analysis (S.E.A.) power balance equation for an isolated subsystem is given by [8],

$$P_{in} = P_{diss} = 2\pi f \eta E_{strain} \quad (2.66)$$

where, P_{in} is the input power, P_{diss} is the dissipated power, η is the loss factor and E_{strain} is the strain energy amplitude of the dynamic response in the subsystem at frequency f (Hz). If the kinetic energy is used in this calculation, the “dissipated power” does not agree well with the input power. This point will be discussed further in the simulation results section. Thus the dissipated power P_{diss} can be calculated by using the total strain energy of the system obtained from equations (2.62), (2.63) and (2.64).

2.6 Simulations for a single beam

In this study MATLAB [9, 10], which is very powerful tool for matrix manipulation, has been used to perform computer simulations for simple structures. Figure 2.2 presents the flow chart for the dynamic analysis of structures using the Dynamic Stiffness Method. In this section the simulation results for a single beam system are presented.

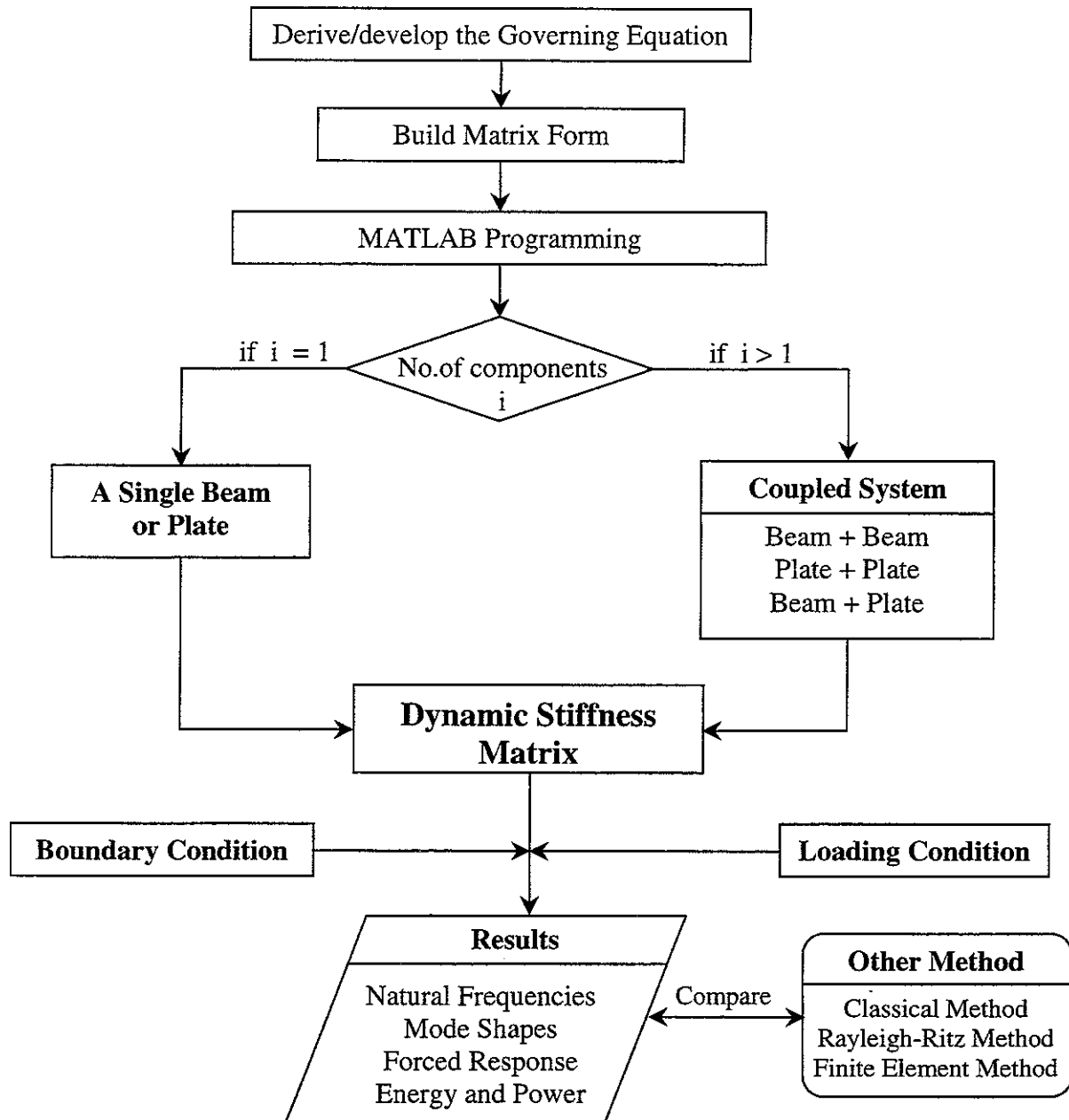


Figure 2.2. The Flow Chart for the Dynamic Analysis of Structures using the Dynamic Stiffness Matrix Method.

2.6.1 Model

Figure 2.3 presents the simulation model for a single beam system that has been studied. Boundary conditions considered are clamped-free (shown) and simply supported at both ends.

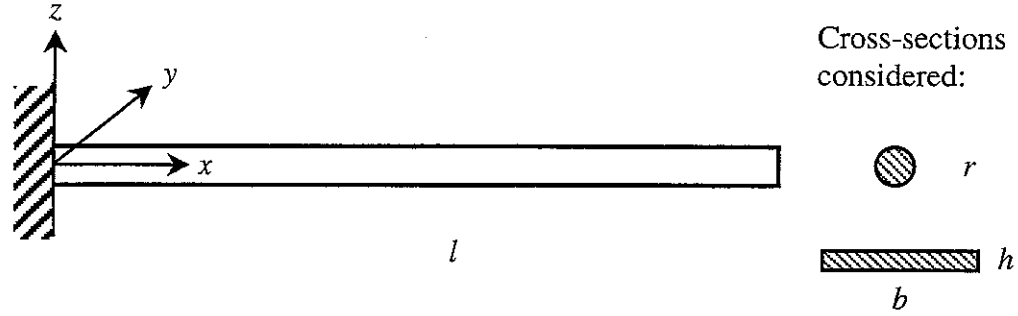


Figure 2.3. Uniform Cantilever beam: Length $l = 500$ mm, Radius $r = 5.0$ mm, Width $b = 12$ mm, Height $h = 2$ mm, Loss factor $\eta = 0.01$, Material: Steel (Young's modulus $E = 2.1 \times 10^{11}$ N/m², Poisson's ratio $\nu = 0.29$, Material density $\rho = 7.86 \times 10^3$ kg/m³).

2.6.2 Natural frequencies

The damped natural frequencies for flexural vibration are determined from the dynamic stiffness matrix considered the hysteretic damping which was defined in equation (2.34). The natural frequencies occur when the constrained dynamic stiffness matrix is singular, i.e. has zero determinant. In Figures 2.4-2.7, the flexural "frequency functions" (that is $\det(\mathbf{K}_f^{-1})$) for the cantilever beam and the simply supported beam, which has two different cross-sections, i.e. circular and rectangular cross-section, are shown.

The undamped natural frequencies may also be determined from the characteristic equation [5] and compared the damped natural frequencies obtained from the dynamic stiffness method.

For a cantilever beam, the characteristic equation is

$$\cos(k_f l) \cosh(k_f l) + 1 = 0 \quad (2.67)$$

where $k_f = (\rho A \omega^2 / EI)^{1/4}$ and l is the length of the beam. The roots of the equation can be solved by analytical or graphical methods.

For a simply supported beam, the characteristic equation is

$$\sin(k_f l) = 0 \quad (2.68)$$

and hence

$$k_f l = n\pi, \quad n=1, 2, 3, \dots \quad (2.69)$$

Therefore

$$f = \frac{\pi}{2} \left(\frac{n}{l} \right)^2 \left(\frac{EI}{\rho A} \right)^{1/2}, \quad n=1, 2, 3, \dots \quad (2.70)$$

The frequency functions which are given by equations (2.67) and (2.68) for a cantilever beam are plotted in Figure 2.8 and for a simply supported beam in Figure 2.9. The minima of these functions correspond to the undamped natural frequencies.

Table 2.3 and Table 2.4 compare the natural frequencies obtained with the dynamic stiffness method and with the analytical method. The results show good agreement between the two methods. In case of the cantilever beam, however, it was very difficult for the frequencies above the third mode to be compared because only two or three peaks are clearly identifiable in Figure 2.4 and 2.5.

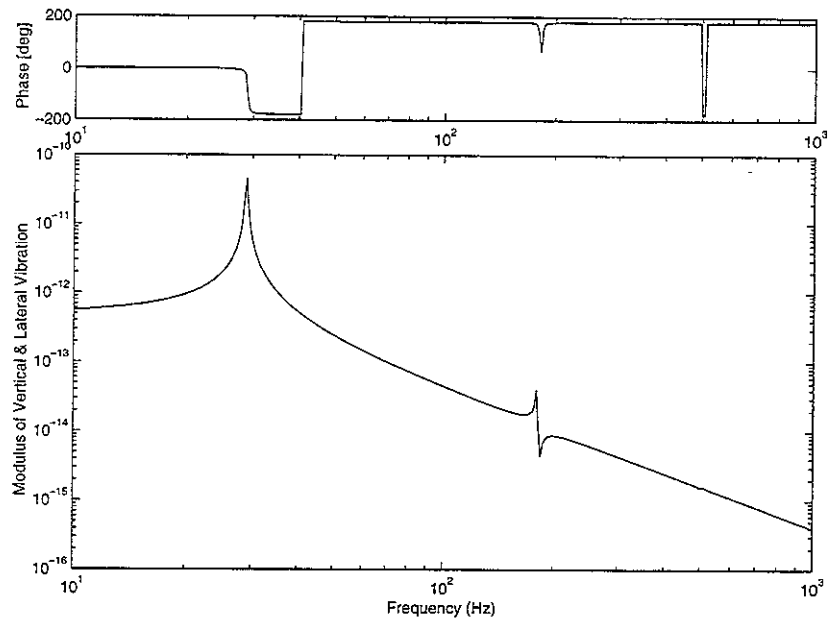


Figure 2.4. The flexural “frequency function” (*i.e.* $\det(\mathbf{K}_f^{-1})$) for the cantilever beam with circular section by the dynamic stiffness method.

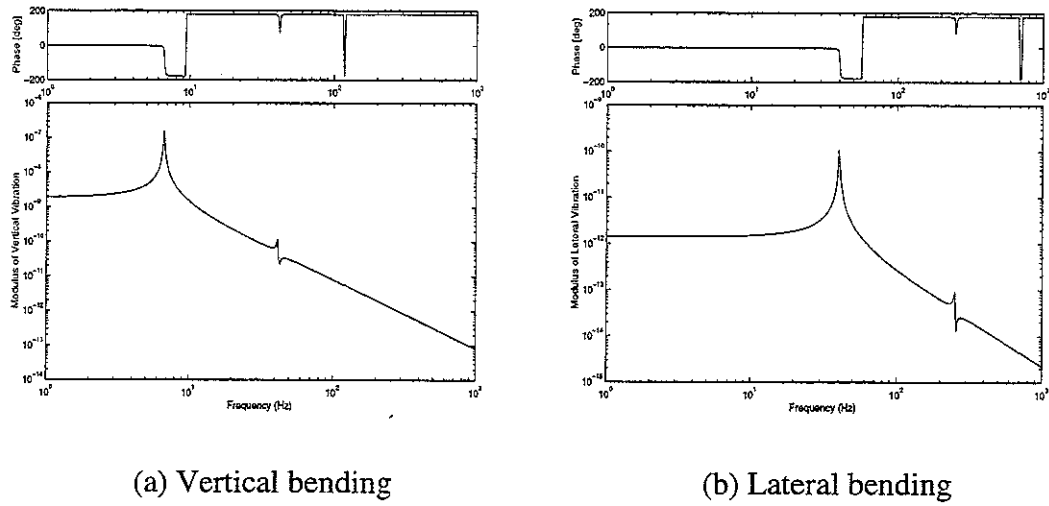


Figure 2.5. The flexural “frequency functions” (*i.e.* $\det(\mathbf{K}_f^{-1})$) for the cantilever beam with rectangular cross-section by the dynamic stiffness method.

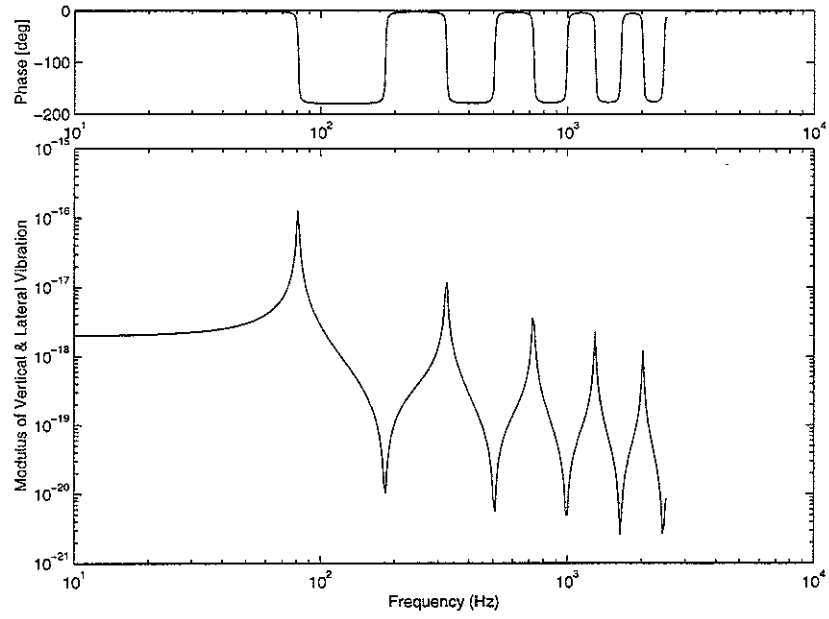


Figure 2.6. The flexural “frequency function” (*i.e.* $\det(\mathbf{K}_f^{-1})$) for the simply supported beam with circular cross-section by the dynamic stiffness method.

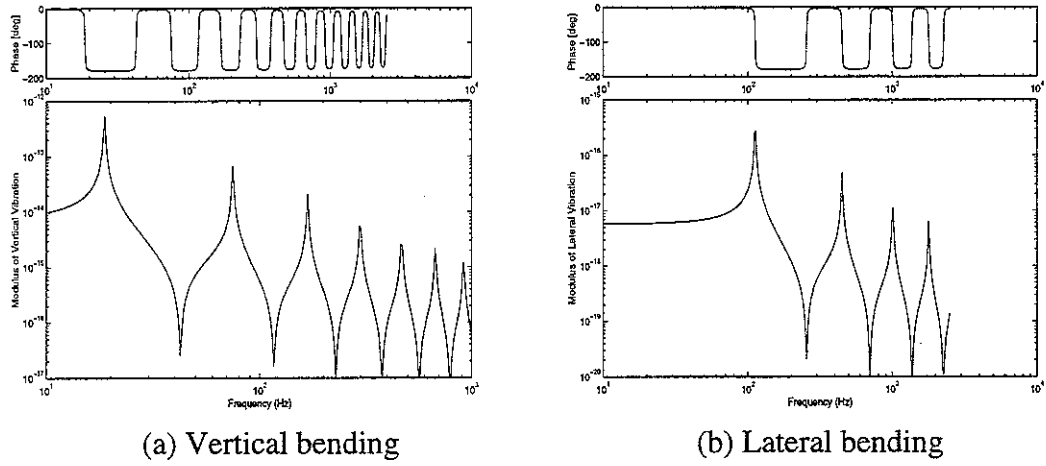
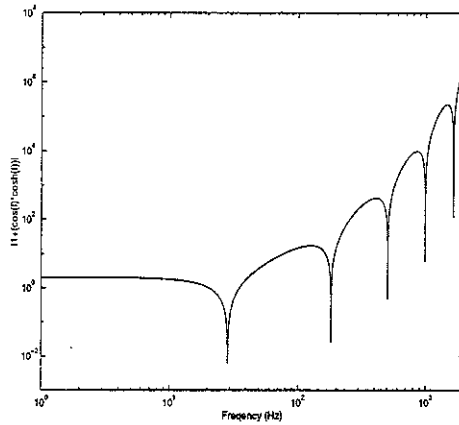


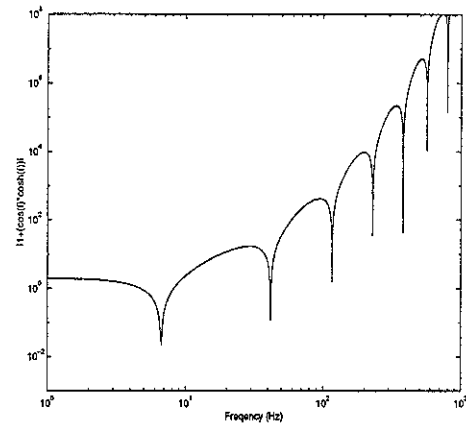
Figure 2.7. The flexural “frequency functions” (*i.e.* $\det(\mathbf{K}_f^{-1})$) for the simply supported beam with rectangular cross-section by the dynamic stiffness method.

Table 2.3. The vertical bending frequencies for the cantilever beam.

Mode	Circular cross-section ($r=5\text{mm}$)		Rectangular cross-section ($12\times 2\text{mm}$)	
	Analytical Method	Dynamic Stiffness Method	Analytical Method	Dynamic Stiffness Method
1	28.9	28.9	6.66	6.67
2	181	181	41.8	41.2
3	506	505	117	117
4	992	-	229	-
5	1640	-	379	-



(a) Circular section



(b) Rectangular section

Figure 2.8. The flexural frequency function of the vertical direction for the cantilever beam by the analytical method.

Table 2.4. The vertical bending frequencies for the simply supported beam.

Mode	Circular cross-section ($r=5\text{mm}$)		Rectangular cross-section ($12\times 2\text{mm}$)	
	Analytical Method	Dynamic Stiffness Method	Analytical Method	Dynamic Stiffness Method
1	81.0	80.9	18.7	18.7
2	324	324	74.8	74.5
3	729	729	168	168
4	1300	1300	299	299
5	2020	2020	468	467

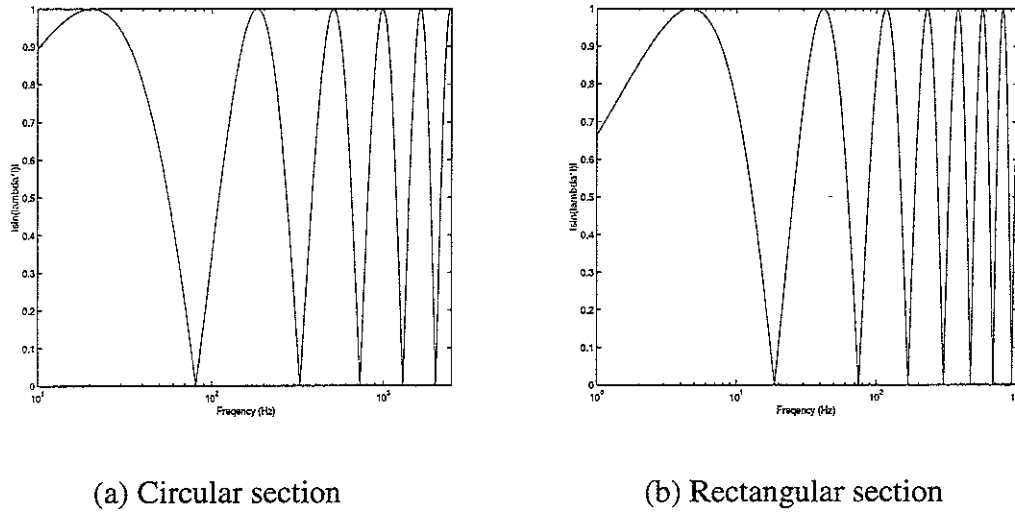


Figure 2.9. The flexural frequency function of the vertical direction for the simply supported beam by the analytical method.

2.6.3 Forced response

If a harmonic force is defined and applied at the free end of the cantilever beam, the forced response for the single beam system can be obtained from equation (2.58). Figure 2.10 shows the forced response for the cantilever beam. Having obtained the forced response at the end point, the displaced shapes can also be determined by using equations (2.59)-(2.61). If the excitation is applied at a natural frequency the mode shapes are obtained. As an example, the displaced shapes for a coupled beam system at some frequency points will be shown in the section 3.2.3.

2.6.4 Power balance

The input power at each frequency can be obtained from equation (2.65). Obtaining the strain energy from equations (2.62)-(2.64), the dissipated power can be calculated by equation (2.66). It should be the same as the input power according to the power balance concept.

The dissipated power obtained from the strain energy agrees well with the input power for all the frequency range considered, as shown in Figure 2.11, whereas the one from the kinetic energy does not, as shown in Figure 2.12. The

error for the former is much smaller than that for the latter. Figure 2.12 shows that the dissipated power is underestimated below resonant peaks and overestimated above these peaks if based on the kinetic energy, although the error becomes smaller as frequency increases.

According to the case study to get good agreement, the accuracy of the results depends on the loss factor and the step size along the length of the beam. The use of a smaller step size produces a more accurate result, but it needs more computing time. In this study the step size of 20mm shows good agreement within the range of acceptable error. It is about 1/7 of the bending wavelength (137mm) at the maximum analysis frequency of 1000 Hz. The bending wavelength λ_{beam} for a beam is obtained from

$$\lambda_{\text{beam}} = 2\pi I(\rho A \omega^2 / EI)^{1/4} \quad (2.71)$$

where ρ is the material density, A is the cross-sectional area, E is Young's modulus and I is the second moment of area of the cross-section. The result of the case study is summarised in Table 2.5 and the error plot is shown in Figure 2.13. The error decreases as the step size and the loss factor decrease.

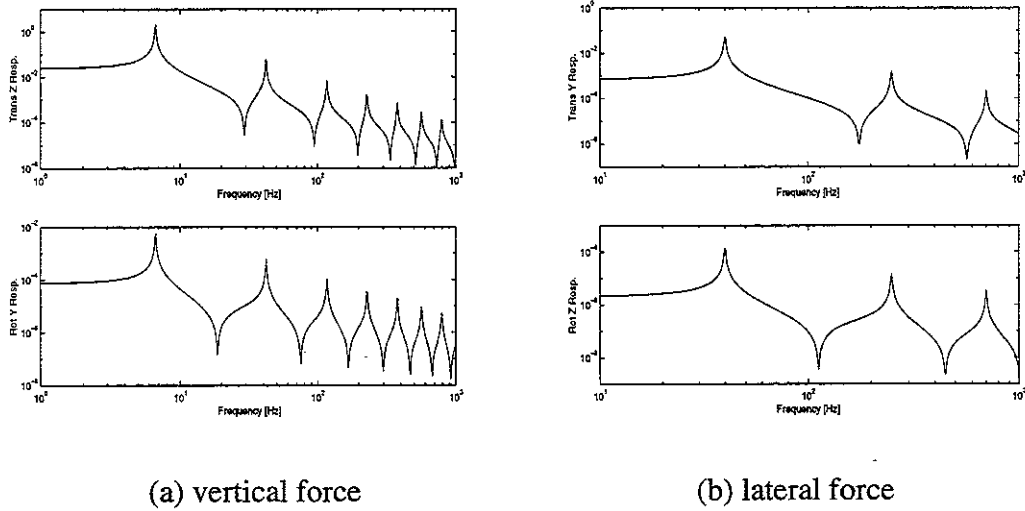
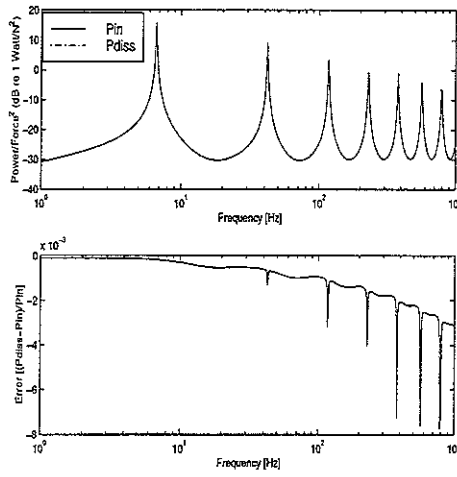
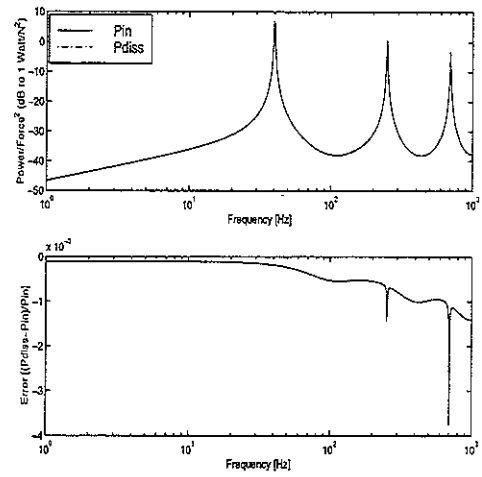


Figure 2.10. The forced response for the rectangular cantilever beam due to separate forces in the (a) vertical and (b) lateral direction applied at the free end. Upper: translational response, lower: rotational response, at the free end.

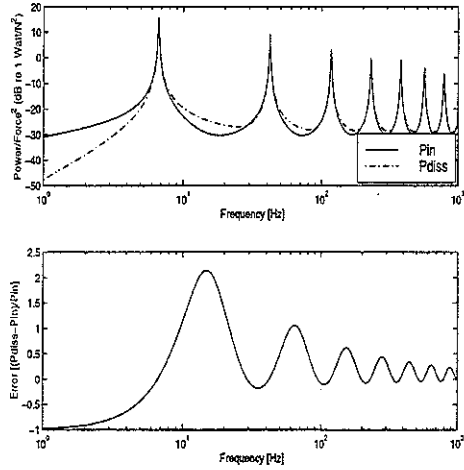


(a) vertical force

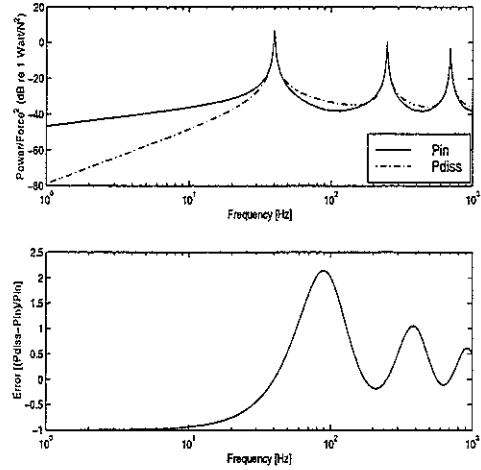


(b) lateral force

Figure 2.11. The input power and dissipated power for the rectangular cantilever beam due to separate forces in the (a) vertical and (b) lateral direction applied at the free end: —, the input power due to the applying force (P_{in}); ---, the dissipated power obtained from strain energy (P_{diss}).



(a) vertical force



(b) lateral force

Figure 2.12. The input power and dissipated power for the rectangular cantilever beam due to separate forces in the (a) vertical and (b) lateral direction applied at the free end: —, the input power due to the applying force (P_{in}); ---, the dissipated power obtained from kinetic energy (P_{diss}).

Table 2.5 Results of the case study for the accuracy of the power calculation

Loss factor	Step size [mm]	Error (%) $[(P_{diss}-P_{in})/P_{in}]\times 100$	
		Vertical force	At the maximum frequency
0.2	40 ($\lambda/3.4$)	-21.34	-29.74
	30 ($\lambda/4.6$)	-19.95	-28.54
	20 ($\lambda/6.9$)	-2.18	-5.58
	10 ($\lambda/13.7$)	-0.56	-1.45
	5 ($\lambda/27.4$)	-0.14	-0.37
	2 ($\lambda/68.5$)	-0.02	-0.06
0.1	40	-15.73	-16.13
	30	-14.29	-14.68
	20	-1.67	-3.48
	10	-0.43	-0.89
	5	-0.11	-0.23
	2	-0.02	-0.04
0.01	40	-9.31	-1.12
	30	-7.99	0.28
	20	-1.14	-1.28
	10	-0.29	-0.32
	5	-0.07	-0.08
	2	-0.01	-0.01
0.001	40	1.70	-0.83
	30	2.57	0.57
	20	-0.50	-1.24
	10	-0.12	-0.31
	5	-0.03	-0.08
	2	0.00	-0.01

Note. P_{diss} = the dissipated power for the beam

P_{in} = the input power for the beam

λ = the bending wavelength for the beam

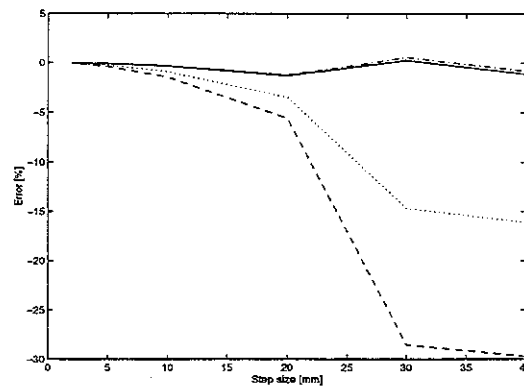


Figure 2.13. The error plot for the beam at the maximum frequency. ---, $\eta = 0.2$; ..., $\eta = 0.1$; —, $\eta = 0.01$; - · -, $\eta = 0.001$.

3. COUPLED BEAM INVESTIGATIONS

3.1 Dynamic Stiffness matrix

In general, a coupled beam system may be analysed by the continuity conditions and the equilibrium equations at the joints. The dynamic stiffness matrix of a coupled beam system is derived by assembling the dynamic stiffness matrices of each beam. As a finite beam has two end points, the dynamic stiffness matrix constitutes a 12×12 matrix, comprising 4 flexural degrees of freedom in each direction, 2 extensional and 2 torsional degrees of freedom. There are defined in a local coordinate system. Although each beam has 12 coupling degrees of freedom, the overall dynamic stiffness matrix can be reduced by applying the continuity conditions and the equilibrium equations at the joints. If a system has n independent degrees of freedom, the overall dynamic stiffness matrix is given by an $n \times n$ matrix. The dynamic stiffness matrix for two perpendicular beams can be defined using the local coordinate system for each beam. It is presented in Appendix B.3.

Although it may be derived by the continuity conditions and the equilibrium equations at the joints, one must be careful and the process is considerably tedious and cannot be automated in this way. Alternatively applying the transformation matrix \mathbf{T}_b that is defined in Appendix B.4, the dynamic stiffness matrix for a coupled beam system joined at an arbitrary angle can be determined in the global coordinate system.

3.2 Simulations for two perpendicular beams

3.2.1 Model

The system studied consists of two beams joined at 90° as shown in Figure 3.1. The dimensions of the beams are given in Table 3.1.

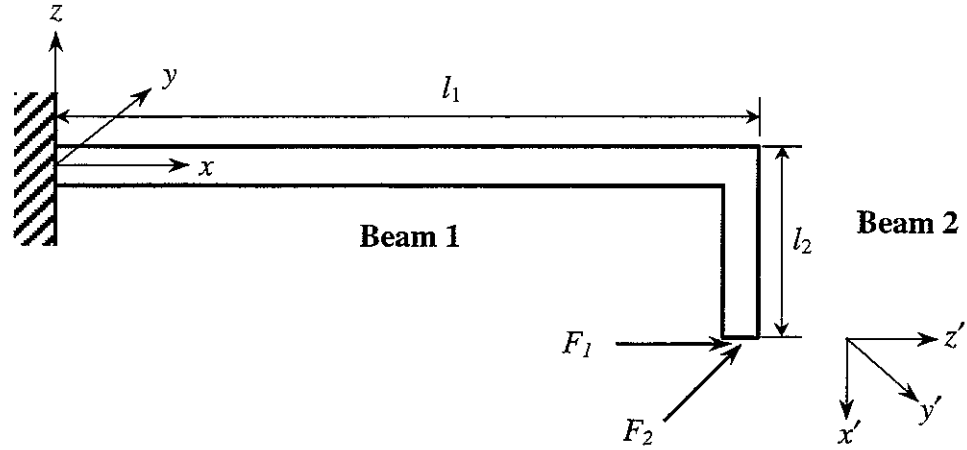


Figure 3.1. Two perpendicular beams.

Table 3.1 The dimensions of the beams

	Beam 1	Beam 2
Cross-section	Rectangular	Rectangular
Length l [mm]	500	200
Width b [mm]	12	3
Height h [mm]	2	6
Material	Steel	Steel
Loss factor η	0.01	0.01

3.2.2 Natural frequencies

The damped natural frequencies for flexural vibration of the coupled beam system, for which the left-hand end is clamped and the other end is free, are obtained from the maxima in the “frequency functions” (that is $\det(\mathbf{K}_f^{-1})$) for the vertical and lateral direction as shown in Figure 3.2.

3.2.3 Forced response

Figure 3.3 presents the forced response at the interface between the two beams when the separate forces (F_1 and F_2) are applied at the free end of Beam 2 in the z' (that is called vertical) and y' (that is called lateral) direction. In the case of the vertical response, the translational z displacement, the rotational y displacement and the translational x displacement are dominant. In the case of the lateral response, the translational y displacement, the rotational z displacement and the rotational x displacement are dominant. Since the other responses are negligible, those responses were excluded from the calculation.

The flexural bending deflection at some frequency points, located near the 2nd, 4th and 6th peaks (22.53, 125.89 and 530.88 Hz) in Figure 3.2(a), is obtained from equation (2.59) and is shown in Figure 3.4. It shows the vertical response of Beam 1 and Beam 2 along the longitudinal direction. In the response zero displacement represents the nodal point at that frequency.

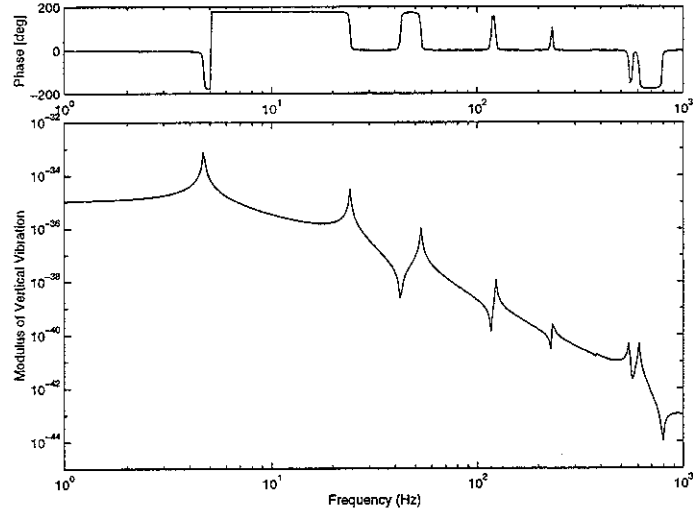
3.2.4 Power balance

If a unit harmonic force is applied at a point, the input power can be determined from equation (2.65). The system divides the total vibrational energy in the form of kinetic energy and strain energy. The dissipated power for the system may be obtained from equation (2.66) and it must be the same as the input power if the system is in steady state. In this calculation, firstly the strain energy for each beam was calculated at the points on the beam axis. The power calculations were performed at each frequency. It is assumed that both beams have the same loss factor of 0.2.

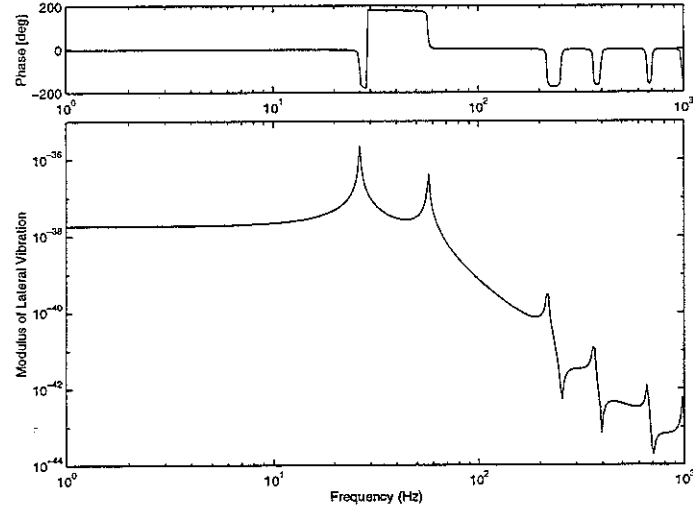
The result for the power calculation for four cases, which are described below the table, is summarised in Table 3.2 and presented in Figures 3.5-3.8. The values in the table are simply the area under the curves which is given for the purpose of comparison without any physical meaning. For all cases for the vertical and the lateral force, the input power shows good agreement with the dissipated power to within calculation limits. The dimension of Case 2, which is a single beam system, is the same as that of Case 1. The cross-section of the beam was considered as

square so that the power calculation for the two different forces would coincide. These show that the program for a coupled beam system is working very well.

The input power P_{in} produced by the applied force divides into the dissipated power P_{diss2} in the driven beam (Beam 2) and the power P_{tr2-1} transmitted to the receiver beam (Beam 1). The transmitted power is dissipated in the receiver beam.

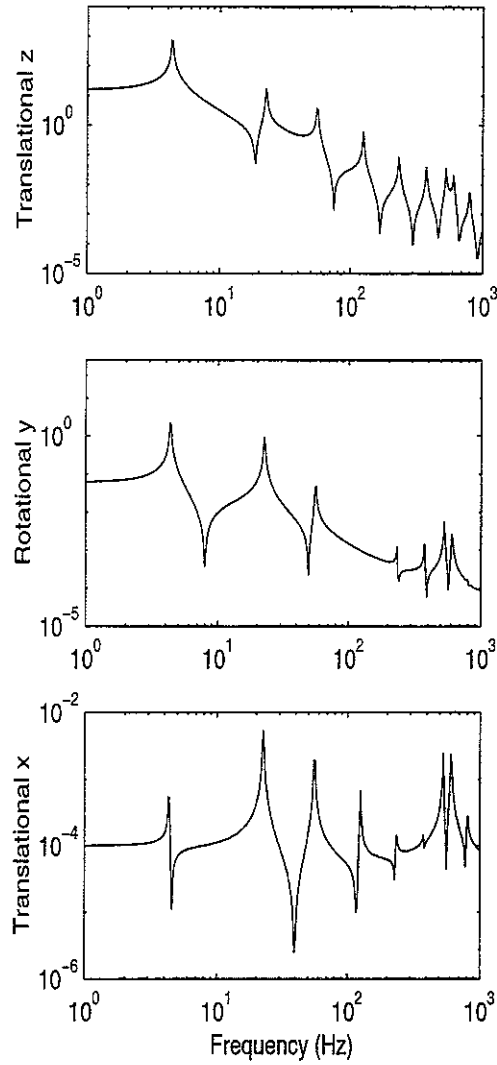


(a) Vertical vibration

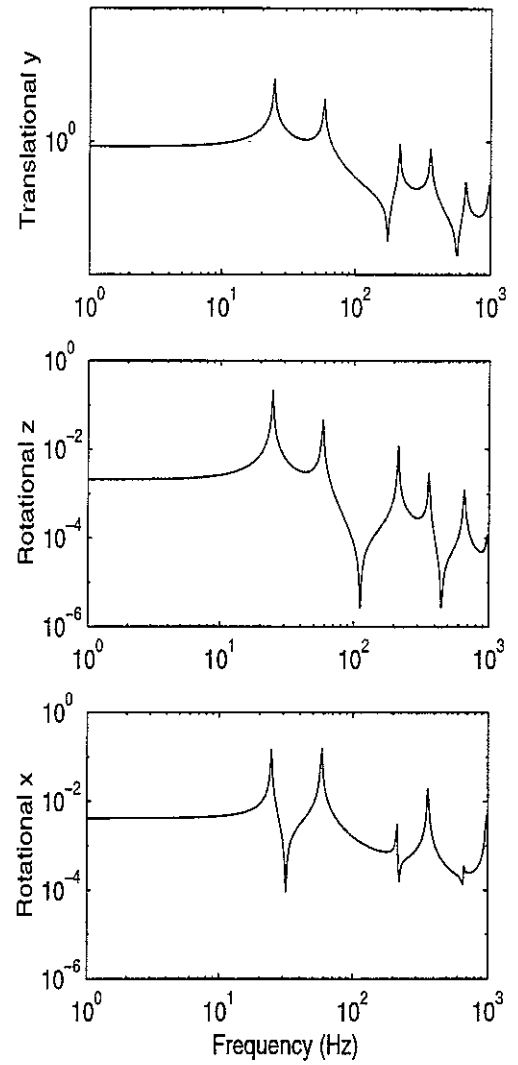


(b) Lateral vibration

Figure 3.2. The flexural “frequency functions” (*i.e.* $\det(\mathbf{K}_f^{-1})$) of a coupled beam system obtained using the dynamic stiffness method.



(a) Vertical force



(b) Lateral force

Figure 3.3. The forced response at the interface between two beams due to separate forces in the vertical (a) and lateral (b) direction applied at the free end.

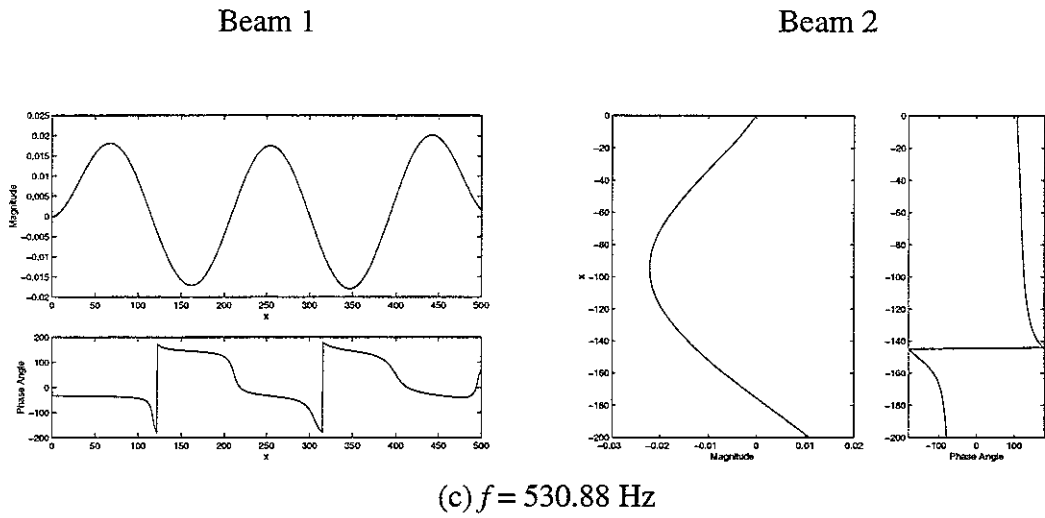
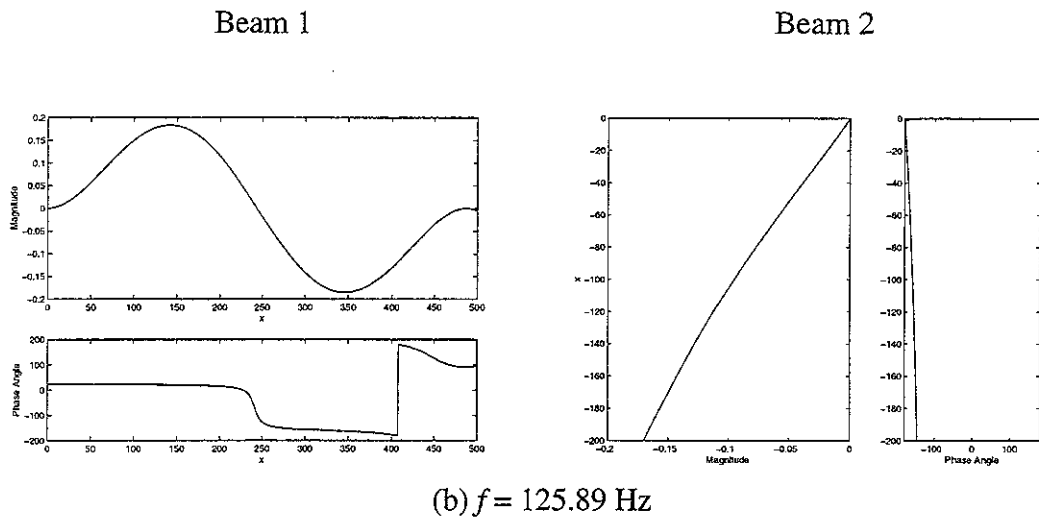
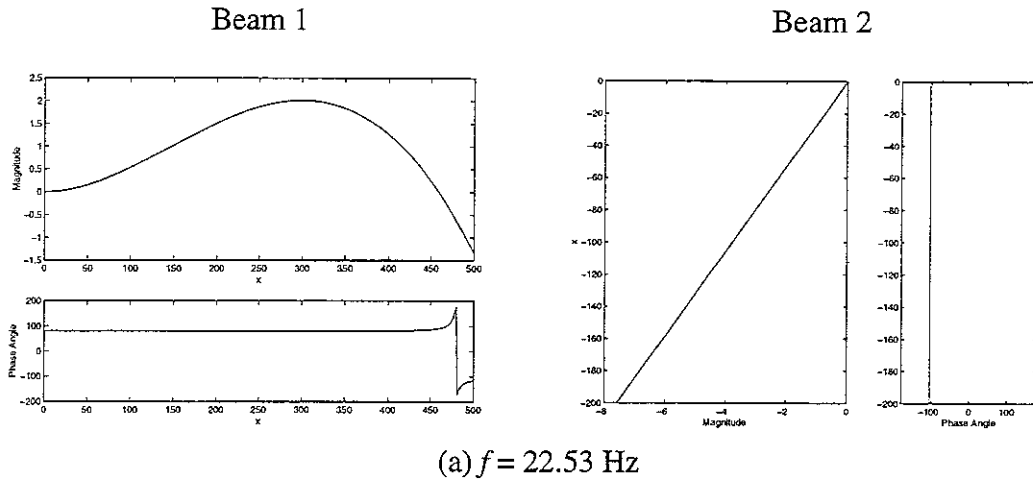


Figure 3.4. The forced response for flexural vibration along the longitudinal axis of both beams at some frequency points due to a unit force in the local z' direction at the free end of Beam 2.

Table 3.2. The input power and the dissipated power for a coupled beam system and a single beam system.

(a) unit vertical force at the free end

	P_{diss1}	P_{tr2-1}	P_{diss2}	$P_{diss1+2}$	P_{in}
Case 1	3.18	3.18	0.78	3.96	3.96
Case 2	-	-	-	3.96	3.96
Case 3	2.71	2.71	1.06	3.78	3.78
Case 4	3.00	3.00	0.85	3.85	3.85

(b) unit lateral force at the free end

	P_{diss1}	P_{tr2-1}	P_{diss2}	$P_{diss1+2}$	P_{in}
Case 1	3.18	3.18	0.78	3.96	3.96
Case 2	-	-	-	3.96	3.96
Case 3	2.96	2.96	0.65	3.61	3.61
Case 4	3.05	3.05	0.63	3.68	3.68

(Unit: Watt/N²)

Note. P_{diss1} = The dissipated power for beam 1
 P_{tr2-1} = The transmitted power from beam 2 to beam 1
 P_{diss2} = The dissipated power for beam 2
 $P_{diss1+2}$ = The total dissipated power
 P_{in} = The input power for the system due to the applied force

The parameter values used in the case studies are as below.

Case 1: Two coplanar beams ($l_1 = 500$ mm, $l_2 = 200$ mm, $\delta = 0^\circ$)

Case 2: A single beam ($l = 700$ mm)

Case 3: Two perpendicular beams ($l_1 = 500$ mm, $l_2 = 200$ mm, $\delta = 90^\circ$)

Case 4: Two angled beams ($l_1 = 500$ mm, $l_2 = 200$ mm, $\delta = 45^\circ$)

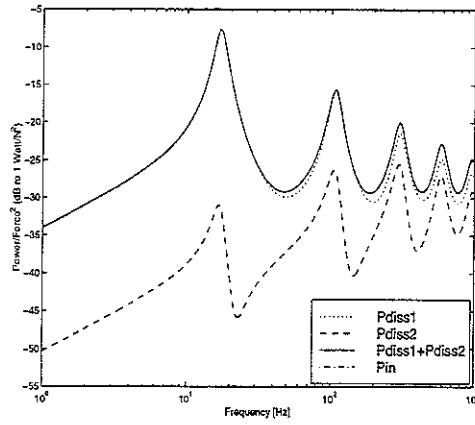
width = 10 mm, height = 10 mm

loss factor = 0.2,

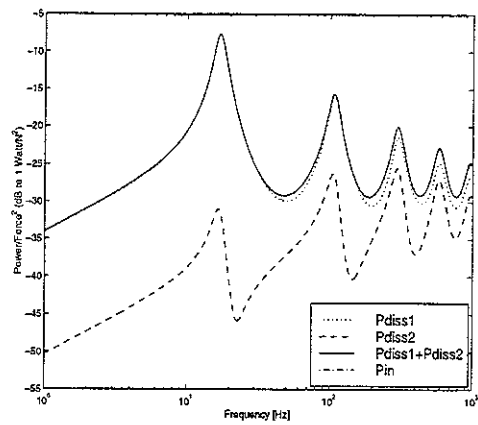
xstep = 5.0 mm,

frequency range = 1 ~ 1000 Hz,

the number of frequency points = 361

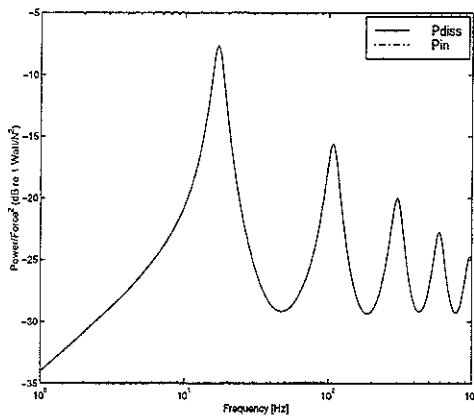


(a) vertical force

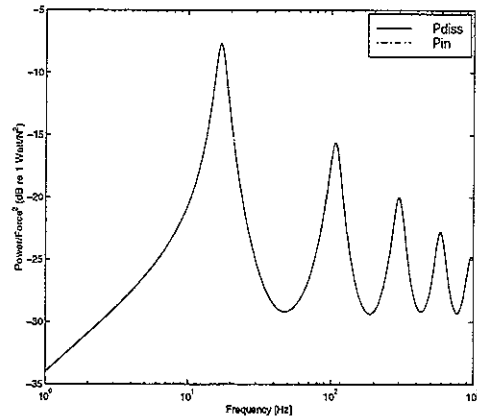


(b) lateral force

Figure 3.5. Power for two coplanar beams [Case 1: $l_1 = 500$ mm, $l_2 = 200$ mm]: ..., the dissipated power for beam 1 (P_{diss1}); ---, the dissipated power for beam 2 (P_{diss2}); —, the total dissipated power ($P_{\text{diss1+2}}$); - · -, the input power due to the applying force (P_{in}).

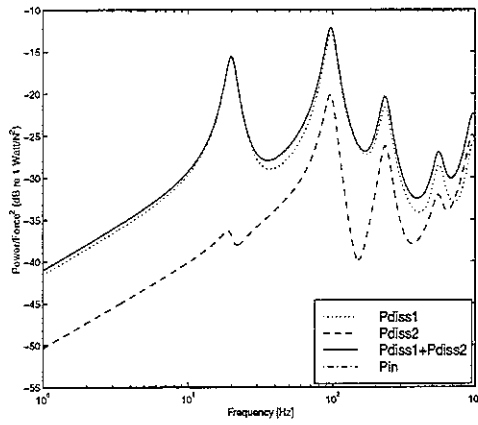


(a) vertical force

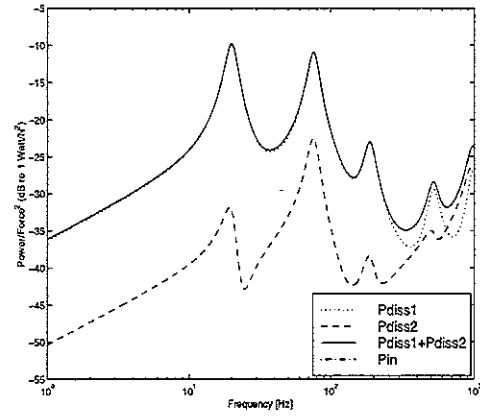


(b) lateral force

Figure 3.6. Power for a single beam [Case 2: $l = 700$ mm].

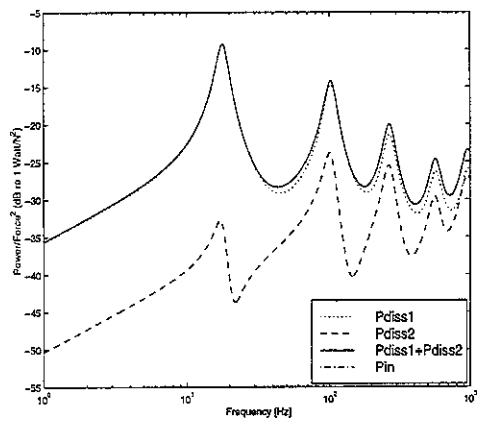


(a) vertical force

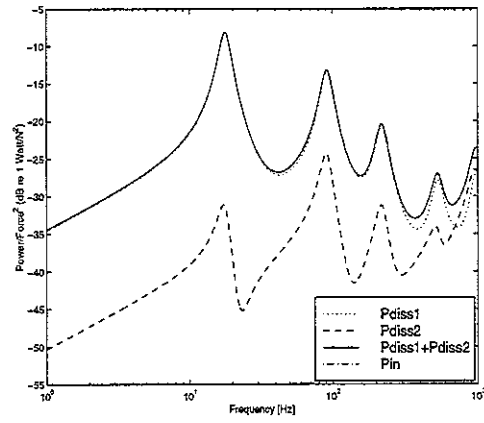


(b) lateral force

Figure 3.7. Power for two perpendicular beams [Case 3: $l_1 = 500$ mm, $l_2 = 200$ mm].



(a) vertical force



(b) lateral force

Figure 3.8. Power for a coupled beam system joined at 45 degrees [Case 4: $l_1 = 500$ mm, $l_2 = 200$ mm].

4. SINGLE PLATE INVESTIGATIONS

4.1 Equations of motion

4.1.1 Flexure

For a uniform plate lying in the x - y plane, the equations of motion are partial differential equations in two space dimensions and time. The differential equation governing the flexural vibrations may be written as [2, 11]

$$D\nabla^4 w + \rho h \ddot{w} = p(x, y, t) \quad (4.1)$$

where w is the out-of-plane deflection, D is the flexural rigidity

($D = Eh^3/12(1-\nu^2)$, E is Young's modulus, h is the thickness of panel and ν is Poisson's ratio, respectively), ρh is the mass per unit area [kg/m^2], and $p(x, y, t)$ represents a distributed load. In equation (4.1), ∇^4 is the bi-harmonic operator of fourth-order,

$$\nabla^4 = \nabla^2 \nabla^2 = \frac{\partial^4}{\partial x^4} + 2 \frac{\partial^4}{\partial x^2 \partial y^2} + \frac{\partial^4}{\partial y^4} \quad (4.2)$$

where ∇^2 is the two-dimensional Laplace operator,

$$\nabla^2 = \frac{\partial^2}{\partial x^2} + \frac{\partial^2}{\partial y^2}. \quad (4.3)$$

If the plate is simply supported along two opposite longitudinal edges ($y = 0$ and $y = b$), that is their displacements and moment are zero, then the deflection may be taken to be of the form

$$w(x, y, t) = \sum_m W_m(x, t) \sin(m\pi y/b) \quad (4.4)$$

where W_m is the out-of-plane displacement, m is the number of half-sine waves along the transverse edge and b is the width of the plate in the transverse direction (y direction in Fig.4.1).

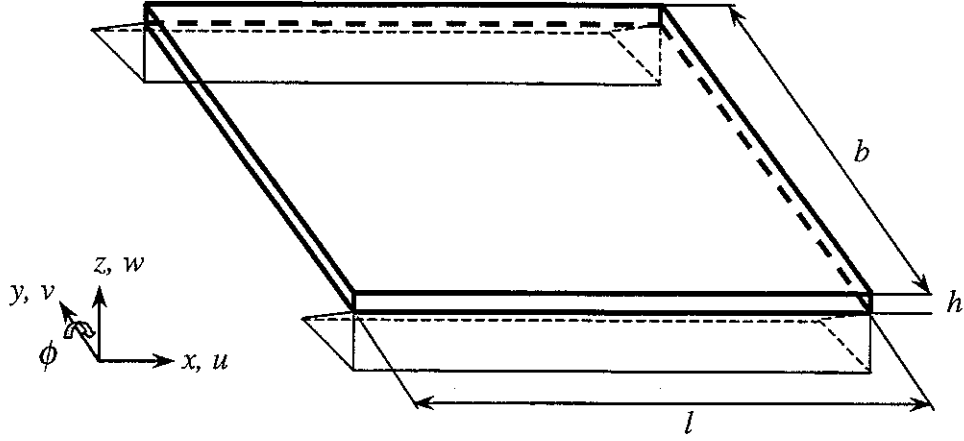


Figure 4.1 Single plate

From equation (4.4),

$$\begin{aligned}
 \frac{\partial w}{\partial x} &= \sum_m W'_m \sin(m\pi y/b), \quad \frac{\partial^2 w}{\partial x^2} = \sum_m W''_m \sin(m\pi y/b), \quad \frac{\partial^4 w}{\partial x^4} = \sum_m W_m^{IV} \sin(m\pi y/b), \\
 \frac{\partial w}{\partial y} &= \sum_m W_m (m\pi/b) \cos(m\pi y/b), \quad \frac{\partial^2 w}{\partial y^2} = -\sum_m W_m (m\pi/b)^2 \sin(m\pi y/b), \\
 \frac{\partial^4 w}{\partial y^4} &= \sum_m W_m (m\pi/b)^4 \sin(m\pi y/b), \quad \frac{\partial^2 w}{\partial x^2 \partial y^2} = -\sum_m W''_m (m\pi/b)^2 \sin(m\pi y/b), \\
 \frac{\partial w}{\partial t} &= \sum_m \dot{W}_m \sin(m\pi y/b), \quad \frac{\partial^2 w}{\partial t^2} = \sum_m \ddot{W}_m \sin(m\pi y/b).
 \end{aligned} \tag{4.5}$$

Substituting equations (4.5) into equation (4.1), then

$$\sum_m \left[DW_m^{IV} - 2D \left(\frac{m\pi}{b} \right)^2 W''_m + D \left(\frac{m\pi}{b} \right)^4 W_m + \rho h \ddot{W}_m \right] \sin(m\pi y/b) = p(x, y, t) \tag{4.6}$$

Taking $k_n = \frac{n\pi}{b}$, multiplying by $\sin(n\pi y/b)$, and integrating over y

$$DW_n^{IV} - 2Dk_n^2 W''_n + Dk_n^4 W_n + \rho h \ddot{W}_n = \frac{2}{b} \int_0^b p(x, y, t) \sin(n\pi y/b) dy \tag{4.7}$$

since on the left-hand side the integral of $\sin(m\pi y/b) \times \sin(n\pi y/b)$ is zero for $m \neq n$ and $b/2$ for $m = n$.

Assuming harmonic time dependence $e^{j\omega t}$, equation (4.7) may be rewritten as follows if there is no excitation.

$$DW_n^{IV} - 2Dk_n^2 W''_n + \{Dk_n^4 - \rho h \omega^2\} W_n = 0 \tag{4.8}$$

where $W_n(x)$ represents a complex amplitude, which can be written as

$$W_n(x) = W_{n0} e^{k_{nr}x}. \quad (4.9)$$

The solution to equation (4.8) yields the general solution

$$W_n(x) = \sum_{r=1}^4 A_{nr} e^{k_{nr}x} \quad (4.10)$$

where the A_{nr} terms are four unknown constants of integration which can be found by ensuring that the solution satisfies the boundary conditions at the ends of the plate and the k_{nr} terms are the four complex roots of the following equation in k_{nr} :

$$Dk_{nr}^4 - 2Dk_n^2 k_{nr}^2 + (Dk_n^4 - \rho h \omega^2) = 0 \quad (4.11)$$

$$k_{nr}^4 - 2k_n^2 k_{nr}^2 + k_n^4 - \rho h \omega^2 / D = 0 \quad (4.12)$$

$$k_{n1, n2} = \pm \sqrt{k_n^2 + k^2}, \quad k_{n3, n4} = \pm j \sqrt{k_n^2 - k^2} \text{ and } k^4 = \rho h \omega^2 / D. \quad (4.13)$$

The first two terms of equation (4.10) represent non-propagating waves which decay exponentially in space. These waves do not transmit energy and they may be called “near field waves”. On the other hand, the last two terms represent true flexural waves which have a sinusoidal distribution in space and propagate from the left to the right or from the right to the left. These waves transmit energy and they may be called “far-field waves” [12].

The solution of equation (4.11) includes all four different k_{nr} terms in the following form

$$w = \sum_{r=1}^4 A_{nr} e^{k_{nr}x} \sin(k_n y) e^{j\omega t}. \quad (4.14)$$

Damping may be considered in the plate by assigning a complex modulus and hence one has $D(1+j\eta)$ for the flexural rigidity.

4.1.2 Extension/shear

The in-plane differential equations for free vibrations of a plate are given by [13, 14]

$$B(1+\gamma) \frac{\partial^2 u}{\partial x^2} + B \frac{\partial^2 u}{\partial y^2} + B\gamma \frac{\partial^2 v}{\partial x \partial y} - \rho \ddot{u} = 0 \quad (4.15)$$

$$B(1+\gamma) \frac{\partial^2 v}{\partial y^2} + B \frac{\partial^2 v}{\partial x^2} + B\gamma \frac{\partial^2 u}{\partial x \partial y} - \rho \ddot{v} = 0 \quad (4.16)$$

where $B = E/(1+\nu)$, $\gamma = (1+\nu)/(1-\nu)$, ρ is the material density $[kg/m^3]$ and u and v are the longitudinal and transverse deflection, respectively.

The loss factor η may be introduced to represent the material damping so that one can replace Young's modulus E by $E(1+j\eta)$.

If the boundary conditions are simply supported along the longitudinal edges, the in-plane deflections, the longitudinal deflection u and the transverse deflection v , may be expressed as

$$u(x, y, t) = \sum_n U_n(x, t) \sin(k_n y) \quad (4.17)$$

$$v(x, y, t) = \sum_n V_n(x, t) \cos(k_n y) \quad (4.18)$$

where $k_n = \frac{n\pi}{b}$ and assuming a harmonic response, U_n and V_n consist of solutions of the form

$$U_n(x, t) = U_{n0} e^{(\lambda_{nr} x + j\omega t)} \quad (4.19)$$

$$V_n(x, t) = V_{n0} e^{(\lambda_{nr} x + j\omega t)}. \quad (4.20)$$

Using equations (4.17) and (4.18), the differential equations (4.15) and (4.16) can be rewritten as

$$B(1+\gamma)U_n'' - B\gamma k_n V_n' - Bk_n^2 U_n - \rho \ddot{U}_n = 0 \quad (4.21)$$

$$BV_n'' + B\gamma k_n U_n' - B(1+\gamma)k_n^2 V_n - \rho \ddot{V}_n = 0. \quad (4.22)$$

Substituting equations (4.19) and (4.20) into the differential equations (4.21) and (4.22)

$$B(1+\gamma)\lambda_{nr}^2 U_{n0} - B\gamma k_n \lambda_{nr} V_{n0} - Bk_n^2 U_{n0} + \rho\omega^2 U_{n0} = 0 \quad (4.23)$$

$$B\lambda_{nr}^2 V_{n0} + B\gamma k_n \lambda_{nr} U_{n0} - B(1+\gamma)k_n^2 V_{n0} + \rho\omega^2 V_{n0} = 0 \quad (4.24)$$

which can be solved for λ_{nr} . The four roots of λ_{nr} for a given n , are

$$\lambda_{1,2} = \pm \sqrt{k_n^2 - k_L^2} \quad \text{and} \quad \lambda_{3,4} = \pm \sqrt{k_n^2 - k_T^2} \quad (4.25)$$

where $k_L^2 = \rho\omega^2(1-\nu^2)/E$ and $k_T^2 = 2\rho\omega^2(1+\nu)/E$.

The general solutions for the in-plane displacements may be written as

$$u(x, y, t) = \left\{ \begin{bmatrix} \lambda_1 & \lambda_2 \end{bmatrix} \begin{bmatrix} C_{n1} e^{\lambda_1 x} \\ C_{n2} e^{\lambda_2 x} \end{bmatrix} + \begin{bmatrix} k_n & k_n \end{bmatrix} \begin{bmatrix} C_{n3} e^{\lambda_3 x} \\ C_{n4} e^{\lambda_4 x} \end{bmatrix} \right\} \sin(k_n y) e^{j\omega t} \quad (4.26)$$

$$v(x, y, t) = \left\{ [k_n \ k_n] \begin{bmatrix} C_{n1} e^{\lambda_1 x} \\ C_{n2} e^{\lambda_2 x} \end{bmatrix} + [\lambda_3 \ \lambda_4] \begin{bmatrix} C_{n3} e^{\lambda_3 x} \\ C_{n4} e^{\lambda_4 x} \end{bmatrix} \right\} \sin(k_n y) e^{j\omega t}. \quad (4.27)$$

4.2 Dynamic stiffness matrix

4.2.1 Flexure

Equation (4.10) may be used to derive a relationship between the displacements and forces at the ends of the plate, and thus the dynamic stiffness matrix of the plate for flexural vibrations with transverse modeshape $\sin(k_n y)$ for each n . The solution of this equation contains four unknown constants A_{nr} of integration which can be found by ensuring that the solution satisfies the four boundary conditions of the plate at the transverse edges, $x = 0$ and $x = l$.

Upon introducing the flexural displacement vector

$$\mathbf{u}_{nf}^T = \{W_n(0) \ W'_n(0) \ W_n(l) \ W'_n(l)\}, \quad (4.28)$$

then

$$\begin{aligned} W_n(0) &= A_{n1} + A_{n2} + A_{n3} + A_{n4} \\ W'_n(0) &= k_{n1}A_{n1} + k_{n2}A_{n2} + k_{n3}A_{n3} + k_{n4}A_{n4} \\ W_n(l) &= A_{n1}e^{k_{n1}l} + A_{n2}e^{k_{n2}l} + A_{n3}e^{k_{n3}l} + A_{n4}e^{k_{n4}l} \\ W'_n(l) &= k_{n1}A_{n1}e^{k_{n1}l} + k_{n2}A_{n2}e^{k_{n2}l} + k_{n3}A_{n3}e^{k_{n3}l} + k_{n4}A_{n4}e^{k_{n4}l} \end{aligned} \quad (4.29)$$

or in matrix form

$$\mathbf{u}_{nf} = \begin{bmatrix} 1 & 1 & 1 & 1 \\ k_{n1} & k_{n2} & k_{n3} & k_{n4} \\ e^{k_{n1}l} & e^{k_{n2}l} & e^{k_{n3}l} & e^{k_{n4}l} \\ k_{n1}e^{k_{n1}l} & k_{n2}e^{k_{n2}l} & k_{n3}e^{k_{n3}l} & k_{n4}e^{k_{n4}l} \end{bmatrix} \begin{Bmatrix} A_{n1} \\ A_{n2} \\ A_{n3} \\ A_{n4} \end{Bmatrix} \quad (4.30)$$

$$\mathbf{u}_{nf} = \mathbf{p}_{1n} \mathbf{A}_n \quad (4.31)$$

where $\mathbf{A}_n^T = \{A_{n1} \ A_{n2} \ A_{n3} \ A_{n4}\}$ and

$$\mathbf{p}_{1n} = \begin{bmatrix} 1 & 1 & 1 & 1 \\ k_{n1} & k_{n2} & k_{n3} & k_{n4} \\ e^{k_{n1}l} & e^{k_{n2}l} & e^{k_{n3}l} & e^{k_{n4}l} \\ k_{n1}e^{k_{n1}l} & k_{n2}e^{k_{n2}l} & k_{n3}e^{k_{n3}l} & k_{n4}e^{k_{n4}l} \end{bmatrix}. \quad (4.32)$$

The longitudinal shear force $S_n(x)$ and bending moment $M_n(x)$ along the free edges may be written as [2, 11]

$$S_n = -D \left[W_n''' - (2-\nu) k_n^2 W_n' \right] \quad (4.33)$$

$$M_n = -D \left[W_n'' - \nu k_n^2 W_n \right] \quad (4.34)$$

where D is the flexural rigidity, ν is Poisson's ratio and $k_n = \frac{n\pi}{b}$.

Upon introducing the restoring force vector

$$\mathbf{F}_{nf}^T = \{-S_n(0) \quad M_n(0) \quad S_n(l) \quad -M_n(l)\} \quad (4.35)$$

$$-S_n(0) = D \left[\sum_{r=1}^4 (k_{nr})^3 A_{nr} - (2-\nu) k_n^2 \left\{ \sum_{r=1}^4 k_{nr} A_{nr} \right\} \right] \quad (4.36)$$

$$M_n(0) = -D \left[\sum_{r=1}^4 (k_{nr})^2 A_{nr} - \nu k_n^2 \sum_{r=1}^4 A_{nr} \right] \quad (4.37)$$

$$S_n(l) = -D \left[\left\{ \sum_{r=1}^4 (k_{nr})^3 A_{nr} e^{k_{nr}l} \right\} - (2-\nu) k_n^2 \left\{ \sum_{r=1}^4 k_{nr} A_{nr} e^{k_{nr}l} \right\} \right] \quad (4.38)$$

$$-M_n(l) = D \left[\sum_{r=1}^4 (k_{nr})^2 A_{nr} e^{k_{nr}l} - \nu k_n^2 \sum_{r=1}^4 A_{nr} e^{k_{nr}l} \right] \quad (4.39)$$

From equation (4.31), $\mathbf{A}_n = \mathbf{p}_{1n}^{-1} \mathbf{u}_{nf}$, substituting this into equations (4.36), (4.37), (4.38) and (4.39), then equation (4.35) can be rewritten in matrix form,

$$\mathbf{F}_{nf} = \mathbf{p}_{2n} \mathbf{A}_n = \mathbf{p}_{2n} \mathbf{p}_{1n}^{-1} \mathbf{u}_{nf} = \mathbf{K}_{nf} \mathbf{u}_{nf} \quad (4.40)$$

$$\mathbf{K}_{nf} = \mathbf{p}_{2n} \mathbf{p}_{1n}^{-1} \quad (4.41)$$

and

$$\mathbf{p}_{2n} = D \begin{bmatrix} (k_{n1})^3 - (2-\nu) k_n^2 k_{n1} & (k_{n2})^3 - (2-\nu) k_n^2 k_{n2} & (k_{n3})^3 - (2-\nu) k_n^2 k_{n3} & (k_{n4})^3 - (2-\nu) k_n^2 k_{n4} \\ -(k_{n1})^2 + \nu k_n^2 & -(k_{n2})^2 + \nu k_n^2 & -(k_{n3})^2 + \nu k_n^2 & -(k_{n4})^2 + \nu k_n^2 \\ -(k_{n1})^3 e^{k_{n1}l} + (2-\nu) k_n^2 k_{n1} e^{k_{n1}l} & -(k_{n2})^3 e^{k_{n2}l} + (2-\nu) k_n^2 k_{n2} e^{k_{n2}l} & -(k_{n3})^3 e^{k_{n3}l} + (2-\nu) k_n^2 k_{n3} e^{k_{n3}l} & -(k_{n4})^3 e^{k_{n4}l} + (2-\nu) k_n^2 k_{n4} e^{k_{n4}l} \\ (k_{n1})^2 e^{k_{n1}l} - \nu k_n^2 e^{k_{n1}l} & (k_{n2})^2 e^{k_{n2}l} - \nu k_n^2 e^{k_{n2}l} & (k_{n3})^2 e^{k_{n3}l} - \nu k_n^2 e^{k_{n3}l} & (k_{n4})^2 e^{k_{n4}l} - \nu k_n^2 e^{k_{n4}l} \end{bmatrix} \quad (4.42)$$

where \mathbf{K}_{nf} is the dynamic stiffness matrix for flexural vibrations.

4.2.2 Extension/shear

Equations (4.17) and (4.18) may be used to derive a relationship between the in-plane displacements and forces at the ends of the plate, and thus the dynamic

stiffness matrix of the plate for in-plane vibrations. The solution of these equations contain four unknown constants C_{nr} of integration for each n which can be found by ensuring that the solution satisfies the four boundary conditions of the plate at the transverse edges, $x = 0$ and $x = l$.

Upon introducing the in-plane displacement vector

$$\mathbf{u}_{ni}^T = \{U_n(0) \quad V_n(0) \quad U_n(l) \quad V_n(l)\}, \quad (4.43)$$

then

$$\begin{aligned} U_n(0) &= \lambda_1 C_{n1} + \lambda_2 C_{n2} + k_n C_{n3} + k_n C_{n4} \\ V_n(0) &= k_n C_{n1} + k_n C_{n2} + \lambda_3 C_{n3} + \lambda_4 C_{n4} \\ U_n(l) &= \lambda_1 e^{\lambda_1 l} C_{n1} + \lambda_2 e^{\lambda_2 l} C_{n2} + k_n e^{\lambda_3 l} C_{n3} + k_n e^{\lambda_4 l} C_{n4} \\ V_n(l) &= k_n e^{\lambda_1 l} C_{n1} + k_n e^{\lambda_2 l} C_{n2} + \lambda_3 e^{\lambda_3 l} C_{n3} + \lambda_4 e^{\lambda_4 l} C_{n4} \end{aligned} \quad (4.44)$$

$$\mathbf{u}_{ni} = \begin{bmatrix} \lambda_1 & \lambda_2 & k_n & k_n \\ k_n & k_n & \lambda_3 & \lambda_4 \\ \lambda_1 e^{\lambda_1 l} & \lambda_2 e^{\lambda_2 l} & k_n e^{\lambda_3 l} & k_n e^{\lambda_4 l} \\ k_n e^{\lambda_1 l} & k_n e^{\lambda_2 l} & \lambda_3 e^{\lambda_3 l} & \lambda_4 e^{\lambda_4 l} \end{bmatrix} \begin{Bmatrix} C_{n1} \\ C_{n2} \\ C_{n3} \\ C_{n4} \end{Bmatrix} \quad (4.45)$$

$$\mathbf{u}_{ni} = \mathbf{r}_{1n} \mathbf{C}_n \quad (4.46)$$

where $\mathbf{C}_n^T = \{C_{n1} \quad C_{n2} \quad C_{n3} \quad C_{n4}\}$ and

$$\mathbf{r}_{1n} = \begin{bmatrix} \lambda_1 & \lambda_2 & k_n & k_n \\ k_n & k_n & \lambda_3 & \lambda_4 \\ \lambda_1 e^{\lambda_1 l} & \lambda_2 e^{\lambda_2 l} & k_n e^{\lambda_3 l} & k_n e^{\lambda_4 l} \\ k_n e^{\lambda_1 l} & k_n e^{\lambda_2 l} & \lambda_3 e^{\lambda_3 l} & \lambda_4 e^{\lambda_4 l} \end{bmatrix}. \quad (4.47)$$

The in-plane longitudinal force $N(x)$ and transverse force $T(x)$ which correspond to the deflections, $U_n(x)$ and $V_n(x)$, may be written as [11, 13]

$$N = hB(1+\gamma) \left[\frac{\partial u}{\partial x} + \nu \frac{\partial v}{\partial y} \right] \quad (4.48)$$

$$T = hB \left[\frac{\partial u}{\partial y} + \frac{\partial v}{\partial x} \right]. \quad (4.49)$$

Upon introducing the restoring force vector

$$\mathbf{F}_{ni}^T = \{-N(0) \quad -T(0) \quad N(l) \quad T(l)\} \quad (4.50)$$

then

$$\mathbf{F}_{ni} = \mathbf{r}_{2n} \mathbf{C}_n \quad (4.51)$$

where

$$\mathbf{r}_{2n} = hB \begin{bmatrix} -(1+\gamma)(\lambda_1^2 - \nu k_n^2) & -(1+\gamma)(\lambda_2^2 - \nu k_n^2) & -(1+\gamma)k_n\lambda_3(1-\nu) & -(1+\gamma)k_n\lambda_4(1-\nu) \\ -2k_n\lambda_1 & -2k_n\lambda_2 & -(k_n^2 + \lambda_3^2) & -(k_n^2 + \lambda_4^2) \\ (1+\gamma)(\lambda_1^2 - \nu k_n^2)e^{\lambda_1 l} & (1+\gamma)(\lambda_2^2 - \nu k_n^2)e^{\lambda_2 l} & (1+\gamma)(1-\nu)k_n\lambda_3e^{\lambda_3 l} & (1+\gamma)(1-\nu)k_n\lambda_4e^{\lambda_4 l} \\ 2k_n\lambda_1e^{\lambda_1 l} & 2k_n\lambda_2e^{\lambda_2 l} & (k_n^2 + \lambda_3^2)e^{\lambda_3 l} & (k_n^2 + \lambda_4^2)e^{\lambda_4 l} \end{bmatrix} \quad (4.52)$$

From equation (4.46), equation (4.51) can be rewritten in matrix form,

$$\mathbf{F}_{ni} = \mathbf{r}_{2n} \mathbf{C}_n = \mathbf{r}_{2n} \mathbf{r}_{1n}^{-1} \mathbf{u}_{ni} = \mathbf{K}_{ni} \mathbf{u}_{ni} \quad (4.53)$$

$$\mathbf{K}_{ni} = \mathbf{r}_{2n} \mathbf{r}_{1n}^{-1} \quad (4.54)$$

where \mathbf{K}_{ni} is the dynamic stiffness matrix for in-plane vibrations.

4.2.3 Dynamic stiffness matrix for a single plate

Each edge has four degrees of freedom, three translational degrees of freedom (u, v, w) and one rotational degree of freedom (ϕ) for each value of n . The dynamic stiffness matrix for flexure and in-plane may be combined in a 8×8 matrix

$$\mathbf{K}_n = \begin{bmatrix} \mathbf{K}_{nf} & \mathbf{0} \\ \mathbf{0} & \mathbf{K}_{ni} \end{bmatrix} \quad (4.55)$$

where \mathbf{K}_{nf} is the dynamic stiffness matrix for flexure and \mathbf{K}_{ni} is the dynamic stiffness matrix for in-plane. Equations (4.40) and (4.53) represent the dynamic properties of a single plate.

4.2.4 The removal of the matrix near singularity

If the length of the plate is large compared with the wavelength, the matrix ($\mathbf{p}_{1n}, \mathbf{p}_{2n}, \mathbf{r}_{1n}$ or \mathbf{r}_{2n}) may be nearly singular. This is caused by the large differences in the relative values of the elements of the matrix. It can be overcome by multiplying by a diagonal scaling matrix \mathbf{H} .

For flexural vibration, write

$$\mathbf{p}_{1n} \mathbf{H} = \mathbf{p}'_{1n}, \quad \mathbf{p}_{2n} \mathbf{H} = \mathbf{p}'_{2n} \quad (4.56)$$

$$\mathbf{K}_{nf} = \mathbf{p}_{2n} \mathbf{p}_{1n}^{-1} = (\mathbf{p}'_{2n} \mathbf{H}^{-1}) (\mathbf{p}'_{1n} \mathbf{H}^{-1})^{-1} = (\mathbf{p}'_{2n} \mathbf{H}^{-1}) (\mathbf{H} \mathbf{p}'_{1n})^{-1} \quad (4.57)$$

$$\mathbf{K}_{nf} = \mathbf{p}_{2n} \mathbf{p}_{1n}^{-1} = \mathbf{p}'_{2n} \mathbf{p}'_{1n}{}^{-1} \quad (4.58)$$

where \mathbf{H} is the diagonal scaling matrix,

$$\mathbf{H} = \begin{bmatrix} e^{-k_{n1}l} & 0 & 0 & 0 \\ 0 & 1 & 0 & 0 \\ 0 & 0 & e^{-k_{n3}l} & 0 \\ 0 & 0 & 0 & 1 \end{bmatrix} \quad (4.59)$$

where $\text{Re}(k_{n1}) \geq 0$ and $\text{Re}(k_{n3}) \geq 0$.

For in-plane vibration,

$$\mathbf{r}_{1n}\mathbf{H} = \mathbf{r}'_{1n}, \quad \mathbf{r}_{2n}\mathbf{H} = \mathbf{r}'_{2n} \quad (4.60)$$

$$\mathbf{K}_{ni} = \mathbf{r}_{2n}\mathbf{r}_{1n}^{-1} = (\mathbf{r}'_{2n}\mathbf{H}^{-1})(\mathbf{r}'_{1n}\mathbf{H}^{-1})^{-1} = (\mathbf{r}'_{2n}\mathbf{H}^{-1})(\mathbf{H}\mathbf{r}'_{1n})^{-1} \quad (4.61)$$

$$\mathbf{K}_{ni} = \mathbf{r}_{2n}\mathbf{r}_{1n}^{-1} = \mathbf{r}'_{2n}\mathbf{r}'_{1n}{}^{-1}. \quad (4.62)$$

This effectively changes the coefficients to scaled coefficients in the description of the wave amplitudes in the plate.

4.3 Concentrated force

In the above, the equations of motion of the plate have been decomposed into a series of half-sine orders. If the excitation is a concentrated force at position y_0 , this needs to be decomposed into its effect on the various orders. If a force is defined by $f(y) = F_0\delta(y - y_0)$ and assumed odd and periodic in $(-b, b)$, then $f(y)$ can be expressed by a half-range Fourier series expansion [15], that is

$$f(y) = \frac{a_0}{2} + \sum_{n=1}^{\infty} \left(a_n \cos \frac{n\pi y}{b} + b_n \sin \frac{n\pi y}{b} \right) \quad (4.63)$$

where $a_0 = 0$, $a_n = 0$, $b_n = \frac{2}{b} \int_0^b f(y) \sin \frac{n\pi y}{b} dy = \frac{2F_0}{b} \sin \frac{n\pi y_0}{b}$ for $n = 1, 2, 3, \dots$

Hence, the force can be represented spatially by the series

$$f(y) = \frac{2F_0}{b} \sum_{n=1}^{\infty} \sin \frac{n\pi y}{b} \sin \frac{n\pi y_0}{b}. \quad (4.64)$$

If the concentrated force is applied at the centre of edge, $y_0 = \frac{b}{2}$, then

$$f(y) = \frac{2F_0}{b} \sum_{\substack{n=1 \\ n, \text{ odd}}}^{\infty} (-1)^{(n-1)/2} \sin \frac{n\pi y}{b} \quad (4.65)$$

or

$$f(y) = \frac{2F_0}{b} \sum_{n=1}^{\infty} (-1)^{n+1} \sin \frac{(2n-1)\pi y}{b} . \quad (4.66)$$

Figure 4.2 shows a reconstruction of a concentrated force at $y_0 = b/2$ using Fourier components up to $n = 11$.

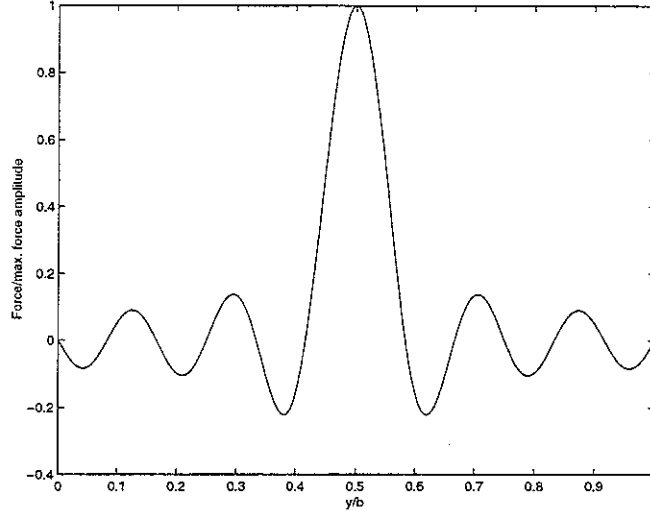


Fig. 4.2 The concentrated force at the middle of the left-hand edge of a coupled plate represented by the Fourier components, $n = 1-11$.

4.4 Strain energies and power

The strain energy for the plate is determined from the following relationships [5].

4.4.1 Strain energy for flexure

The strain energy for flexural vibration is given by

$$U_f = \frac{D}{2} \int_0^b \int_0^l \left[\left(\frac{\partial^2 w}{\partial x^2} \right)^2 + \left(\frac{\partial^2 w}{\partial y^2} \right)^2 + 2\nu \left(\frac{\partial^2 w}{\partial x^2} + \frac{\partial^2 w}{\partial y^2} \right) + 2(1-\nu) \left(\frac{\partial^2 w}{\partial x \partial y} \right)^2 \right] dx dy \quad (4.67)$$

where D is the flexural rigidity, ν is Poisson's ratio, w is the out-of-plane displacement and b and l are the width and length of the plate.

4.4.2 Strain energy for in-plane

The strain energy for in-plane vibration is given by

$$U_i = \frac{1}{2} \frac{Eh}{1-\nu^2} \int_0^b \int_0^l \left[\left(\frac{\partial u}{\partial x} \right)^2 + \left(\frac{\partial v}{\partial y} \right)^2 + 2\nu \left(\frac{\partial u}{\partial x} + \frac{\partial v}{\partial y} \right) + \frac{(1-\nu)}{2} \left(\frac{\partial u}{\partial y} + \frac{\partial v}{\partial x} \right)^2 \right] dx dy . \quad (4.68)$$

where E is Young's modulus, h is the thickness of the plate, ν is Poisson's ratio, u is the extensional displacement and v is the transverse displacement.

4.4.3 Power

The input power and the dissipated power are obtained from the same equations, (2.65) and (2.66) respectively, as for the beam.

4.5 Simulations for a single plate

4.5.1 Model

The model was selected to compare the results with previously published data [16]. It is shown in Figure 4.3 and comprises a square aluminium plate simply supported along two edges, free along the other edges. For this model, only the flexural vibration is considered.

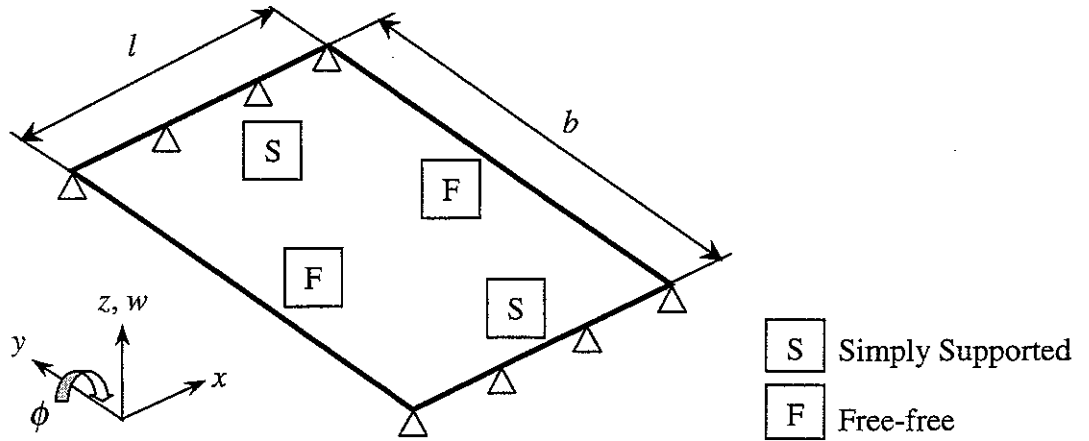


Figure 4.3. A single plate: Width $b = 254$ mm, Length $l = 254$ mm, Thickness $h = 3.175$ mm, Material: Aluminium (Young's modulus $E = 7.24 \times 10^{10}$ N/m², Poisson's ratio $\nu = 0.333$, Material density $\rho = 2.794 \times 10^3$ kg/m³).

4.5.2 Natural frequencies

For free vibration problems \mathbf{F}_n is zero and the natural frequencies for flexural vibration are determined from the equation

$$\det(\mathbf{K}_{nf}) = 0 \quad (4.69)$$

where \mathbf{K}_{nf} is the dynamic stiffness matrix for flexure reduced as appropriate according to the boundary conditions at $x = 0$ and $x = l$.

Figure 4.4 shows the flexural “frequency functions” (that is $\det(\mathbf{K}_{ff}^{-1})$) for a single plate according to the number of half-sine waves along the y-direction. In the plot n implies the number of half-sine waves from $y = 0$ to $y = b$ in the direction across the plate.

The natural frequencies of a single plate obtained by the dynamic stiffness method (Figure 4.4 and Table 4.2) agree well with previously published data [16] as shown in Table 4.1.

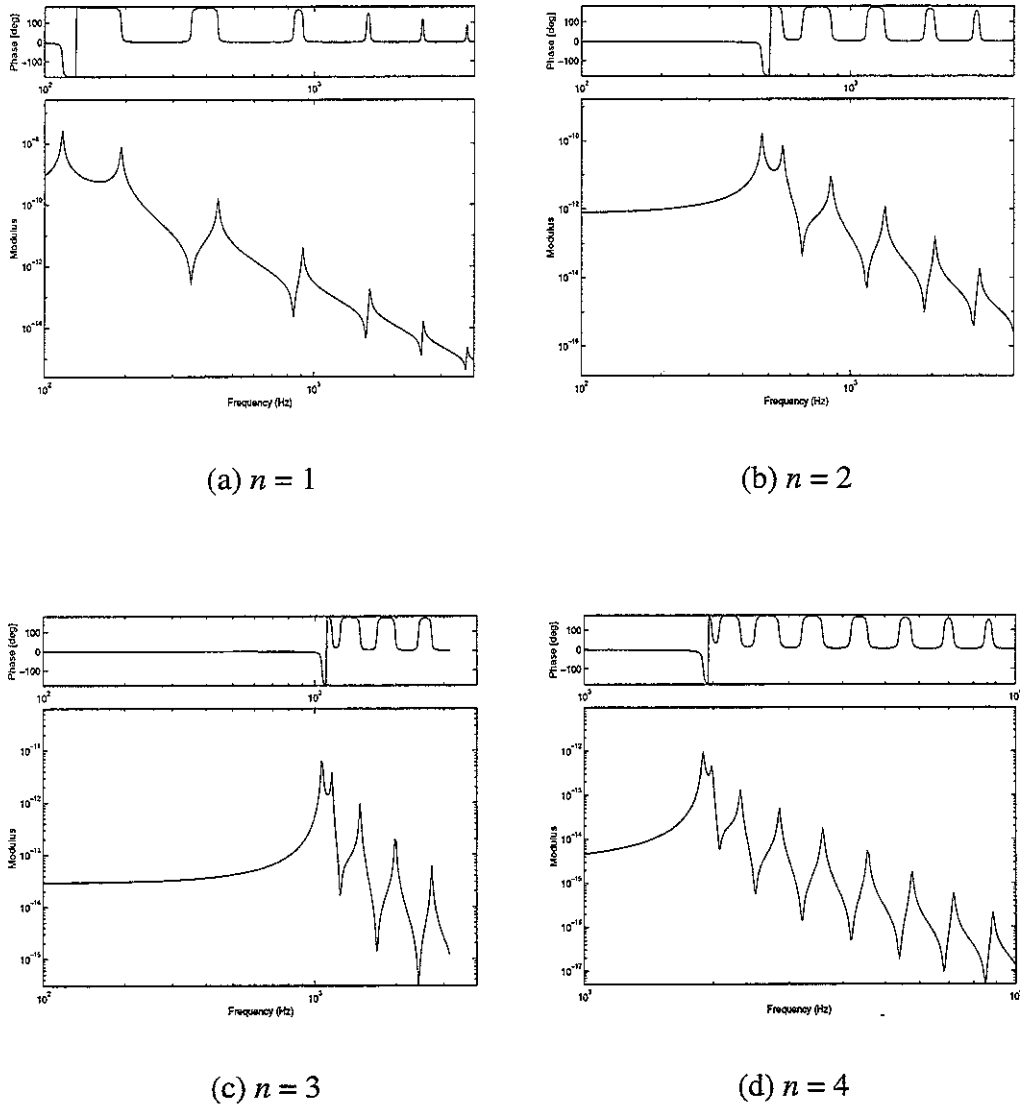


Figure 4.4. The flexural “frequency functions” (*i.e.* $\det(\mathbf{K}_f^{-1})$) for a single plate for 4 different half-sine wave orders.

Table 4.1. The natural frequencies for a single plate obtained from published data [16]

$$\lambda^2 = \omega l^2 \sqrt{\rho/D} \quad (b = 254mm, l = 254mm, \nu = 0.333)$$

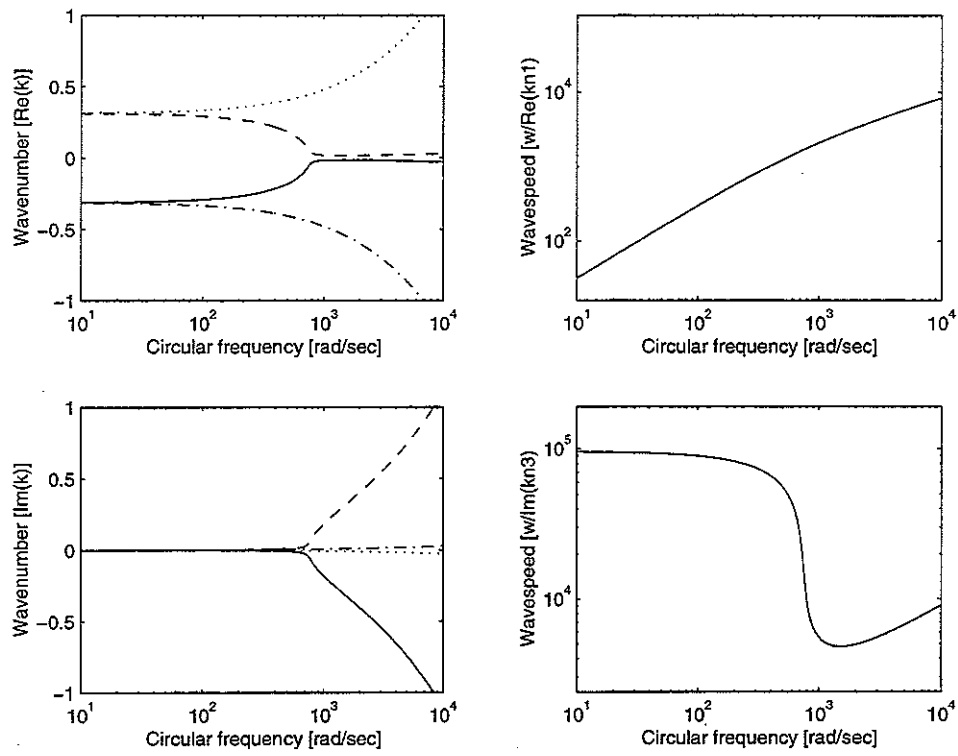
$n \quad m$	1	2	3	4
1	115.9	192.4	441.2	908.8
2	469.9	561.2	849.9	1337.3
3	1062.8	1156.6	1469.4	1984.2
4	1894.6	1987.8	2313.7	2849.1

Table 4.2. Comparison of the natural frequencies for the first mode of each n ($m=1$)

n	Gorman	Dynamic Stiffness Method
1	115.9	115.86 (-0.03%)
2	469.9	470.09 (0.04%)
3	1062.8	1063.18 (0.04%)
4	1894.6	1895.26 (0.03%)

4.5.3 Dispersion relationships of flexural vibration for a single plate

Figure 4.5 shows the dispersion curves, the relationship between wavenumber and frequency, and also the wavespeed, for a single plate for the first 4 different half-sine orders across the plate. There are four complex roots from equation (4.12) for each n . For two complex roots, k_{n1} and k_{n2} , the real parts of the wavenumbers that are the evanescent component are greater than the imaginary parts and these waves are not propagating but decaying along the plate. For the other two complex roots, k_{n3} and k_{n4} , on the other hand, the imaginary parts are greater than the real parts and these waves are propagating in negative and positive directions, respectively and each of these waves transmits energy along the plate. The wavespeeds of these propagating waves change rapidly around the cut-on frequency, which corresponds to the first mode of an infinitely long plate.



(a) wavenumber vs. frequency

(b) wavespeed vs. frequency

Figure 4.5. The dispersion curves for a single plate [$n = 1$]: (a) wavenumber k vs. frequency: ..., k_{n1} ; - · -, k_{n2} ; ---, k_{n3} ; —, k_{n4} (b) wavespeed of k_{n1} and k_{n3} vs. frequency.

5. COUPLED PLATE INVESTIGATIONS

5.1 Dynamic Stiffness matrix

Assuming a distributed harmonic force is applied at a transverse edge, a coupled plate system may be analysed by using the same concept as the previous beam system. The plates are assumed to be simply supported along opposite edges and connected along the other edges. The dynamic stiffness matrix of a coupled plate system is derived from assembling the dynamic stiffness matrix of each plate and applying the compatibility and equilibrium condition at the joint. As for the single plate, the system is analysed for each half-sine order separately.

The dynamic stiffness matrix of a coupled plate system joined at an arbitrary angle is given by (Appendix B.5),

$$\mathbf{K}_p = \mathbf{T}_p^T \mathbf{K}_{(l+2)} \mathbf{T}_p \quad (5.1)$$

where \mathbf{K}_p is a 12×12 matrix for a coupled plate system, $\mathbf{K}_{(l+2)}$ is a 16×16 assembled matrix for two plates and \mathbf{T}_p is the transformation matrix for plates defined in Appendix B.6.

The forced response is determined by premultiplying \mathbf{K}_p^{-1} to the equation

$$\mathbf{F}_p = \mathbf{K}_p \mathbf{u}_p, \text{ then}$$

$$\mathbf{u}_p = \mathbf{K}_p^{-1} \mathbf{F}_p \quad (5.2)$$

where the force vector:

$$\mathbf{F}_p^T = \{-S_1, M_1, -N_1, -T_1, S_2, -M_2, N_2, T_2, S_4, -M_4, N_4, T_4\}, \mathbf{F}_p = \mathbf{T}_p \mathbf{F}_{(l+2)} \quad (5.3)$$

and the displacements vector:

$$\mathbf{u}_p^T = \{w_1, \phi_1, u_1, v_1, w_2, \phi_2, u_2, v_2, w_4, \phi_4, u_4, v_4\}, \mathbf{u}_p = \mathbf{T}_p \mathbf{u}_{(l+2)}. \quad (5.4)$$

5.2 Simulations for two coplanar plates with flexural vibration only

5.2.1 Model

The system studied consists of two plates joined at 0 degree as shown in Figure 5.1. The model is selected to compare the natural frequencies and forced response between a single plate system and a coupled plate system which have the same width and overall length. For this model, only the flexural vibration is considered.

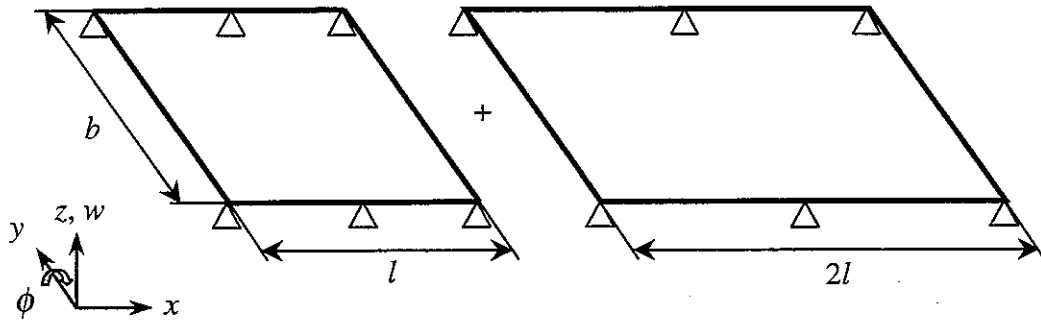
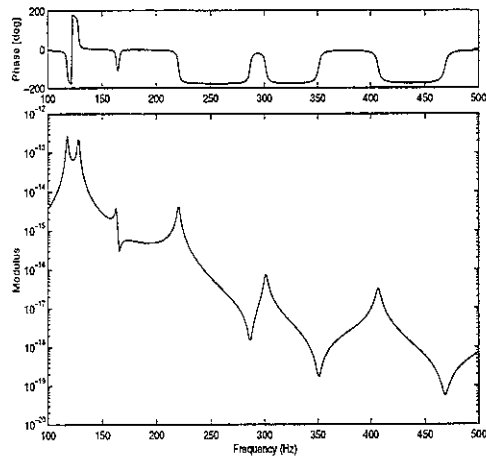


Figure 5.1. Two coplanar plates: Width $b = 254$ mm, Length $l = 254$ mm, Thickness $h = 3.175$ mm, Material: Aluminium (Young's modulus $E = 7.24 \times 10^{10}$ N/m², Poisson's ratio $\nu = 0.333$, Material density $\rho = 2.794 \times 10^3$ kg/m³).

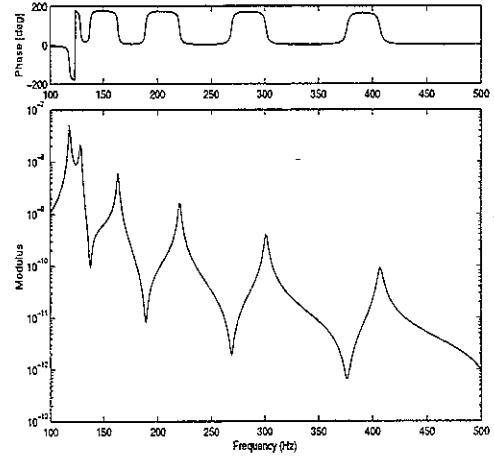
5.2.2 Natural frequencies

The flexural “frequency functions” (that is $\det(\mathbf{K}_f^{-1})$) for a coupled plate system of total length $3l = 762$ mm and a single plate which has the same dimension, are shown in Figure 5.2. These have been compared to check the accuracy of the analysis and the numerical implementation. In the plot n presents the number of half-sine waves, from $y = 0$ to $y = b$, in the direction across the plate.

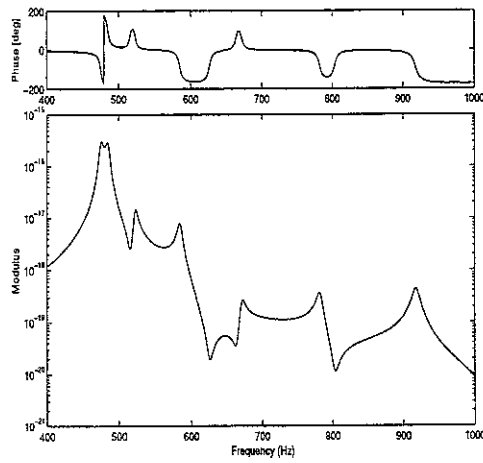
In Figure 5.2 the natural frequencies of a coupled plate system of total length $3l$ shows good agreement with a single plate of the same length as a coupled plate system although the magnitudes and shapes of the frequency functions are quite different. The resonances are easier to identify for the single plate system.



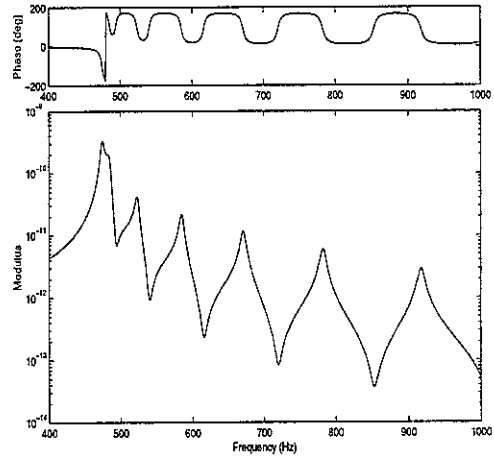
(a) Two plates ($n = 1$)



(b) Single plate ($n = 1$)

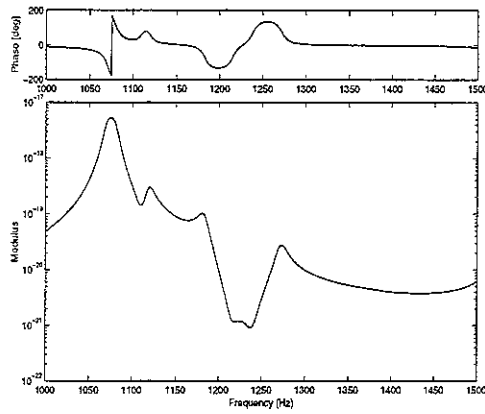


(c) Two plates ($n = 2$)

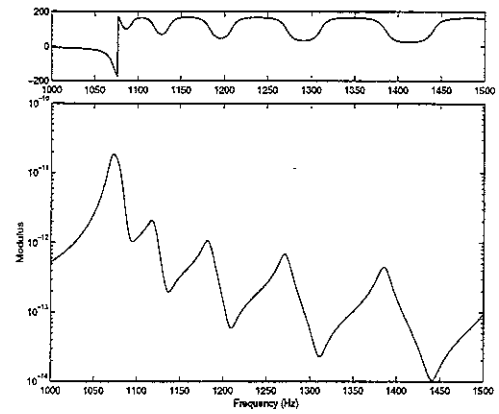


(d) Single plate ($n = 2$)

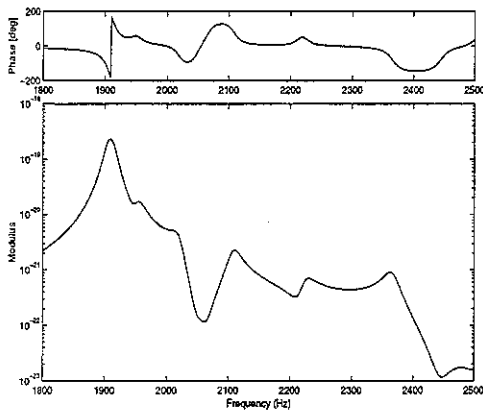
Figure 5.2. The comparison of the frequency functions of a coupled plate system and a single plate.



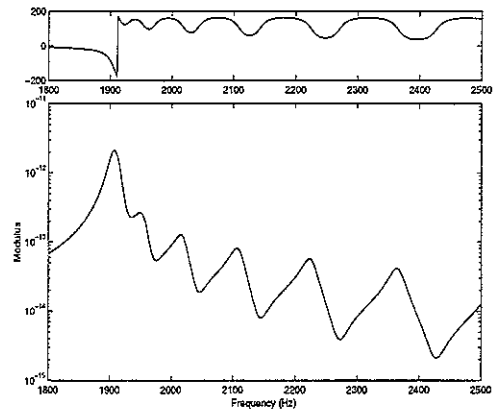
(e) Two plates ($n = 3$)



(f) Single plate ($n = 3$)



(g) Two plates ($n = 4$)



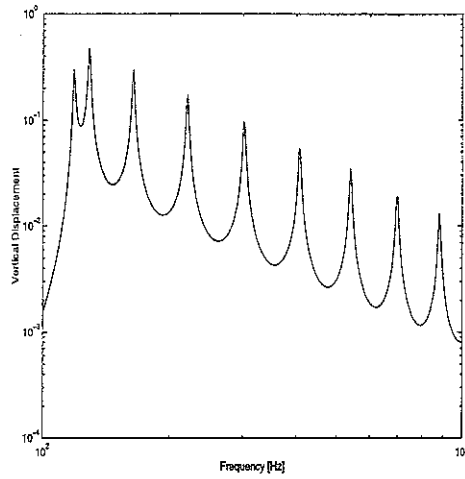
(h) Single plate ($n = 4$)

Figure 5.2 (cont'd). The comparison of the frequency functions of two coupled plates and a single plate.

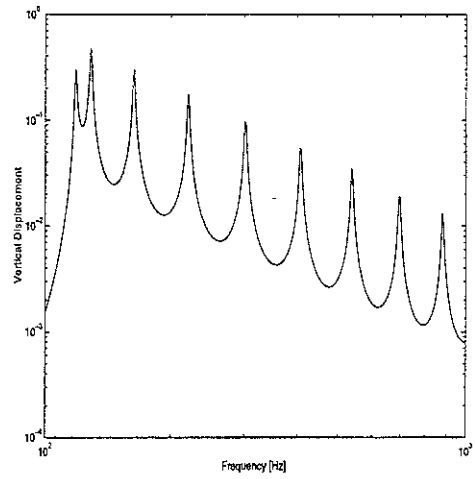
5.2.3 Forced response

Figure 5.3 shows the forced response when a unit amplitude distributed force with a half-sine wave spatial variation is applied at the free end of right-hand side edge, $x = 3l$. As expected, the result shows exact agreement between a single plate and a coupled plate system.

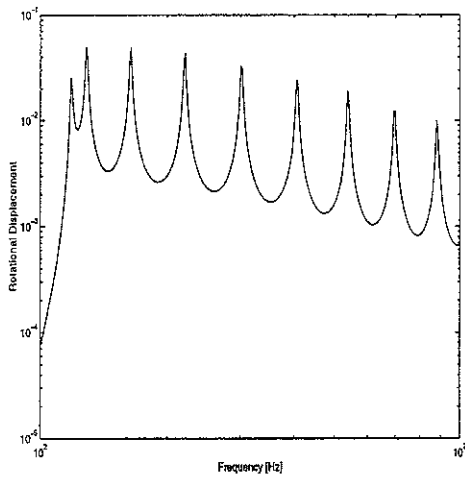
The forced response for a coupled plate system is also calculated when a unit force is applied at the middle edge, *i.e.* $x = l$, where Plate 1 is connected with Plate 2. The vertical displacement is presented in Figure 5.4 and the rotational displacement in Figure 5.5.



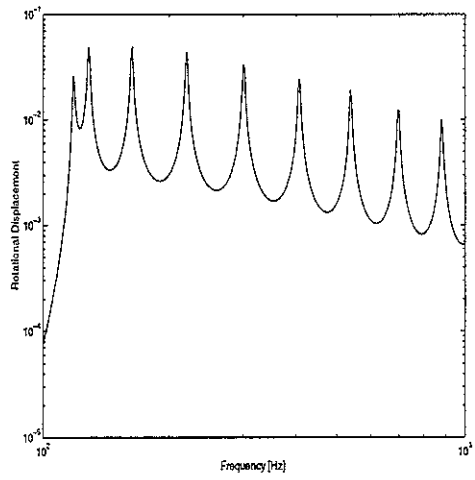
(a) Vertical displacement for two plates



(b) Vertical displacement for a single plate

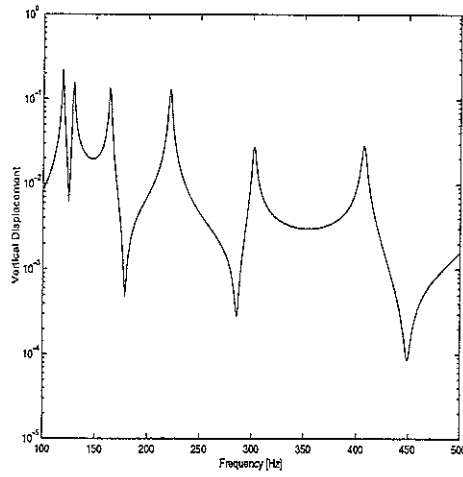


(c) Rotational displacement for two plates

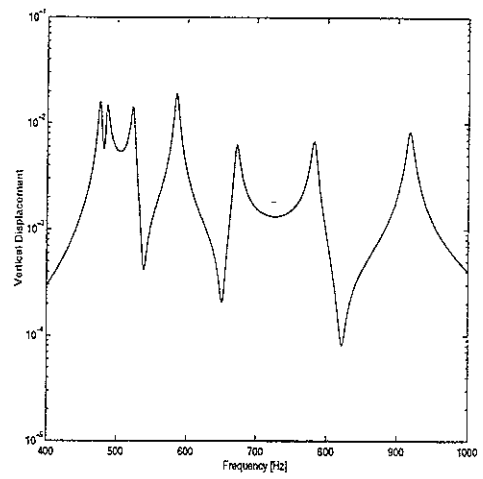


(d) Rotational displacement for a single plate

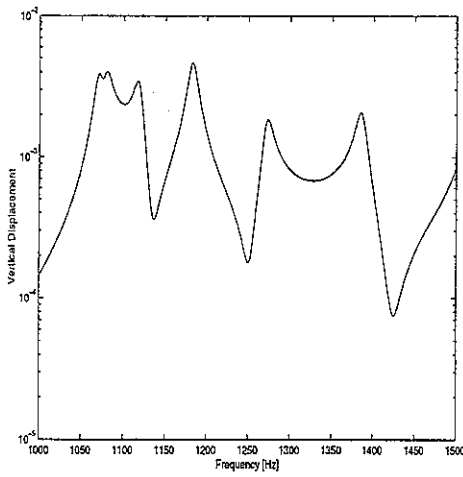
Figure 5.3. The forced response comparison of a coupled plates with a single plate due to a unit amplitude distributed force [$n = 1$] applied at the right-hand side free edge.



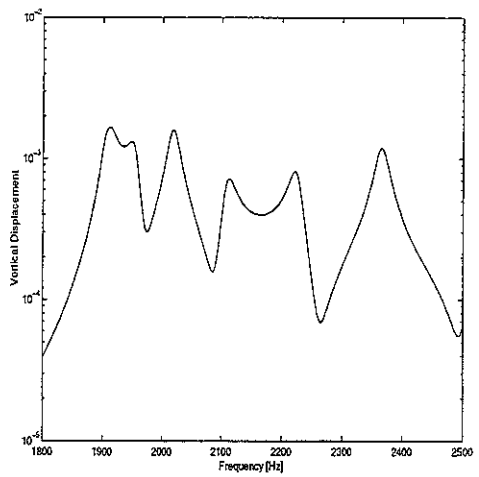
(a) $n = 1$



(b) $n = 2$

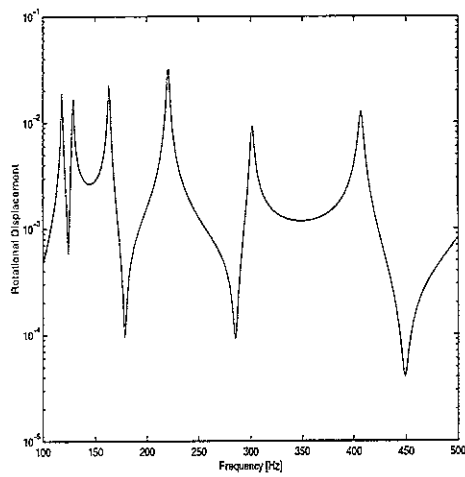


(c) $n = 3$

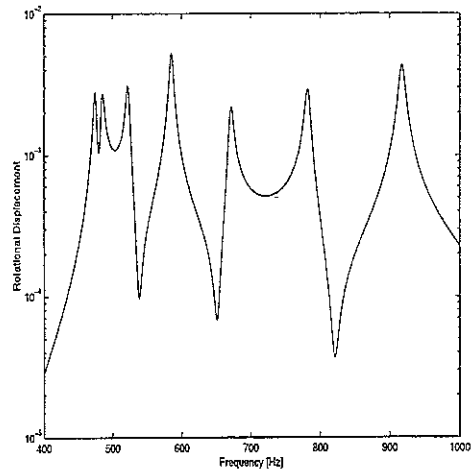


(b) $n = 4$

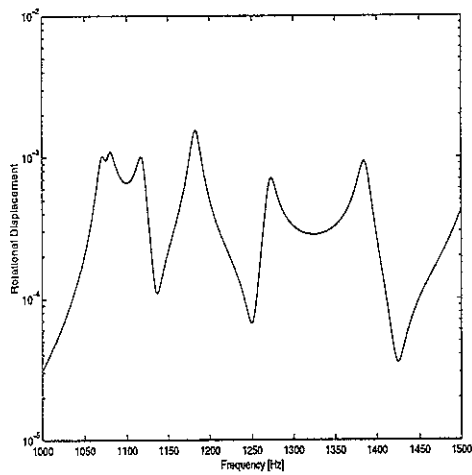
Figure 5.4. The vertical displacement for a coupled plate system at the left-hand side edge due to a unit amplitude distributed force applied at the middle edge.



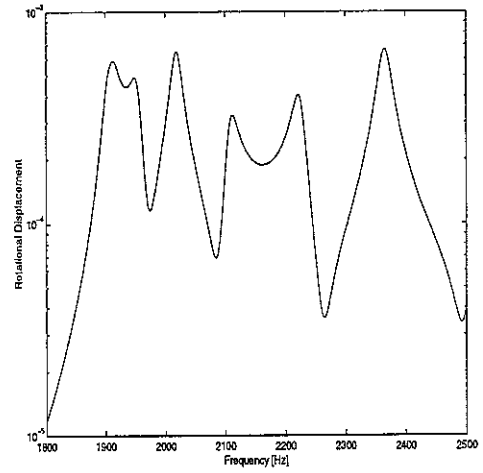
(a) $n = 1$



(b) $n = 2$



(c) $n = 3$



(d) $n = 4$

Figure 5.5. The rotational displacement for a coupled plate system at the left-hand side edge due to a unit amplitude distributed force applied at the middle edge.

5.3 Simulations for two perpendicular plates considering in-plane vibrations

5.3.1 Model

The system studied in this section consists of two perpendicular plates which have both flexural and in-plane vibrations, as shown in Figure 5.6. It is assumed that the two opposite edges along the longitudinal direction, $y = 0$ and $y = b$, are simply supported and the other edges are free along the y direction. The model is used to compare the input power due to the excitation with the total dissipated power for two plates.

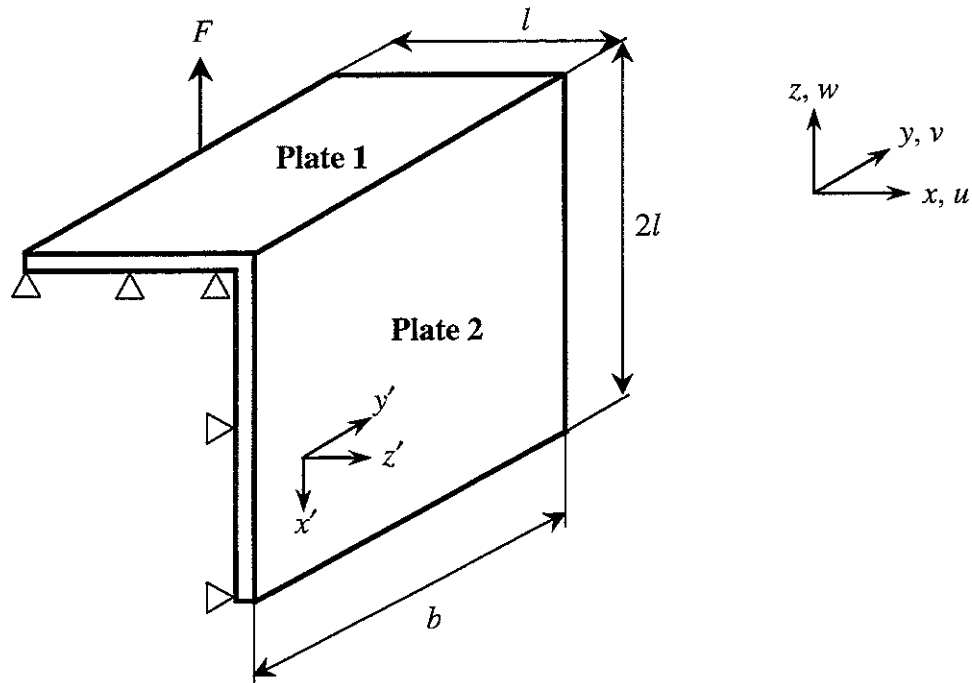


Figure 5.6. Two perpendicular plates: Width $b = 200$ mm, Length $l = 100$ mm, Thickness $h = 3.0$ mm, Material: Aluminium (Young's modulus $E = 7.24 \times 10^{10}$ N/m², Poisson's ratio $\nu = 0.333$, Material density $\rho = 2.794 \times 10^3$ kg/m³).

5.3.2 Power balance

In this analysis, the in-plane vibration was introduced and a concentrated force was applied at the centre of the left-hand side edge of Plate 1, that is $x = 0$ and $y = b/2$.

Since the concentrated force excites components of vibration with different values of n , a study has been performed to establish how many components should be included to achieve convergence of the solution. The force acts at the centre of the edge so only odd values of n need to be included. The total input power has been calculated using $n = 1$ to 15 and converted into one-third octave band levels. The same calculation has been performed for a truncated series using $n = 1$ to n_{max} for different values of n_{max} . These results have then been normalised by the result for $n_{max} = 15$ in each band. Figure 5.7 shows these normalised input powers. As frequency increases the number of components that need to be included, n_{max} , increases. Thus below 200 Hz $n_{max} = 1$ is sufficient whereas at 10 kHz $n_{max} = 11$ is required. These results are also listed in Table 5.1.

The choice of n_{max} should ideally be made beforehand, for example from a knowledge of the cut-on frequency for each n . Below the appropriate cut-on frequency the contribution of a given n is likely to be small. In the table, values are shown in italics where n_{max} is chosen such that only components with cut-on frequencies below the current band centre frequency are included. This results in inaccuracies especially in the 250 Hz and 315 Hz bands. The shaded values are those for which n_{max} is chosen so that components with $f_{cut-on}/2$ less than the band centre frequency are included. This gives more accurate results, as also shown in Figure 5.8 and means that $n_{max} = 15$ is required for the 8 kHz band.

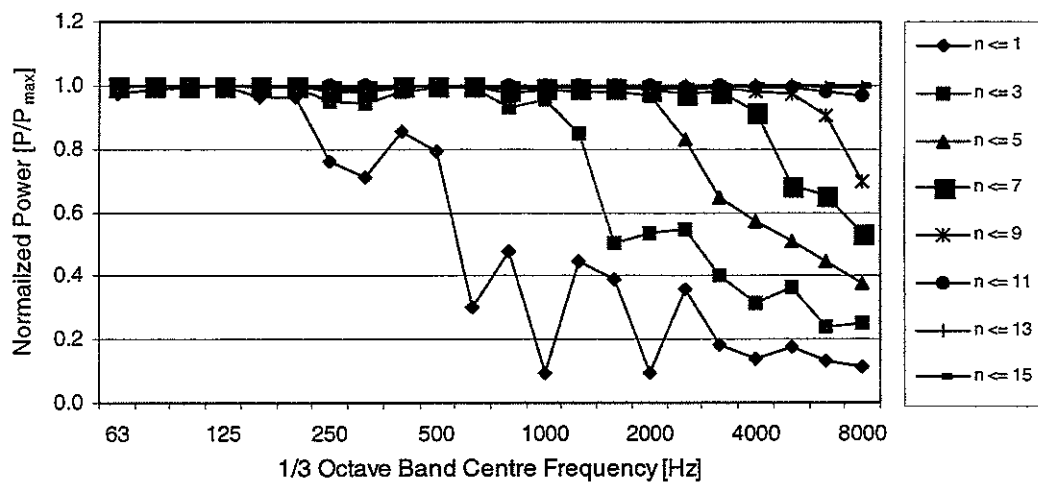


Figure 5.7 The convergence of the input power for the number of Fourier components.

Table 5.1 The normalised power by the maximum input power of each 1/3 octave frequency band for each n_{max}

n_{max}	1	3	5	7	9	11	13	15
f_{cut-on}	55.0	500.0	1477.0	2800.0	4800.0	7200.0	10027.0	13570.0
f_c								
50	<i>0.955</i>	0.988	0.995	0.997	0.999	0.999	1.000	1.000
63	<i>0.974</i>	0.993	0.997	0.999	0.999	1.000	1.000	1.000
80	<i>0.986</i>	0.996	0.998	0.999	1.000	1.000	1.000	1.000
100	<i>0.995</i>	0.999	0.999	1.000	1.000	1.000	1.000	1.000
125	<i>0.998</i>	0.999	1.000	1.000	1.000	1.000	1.000	1.000
160	<i>0.964</i>	0.991	0.996	0.998	0.999	1.000	1.000	1.000
200	<i>0.961</i>	0.991	0.996	0.998	0.999	0.999	1.000	1.000
250	<i>0.759</i>	<i>0.946</i>	0.978	0.989	0.994	0.997	0.999	1.000
315	<i>0.708</i>	<i>0.944</i>	0.977	0.989	0.994	0.997	0.999	1.000
400	<i>0.856</i>	<i>0.981</i>	0.992	0.996	0.998	0.999	1.000	1.000
500	<i>0.794</i>	<i>0.991</i>	0.997	0.998	0.999	1.000	1.000	1.000
630	<i>0.304</i>	<i>0.990</i>	0.996	0.998	0.999	1.000	1.000	1.000
800	<i>0.477</i>	<i>0.932</i>	<i>0.977</i>	0.989	0.994	0.997	0.999	1.000
1000	<i>0.095</i>	<i>0.952</i>	<i>0.987</i>	0.994	0.997	0.998	0.999	1.000
1250	<i>0.445</i>	<i>0.850</i>	<i>0.979</i>	0.991	0.995	0.998	0.999	1.000
1600	<i>0.387</i>	<i>0.505</i>	<i>0.981</i>	<i>0.992</i>	0.996	0.998	0.999	1.000
2000	<i>0.093</i>	<i>0.536</i>	<i>0.967</i>	<i>0.989</i>	0.994	0.997	0.999	1.000
2500	<i>0.358</i>	<i>0.548</i>	<i>0.830</i>	0.971	<i>0.987</i>	0.994	0.998	1.000
3150	<i>0.182</i>	<i>0.403</i>	<i>0.646</i>	<i>0.979</i>	<i>0.992</i>	0.996	0.999	1.000
4000	<i>0.141</i>	<i>0.312</i>	<i>0.571</i>	<i>0.918</i>	0.979	<i>0.991</i>	0.997	1.000
5000	<i>0.175</i>	<i>0.363</i>	<i>0.507</i>	<i>0.682</i>	<i>0.976</i>	<i>0.991</i>	0.997	1.000
6300	<i>0.130</i>	<i>0.238</i>	<i>0.449</i>	<i>0.652</i>	<i>0.908</i>	<i>0.983</i>	<i>0.995</i>	1.000
8000	<i>0.111</i>	<i>0.253</i>	<i>0.380</i>	<i>0.535</i>	<i>0.696</i>	<i>0.969</i>	<i>0.993</i>	<i>1.000</i>

Note. n = the number of Fourier component

f_c = the one-third octave centre frequency

f_{cut-on} = the cut-on frequency

italic values = the maximum analysis frequency is greater than the cut-on frequency ($f > f_{cut-on}$)

shaded values = the maximum analysis frequency is greater than the half of the cut-on frequency ($f > f_{cut-on}/2$)

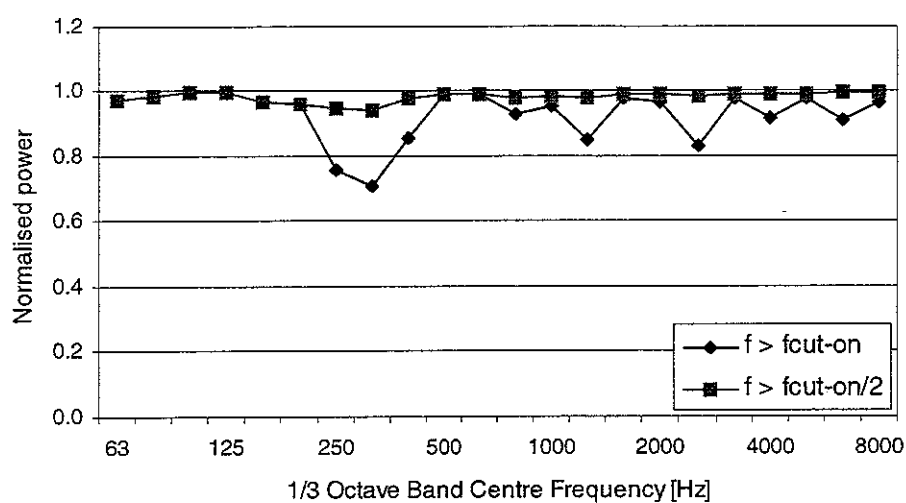


Figure 5.8 The convergence of the input power determined from the relationship between the cut-on frequency and the analysis frequency.

Table 5.2 The guideline for the selection of the number of Fourier component n depending on the analysis frequency

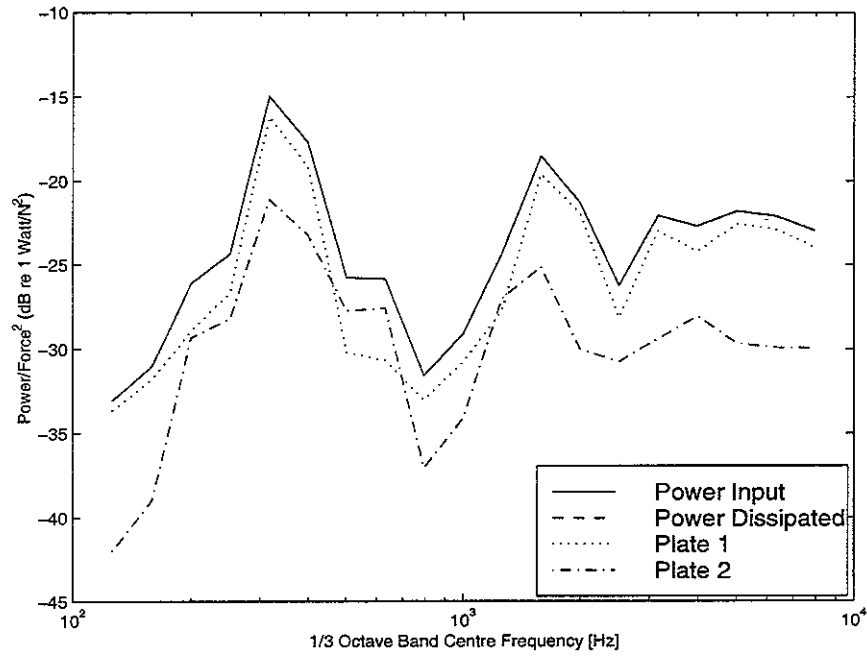
$f > f_{\text{cut-on}}$		$f > f_{\text{cut-on}}/2$	
Frequency range	n	Frequency range	n
50-400	1	50-200	1
500-1250	1,3	250-630	1,3
1600-2500	1,3,5	800-1250	1,3,5
3150-4000	1,3,5,7	1600-2000	1,3,5,7
5000-6300	1,3,5,7,9	2500-3150	1,3,5,7,9
8000	1,3,5,7,9,11	4000-5000	1,3,5,7,9,11
		6300	1,3,5,7,9,11,13
		8000	1,3,5,7,9,11,13,15

Figure 5.9 is the power calculation result for the two perpendicular plates with $n_{max} = 15$ for all frequencies and shows that the input power and the dissipated power agree with each other. The effect of the in-plane vibration is only significant above about 3000 Hz.

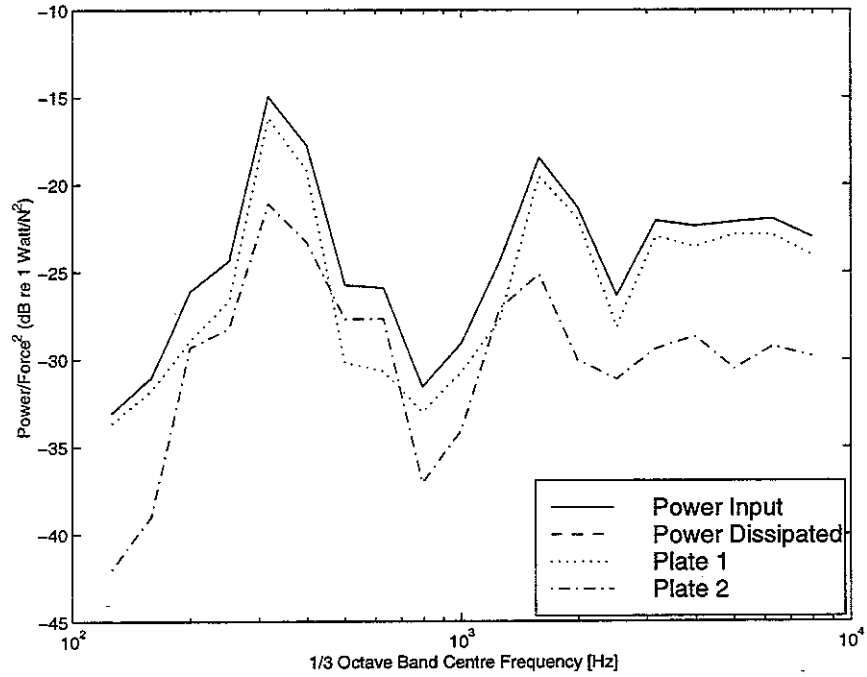
In this study the step size of 9mm used in calculating the strain energy shows good agreement within the range of acceptable error. It is 1/6 of the bending wavelength (54 mm) to the maximum analysis frequency 10 kHz. The bending wavelength λ_{plate} for plate is obtained from

$$\lambda_{plate} = 2\pi / (\rho h \omega^2 / D)^{1/4} \quad (5.5)$$

where ρ is the material density, h is the thickness of plate and D is the flexural rigidity. The result of the case study is summarised in Table 5.3 and the error plot is shown in Figure 5.10. The error decreases as the step size decreases and the loss factor increases.



(a) flexural vibration only



(b) considering in-plane vibration

Figure 5.9. The input power and the dissipated power for two perpendicular plates due to a unit concentrated force (the number of Fourier component $n_{max} = 15$) applied at the centre of the left-hand side edge of plate 1: ..., the dissipated power for plate 1; ---, the dissipated power for plate 2; ---, the total dissipated power; —, the input power.

Table 5.3 Results of the case study for the accuracy of the power calculation

Loss factor	Step size [mm]	Error (%) $[(P_{diss}-P_{in})/P_{in}]\times 100$	
		Total area	At the maximum frequency
0.2	27 ($\lambda/2$)	2.64	-15.84
	18 ($\lambda/3$)	3.25	10.91
	9 ($\lambda/6$)	-0.81	0.01
	4.5 ($\lambda/12$)	-0.41	0.25
	2 ($\lambda/27$)	-0.03	-0.11
0.1	27	-0.68	1.75
	18	2.06	6.87
	9	-0.96	0.31
	4.5	-0.51	0.46
	2	-0.03	-0.03
0.01	27	-5.68	53.62
	18	1.06	0.07
	9	-1.13	0.84
	4.5	-0.63	0.76
	2	-0.04	0.00
0.001	27	-6.46	57.14
	18	0.23	-0.10
	9	-1.21	0.79
	4.5	-0.85	0.76
	2	-0.03	0.00

Note. P_{diss} = the dissipated power for the perpendicular plates
 P_{in} = the input power for the driven plate
 λ = the bending wavelength for the plate

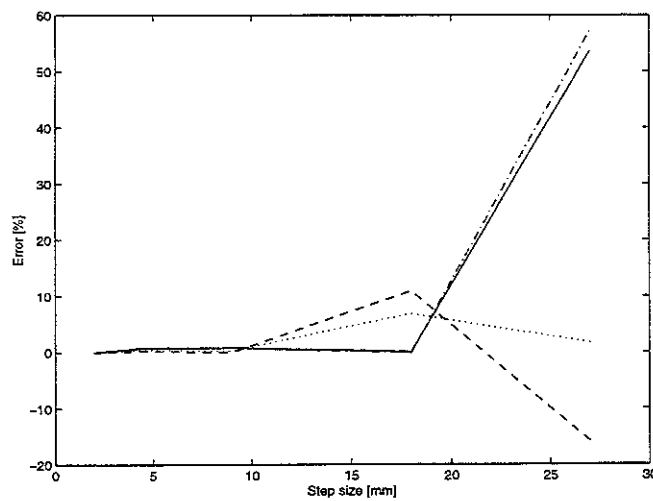


Figure 5.10. The error plot for the perpendicular plates at the maximum frequency. ---, $\eta = 0.2$; ..., $\eta = 0.1$; —, $\eta = 0.01$; - · -, $\eta = 0.001$.

6. CONCLUSIONS

The dynamic stiffness method provides a means of determining exactly the high frequency behaviour of idealised beam and plate structures. In this report, the dynamic stiffness matrices of beams and plates have been derived, including flexural, in-plane and (for the beam) torsional degrees of freedom and examples have been presented of single and coupled beams and plates. Natural frequencies have been predicted and compared with analytical results to provide validation of the software. Comparisons between natural frequencies and of the forced responses have been made for systems comprising a single element or the same system divided into two elements as validation of the software for the coupled case.

The objective in using the method in the current research is to study the power flow in a system of plates and/or beams. The input power due to excitation by a force has been obtained and the dissipated power has been determined by using the strain energy. This provides the tools for a study of coupling between beams and plates in terms of their coupling loss factors which is the next stage of the research. It has been found that significant errors occur in the dissipated calculation if kinetic energy is used instead of strain energy, particularly at low frequencies. The refinement in the numerical integration of strain energy has been investigated, as have the criteria for selecting the number of terms required in the Fourier series of the plate vibration in the transverse direction.

7. REFERENCES

1. ESDU 1997 Item No. 97033. Methods for analysis of the dynamic response of structures.
2. R. S. Langley 1989 *Journal of Sound and Vibration* **135**(2), 319-331. Application of the dynamic stiffness method to the free and forced vibrations of aircraft panels.
3. R. S. Langley 1990 *Journal of Sound and Vibration* **136**(3), 439-452. Analysis of power flow in beams and frameworks using the direct-dynamic stiffness method.
4. R. S. Langley 1992 *Journal of Sound and Vibration* **156**(3), 521-540. A dynamic stiffness technique for the vibration analysis of stiffened shell structures.
5. G. B. Warburton 1976 *The Dynamical Behaviour of Structures*. Oxford: Pergamon Press; second edition.
6. R. E. D. Bishop and D. C. Johnson 1960 *The Mechanics of Vibration*. Cambridge: Cambridge University Press.
7. M. Lalanne, P. Berthier and J. D. Hagopian 1983 *Mechanical Vibrations for Engineers*. New York: John Wiley & Sons.
8. R. H. Lyon and R. G. DeJong 1995 *Theory and Application of Statistical Energy Analysis*. Boston: Butterworth-Heinemann; second edition.
9. A. Biran and M. Breiner 1995 *MATLAB for Engineers*. Addison-Wesley.
10. The Math Works, Inc. 1995 *The Student Edition of MATLAB, Version 4 User's Guide*.
11. S. Timishenko and S. Woinowsky-Krieger 1959 *Theory of Plates and Shells*. New York: McGraw-Hill; second edition.
12. D. J. Mead 1982 in *Noise and Vibration* (R.G. White and J.G. Walker editors). Chapter 9: Structural wave motion. Chichester: Ellis Horwood.
13. A. N. Bercin and R. S. Langley 1996 *Computers & Structures* **59**(5), 869-875. Application of the Dynamic Stiffness Technique to the In-plane Vibrations of Plate Structures.
14. P. G. Craven and B. M. Gibbs 1981 *Journal of Sound and Vibration* **77**(3), 417-427. Sound transmission and mode coupling at junctions of thin plates, part i: representation of the problem.

15. R. Szilard 1974 *Theory and Analysis of Plates: Classical and Numerical Methods*. New Jersey: Prentice-Hall, Inc.
16. D. J. Gorman 1982 *Free Vibration Analysis of Rectangular Plates*. New York: Elsevier.

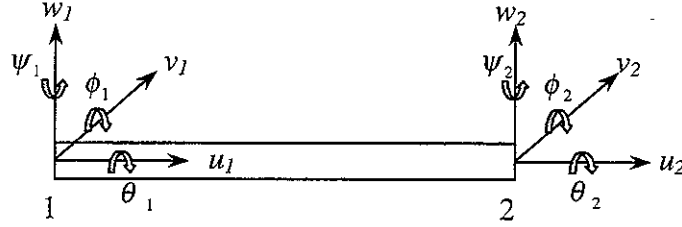
Appendix A. List of Symbols

a_n	Fourier coefficient of $\cos\left(\frac{n\pi y}{b}\right)$
b	Width of rectangular beam
b_n	Fourier coefficient of $\sin\left(\frac{n\pi y}{b}\right)$
c_f, c_e, c_t	Flexural, extensional, torsional wavespeed
f	frequency $\left(= \frac{\omega}{2\pi}\right)$
f_c	One-third octave centre frequency
$f_{\text{cut-on}}$	Cut-on frequency
h	Height of rectangular beam, thickness of plate
j	Complex operator $(=\sqrt{-1})$
k_n	$\frac{n\pi}{b}$
k_{nr}	Four complex roots of free vibration of plate
k_{bf}, k_{be}, k_{bt}	Flexural, extensional, torsional wavenumber for beam
k_{pf}, k_{pe}	Flexural, extensional wavenumber for plate
l	Length of beam and plate
n	Number of half-sine waves along transverse edge
p	Force, distributed force
r	Radius of circular beam
x, y, z	Global Cartesian coordinates
x', y', z'	Local Cartesian coordinates
u, v, w	Translational displacements in x, y, z directions, respectively
A	Cross-sectional area
A_{nr}, C_{nr}	Constants of integration
B	$\frac{E}{2(1+\nu)}$
B_i	Constants
D	Flexural rigidity $\left(\frac{Eh^3}{12(1-\nu^2)}\right)$
E	Young's modulus
E_{strain}	Strain energy amplitude of the dynamical response
F_A, F_B, S_n	Longitudinal shear force
G	Shear modulus
I	Second moment of inertia of area
J	Polar second moment of inertia of area
M_A, M_B, M_n	Bending moment
N	Axial force
P_{in}, P_{diss}	Input, dissipated power
T	Transverse force
U_f, U_e, U_t, U_{pi}	Strain energy for flexure, extension, torsion, in-plane

U, V, W	Amplitude of extensional, transverse and vertical displacement
Y	Mobility
Z	Impedance
\mathbf{b}	Constant vector
$\mathbf{p}_{1n}, \mathbf{p}_{2n}, \mathbf{r}_{1n}, \mathbf{r}_{2n}$	Matrix for plate used in dynamic stiffness matrix calculation
\mathbf{u}	Displacement vector
\mathbf{A}_n	Coefficient of n^{th} complementary function
\mathbf{C}_m	Constant vector of integration
\mathbf{D}	Constant vector
$\mathbf{F}_f, \mathbf{F}_e, \mathbf{F}_t, \mathbf{F}_{nf}, \mathbf{F}_{ni}$	Force vector
\mathbf{H}	Diagonal scaling matrix
$\mathbf{K}_f, \mathbf{K}_{nf}$	Dynamic stiffness matrix for flexure of beam and plate
\mathbf{K}_e	Dynamic stiffness matrix for extension of beam
\mathbf{K}_{ni}	Dynamic stiffness matrix for in-plane of plate
\mathbf{K}_t	Dynamic stiffness matrix for torsion of beam
$\mathbf{T}_b, \mathbf{T}_p$	Transformation matrix
γ	$\left(\frac{1+\nu}{1-\nu} \right)$
δ	Angle of assembly
ε	Strain
η	Hysteretic damping constant, loss factor
κ	Shape factor for non-circular beam
λ	Four roots of in-plane equations
ν	Poisson's ratio
θ, ϕ, ψ	Rotational displacement in x, y, z directions, respectively
ρ	Material density
σ	Stress
ω	Circular frequency
Θ, Φ	Rotational displacement

Appendix B Dynamic Stiffness and Transformation Matrices

B.1 Dynamic Stiffness Matrix for a single beam 1



$$\begin{bmatrix} F_{z1} \\ M_{y1} \\ F_{z2} \\ M_{y2} \\ F_{y1} \\ M_{z1} \\ F_{y2} \\ M_{z2} \\ F_{x1} \\ F_{x2} \\ M_{x1} \\ M_{x2} \end{bmatrix} = \begin{bmatrix} j_{a11} & j_{c11} & j_{b11} & j_{d11} \\ j_{c11} & j_{e11} & -j_{d11} & j_{f11} \\ j_{b11} & -j_{d11} & j_{a11} & -j_{c11} \\ j_{d11} & j_{f11} & -j_{c11} & j_{e11} \\ & & & j_{a12} & j_{c12} & j_{b12} & j_{d12} \\ & & & j_{c12} & j_{e12} & -j_{d12} & j_{f12} \\ & & & j_{b12} & -j_{d12} & j_{a12} & -j_{c12} \\ & & & j_{d12} & j_{f12} & -j_{c12} & j_{e12} \\ & & & & & j_{g1} & j_{h1} \\ & & & & & j_{h1} & j_{g1} \\ & & & & & & j_{k1} & j_{l1} \\ & & & & & & j_{l1} & j_{k1} \end{bmatrix} \begin{bmatrix} w_1 \\ \phi_1 \\ w_2 \\ \phi_2 \\ v_1 \\ \psi_1 \\ v_2 \\ \psi_2 \\ u_1 \\ u_2 \\ \theta_1 \\ \theta_2 \end{bmatrix}$$

$$\begin{aligned} j_{a11} &= -K_{11} k_{f11}^3 (\cos k_{f11} l_1 \sinh k_{f11} l_1 + \sin k_{f11} l_1 \cosh k_{f11} l_1) & j_{a12} &= -K_{12} k_{f12}^3 (\cos k_{f12} l_1 \sinh k_{f12} l_1 + \sin k_{f12} l_1 \cosh k_{f12} l_1) \\ j_{b11} &= K_{11} k_{f11}^3 (\sin k_{f11} l_1 + \sinh k_{f11} l_1) & j_{b12} &= K_{12} k_{f12}^3 (\sin k_{f12} l_1 + \sinh k_{f12} l_1) \\ j_{c11} &= -K_{11} k_{f11}^2 \sin k_{f11} l_1 \sinh k_{f11} l_1 & j_{c12} &= -K_{12} k_{f12}^2 \sin k_{f12} l_1 \sinh k_{f12} l_1 \\ j_{d11} &= K_{11} k_{f11}^2 (\cos k_{f11} l_1 - \cosh k_{f11} l_1) & j_{d12} &= K_{12} k_{f12}^2 (\cos k_{f12} l_1 - \cosh k_{f12} l_1) \\ j_{e11} &= K_{11} k_{f11} (\cos k_{f11} l_1 \sinh k_{f11} l_1 - \sin k_{f11} l_1 \cosh k_{f11} l_1) & j_{e12} &= K_{12} k_{f12} (\cos k_{f12} l_1 \sinh k_{f12} l_1 - \sin k_{f12} l_1 \cosh k_{f12} l_1) \\ j_{f11} &= K_{11} k_{f11} (\sin k_{f11} l_1 - \sinh k_{f11} l_1) & j_{f12} &= K_{12} k_{f12} (\sin k_{f12} l_1 - \sinh k_{f12} l_1) \\ j_{g1} &= L_1 \cot(k_{e11} l_1) & K_{11} &= E_1 I_{1a} / (\cos k_{f11} l_1 \cosh k_{f11} l_1 - 1) \\ j_{h1} &= -L_1 \operatorname{cosec}(k_{e11} l_1) & \lambda_{11} &= (\rho_1 A_1 \omega^2 / E_1 I_{1a})^{1/4} \\ j_{k1} &= N_1 \cot(k_{r11} l_1) & K_{12} &= E_1 I_{1b} / (\cos k_{f12} l_1 \cosh k_{f12} l_1 - 1) \\ j_{l1} &= -N_1 \operatorname{cosec}(k_{r11} l_1) & \lambda_{12} &= (\rho_1 A_1 \omega^2 / E_1 I_{1b})^{1/4} \end{aligned}$$

$$L_1 = E_1 A_1 k_{e11}$$

$$k_{e11} = (E_1 / \rho_1)^{1/2}$$

$$N_1 = G_1 J_1 k_{r11}$$

$$k_{r11} = (\kappa G_1 / \rho_1)^{1/2},$$

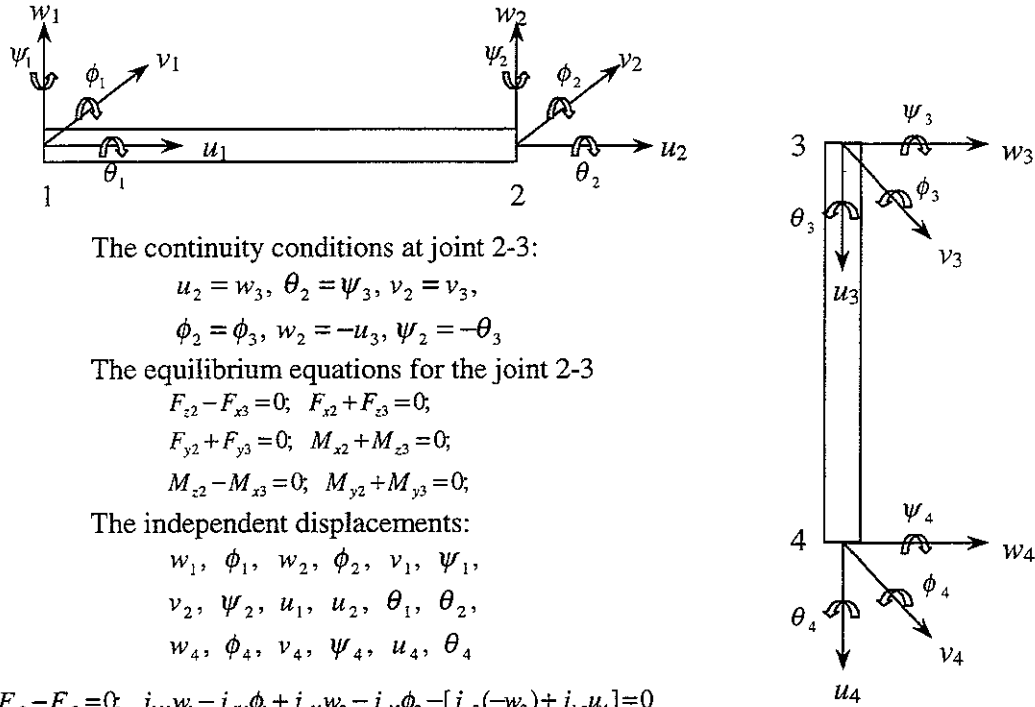
κ = Shape factor for non-circular section

B.2 Dynamic Stiffness Matrix for a single beam 2

$$\begin{bmatrix} F_{z3} \\ M_{y3} \\ F_{z4} \\ M_{y4} \\ F_{x3} \\ M_{z3} \\ F_{x4} \\ M_{z4} \end{bmatrix} = \begin{bmatrix} j_{d21} & j_{c21} & j_{b21} & j_{d21} & & & & \\ j_{c21} & j_{d21} & -j_{d21} & j_{f21} & & & & \\ j_{b21} & -j_{d21} & j_{d21} & -j_{c21} & & & & \\ j_{d21} & j_{f21} & -j_{c21} & j_{d21} & & & & \\ & & & & j_{d22} & j_{c22} & j_{b22} & j_{d22} \\ & & & & j_{c22} & j_{d22} & -j_{d22} & j_{f22} \\ & & & & j_{b22} & -j_{d22} & j_{d22} & -j_{c22} \\ & & & & j_{d22} & j_{f22} & -j_{c22} & j_{d22} \\ & & & & & j_{g2} & j_{h2} & \\ & & & & & j_{h2} & j_{g2} & \\ & & & & & & j_{k2} & j_{l2} \\ & & & & & & j_{l2} & j_{k2} \end{bmatrix} \begin{bmatrix} w_3 \\ \phi_3 \\ w_4 \\ \phi_4 \\ v_3 \\ \psi_3 \\ v_4 \\ \psi_4 \\ u_3 \\ u_4 \\ \theta_3 \\ \theta_4 \end{bmatrix}$$

$$\begin{aligned}
 j_{d21} &= -K_{21} k_{f21}^3 (\cos k_{f21} L_2 \sinh k_{f21} L_2 + \sin k_{f21} L_2 \cosh k_{f21} L_2) & j_{d22} &= -K_{22} k_{f22}^3 (\cos k_{f22} L_2 \sinh k_{f22} L_2 + \sin k_{f22} L_2 \cosh k_{f22} L_2) \\
 j_{b21} &= K_{21} k_{f21}^3 (\sin k_{f21} L_2 + \sinh k_{f21} L_2) & j_{b22} &= K_{22} k_{f22}^3 (\sin k_{f22} L_2 + \sinh k_{f22} L_2) \\
 j_{c21} &= -K_{21} k_{f21}^2 \sin k_{f21} L_2 \sinh k_{f21} L_2 & j_{c22} &= -K_{22} k_{f22}^2 \sin k_{f22} L_2 \sinh k_{f22} L_2 \\
 j_{d21} &= K_{21} k_{f21}^2 (\cos k_{f21} L_2 - \cosh k_{f21} L_2) & j_{d22} &= K_{22} k_{f22}^2 (\cos k_{f22} L_2 - \cosh k_{f22} L_2) \\
 j_{e21} &= K_{21} k_{f21} (\cos k_{f21} L_2 \sinh k_{f21} L_2 - \sin k_{f21} L_2 \cosh k_{f21} L_2) & j_{e22} &= K_{22} k_{f22} (\cos k_{f22} L_2 \sinh k_{f22} L_2 - \sin k_{f22} L_2 \cosh k_{f22} L_2) \\
 j_{f21} &= K_{21} k_{f21} (\sin k_{f21} L_2 - \sinh k_{f21} L_2) & j_{f22} &= K_{22} k_{f22} (\sin k_{f22} L_2 - \sinh k_{f22} L_2) \\
 j_{g2} &= L_2 \cot(k_{e21} L_2) & K_{21} &= E_2 I_{2a} / (\cos k_{f21} L_2 \cosh k_{f21} L_2 - 1) \\
 j_{h2} &= -L_2 \operatorname{cosec}(k_{e21} L_2) & k_{f21} &= (\rho_2 A_2 \omega^2 / E_2 I_{2a})^{1/4} \\
 j_{k2} &= N_2 \cot(k_{i21} L_2) & K_{22} &= E_2 I_{2b} / (\cos k_{f22} L_2 \cosh k_{f22} L_2 - 1) \\
 j_{l2} &= -N_2 \operatorname{cosec}(k_{i21} L_2) & k_{f22} &= (\rho_2 A_2 \omega^2 / E_2 I_{2b})^{1/4} \\
 & & L_2 &= E_2 A_2 k_{e21} \\
 & & k_{e21} &= (E_2 / \rho_2)^{1/2} \\
 & & N_2 &= G_2 J_2 k_{i21} \\
 & & k_{i21} &= (\kappa G_2 / \rho_2)^{1/2}, \\
 & & \kappa &= \text{Shape factor for non-circular section}
 \end{aligned}$$

B.3 Dynamic Stiffness Matrix for two perpendicular beams



The continuity conditions at joint 2-3:

$$u_2 = w_3, \theta_2 = \psi_3, v_2 = v_3,$$

$$\phi_2 = \phi_3, w_2 = -u_3, \psi_2 = -\theta_3$$

The equilibrium equations for the joint 2-3

$$F_{z2} - F_{x3} = 0; \quad F_{x2} + F_{z3} = 0;$$

$$F_{y2} + F_{y3} = 0; \quad M_{x2} + M_{z3} = 0;$$

$$M_{z2} - M_{x3} = 0; \quad M_{y2} + M_{y3} = 0;$$

The independent displacements:

$$w_1, \phi_1, w_2, \phi_2, v_1, \psi_1,$$

$$v_2, \psi_2, u_1, u_2, \theta_1, \theta_2,$$

$$w_4, \phi_4, v_4, \psi_4, u_4, \theta_4$$

$$F_{z2}-F_{z3}=0; \quad j_{b11}w_1-j_{d11}\phi_1+j_{a11}w_2-j_{c11}\phi_2-[j_{g2}(-w_2)+j_{h2}u_4]=0$$

$$F_{x_2} + F_{x_3} = 0; \quad j_{h1}u_1 + j_{g1}u_2 + [j_{a21}u_2 + j_{c21}\phi_2 + j_{b21}w_4 + j_{d21}\phi_4] = 0$$

$$F_{y_2} + F_{y_3} = 0; \quad j_{b12}v_1 - j_{d12}\psi_1 + j_{a12}v_2 - j_{c12}\psi_2 + [j_{a22}v_2 + j_{c22}\theta_2 + j_{b22}v_4 + j_{d22}\psi_4] = 0$$

$$M_{x2} + M_{z3} = 0; \quad j_{i1}\theta_1 + j_{k1}\theta_2 + [j_{c22}v_2 + j_{e22}\theta_2 - j_{d22}v_4 + j_{f22}\psi_4] = 0$$

$$M_{z2}-M_{x3}=0; \quad j_{d12}v_1+j_{f12}\psi_1-j_{c12}v_2+j_{e12}\psi_2-[j_{k2}(-\psi_2)+j_{l2}\theta_4]=0$$

$$M_{y_2} + M_{y_3} = 0; \quad j_{d11}w_1 + j_{f11}\phi_1 - j_{c11}\phi_2 + [j_{c21}u_2 + j_{e21}\phi_2 - j_{d21}w_4 + j_{f21}\phi_4] = 0$$

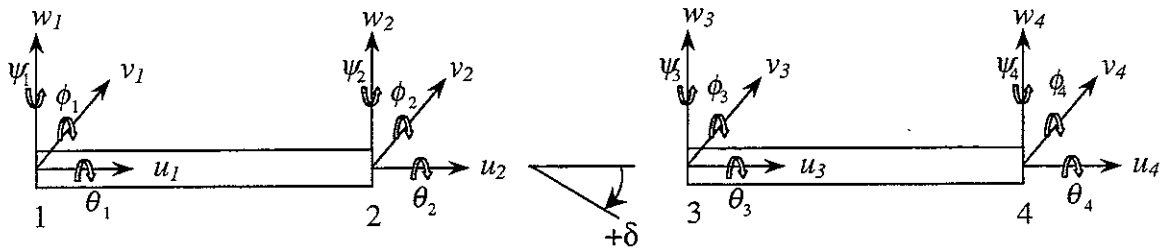
$$\mathbf{F} = \mathbf{K} \mathbf{u}$$

[illegible]

$$\mathbf{F}^T = \{F_{z1} \quad M_{y1} \quad F_{x2} - F_{x3} \quad M_{y2} + M_{y3} \quad F_{y1} \quad M_{z1} \quad F_{y2} + F_{y3} \quad M_{z2} - M_{z3} \quad F_{x1} \quad F_{x2} + F_{x3} \quad M_{x1} \quad M_{x2} + M_{x3} \quad F_{z4} \quad M_{y4} \quad F_{y4} \quad M_{z4} \quad F_{x4} \quad M_{x4}\}$$

$$\mathbf{u}^T = \{w_1 \quad \phi_1 \quad w_2 \quad \phi_2 \quad v_1 \quad \psi_1 \quad v_2 \quad \psi_2 \quad u_1 \quad u_2 \quad \theta_1 \quad \theta_2 \quad w_4 \quad \phi_4 \quad v_4 \quad \psi_4 \quad u_4 \quad \theta_4\}$$

B.4 Transformation Matrix \mathbf{T}_b for a coupled beam system



The continuity conditions at joint 2-3:

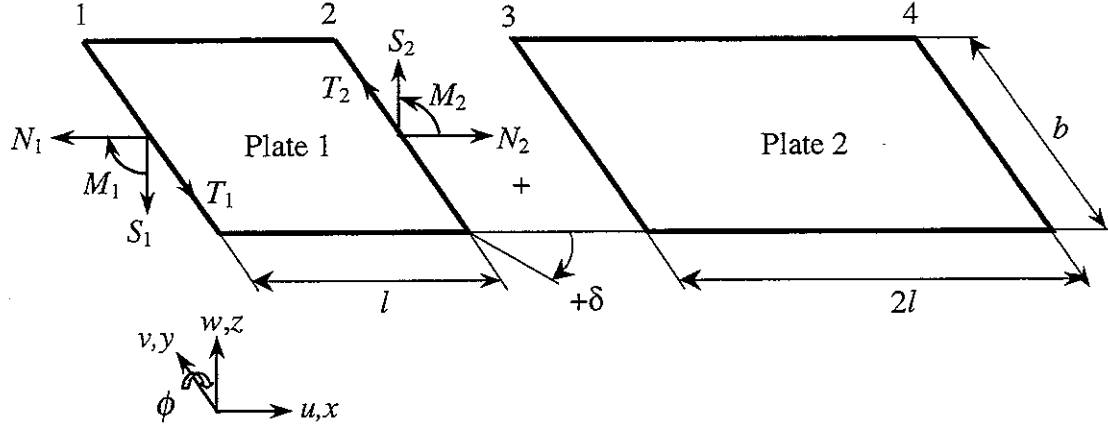
$$\begin{aligned} u_2 &= u_3 \cos \delta + w_3 \sin \delta, & \theta_2 &= \theta_3 \cos \delta + v_3 \sin \delta \\ w_2 &= -u_3 \sin \delta + w_3 \cos \delta, & \psi_2 &= -\theta_3 \sin \delta + v_3 \cos \delta \\ v_2 &= v_3, & \phi_2 &= \phi_3 \end{aligned}$$

The independent displacements:

$$\begin{array}{ccccccc} w_1, & \phi_1, & w_2, & \phi_2, & v_1, & \psi_1, & \\ v_2, & \psi_2, & u_1, & u_2, & \theta_1, & \theta_2, & \\ w_4, & \phi_4, & v_4, & \psi_4, & u_4, & \theta_4 & \end{array}$$

[illegible]

B.5 Dynamic Stiffness Matrix for a coupled plate system



For the flexural vibration for plate 1 and plate 2, $\mathbf{F}_{f1} = \mathbf{K}_{f1} \mathbf{u}_{f1}$ and $\mathbf{F}_{f2} = \mathbf{K}_{f2} \mathbf{u}_{f2}$ where

$$\mathbf{F}_{f1}^T = \{-S_1 \quad M_1 \quad S_2 \quad -M_2\}, \quad \mathbf{F}_{f2}^T = \{-S_3 \quad M_3 \quad S_4 \quad -M_4\},$$

$$\mathbf{u}_{f1}^T = \{w_1 \quad \phi_1 \quad w_2 \quad \phi_2\}, \quad \mathbf{u}_{f2}^T = \{w_3 \quad \phi_3 \quad w_4 \quad \phi_4\}$$

and the dynamic stiffness matrix for flexure, \mathbf{K}_{f1} and \mathbf{K}_{f2} , was defined from equation (4.41).

For the in-plane vibration for plate 1 and plate 2, $\mathbf{F}_{i1} = \mathbf{K}_{i1} \mathbf{u}_{i1}$ and $\mathbf{F}_{i2} = \mathbf{K}_{i2} \mathbf{u}_{i2}$ where

$$\mathbf{F}_{i1}^T = \{-N_1 \quad -T_1 \quad N_2 \quad T_2\}, \quad \mathbf{F}_{i2}^T = \{-N_3 \quad -T_3 \quad N_4 \quad T_4\},$$

$$\mathbf{u}_{i1}^T = \{u_1 \quad v_1 \quad u_2 \quad v_2\}, \quad \mathbf{u}_{i2}^T = \{u_3 \quad v_3 \quad u_4 \quad v_4\}$$

and the dynamic stiffness matrix for in-plane, \mathbf{K}_{i1} and \mathbf{K}_{i2} , was defined from equation (4.54).

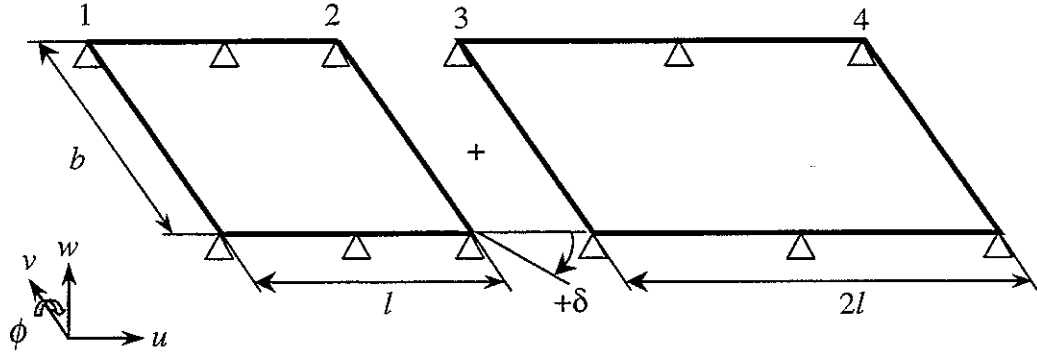
Assembling the dynamic stiffness matrices for flexure and in-plane and multiplying the transformation matrix in Appendix B.6, the force-displacement relationship for a coupled plate system can be obtained from.

$$\mathbf{F}_p = \mathbf{K}_p \mathbf{u}_p$$

where

$$\mathbf{F}_p = \mathbf{T}_p^T \begin{bmatrix} \mathbf{F}_{f1} \\ \mathbf{F}_{f2} \\ \mathbf{F}_{i1} \\ \mathbf{F}_{i2} \end{bmatrix}, \quad \mathbf{u}_p = \mathbf{T}_p^T \begin{bmatrix} \mathbf{u}_{f1} \\ \mathbf{u}_{f2} \\ \mathbf{u}_{i1} \\ \mathbf{u}_{i2} \end{bmatrix} \quad \text{and} \quad \mathbf{K}_p = \mathbf{T}_p^T \begin{bmatrix} \mathbf{K}_{f1} & 0 & 0 & 0 \\ 0 & \mathbf{K}_{f2} & 0 & 0 \\ 0 & 0 & \mathbf{K}_{i1} & 0 \\ 0 & 0 & 0 & \mathbf{K}_{i2} \end{bmatrix} \mathbf{T}_p.$$

B.6 Transformation Matrix \mathbf{T}_p for a coupled plate system



The continuity conditions at joint $x = l$:

$$w_2 = w_3 \cos \delta - u_3 \sin \delta, \quad u_2 = w_3 \sin \delta + u_3 \cos \delta, \quad v_2 = v_3, \quad \phi_2 = \phi_3$$

The independent displacements:

$$w_1, \phi_1, w_2, \phi_2, w_4, \phi_4, u_1, v_1, u_2, v_2, u_4, v_4$$

$$\mathbf{T}_p = \begin{bmatrix} 1 & . & . & . & . & . & . & . & . & . & . & . \\ . & 1 & . & . & . & . & . & . & . & . & . & . \\ . & . & 1 & . & . & . & . & . & . & . & . & . \\ . & . & . & 1 & . & . & . & . & . & . & . & . \\ . & . & \cos \delta & . & . & . & . & \sin \delta & . & . & . & . \\ . & . & . & 1 & . & . & . & . & . & . & . & . \\ . & . & . & . & 1 & . & . & . & . & . & . & . \\ . & . & . & . & . & 1 & . & . & . & . & . & . \\ . & . & . & . & . & . & 1 & . & . & . & . & . \\ . & . & . & . & . & . & . & 1 & . & . & . & . \\ . & . & . & . & . & . & . & . & 1 & . & . & . \\ . & . & . & . & . & . & . & . & . & 1 & . & . \\ . & . & . & . & . & . & . & . & . & . & 1 & . \\ . & . & . & . & . & . & . & . & . & . & . & 1 \end{bmatrix} \begin{matrix} w_1 \\ \phi_1 \\ w_2 \\ \phi_2 \\ w_3 \\ \phi_3 \\ w_4 \\ \phi_4 \\ u_1 \\ v_1 \\ u_2 \\ v_2 \\ u_3 \\ v_3 \\ u_4 \\ v_4 \end{matrix}$$

$$\mathbf{u}_p = \mathbf{T}_p^T \mathbf{u}_{(I+2)}$$

where $\mathbf{u}_p = \{w_2 \ \phi_1 \ w_2 \ \phi_2 \ w_4 \ \phi_4 \ u_1 \ v_1 \ u_2 \ v_2 \ u_4 \ v_4\}^T$ and

$$\mathbf{u}_{(I+2)} = \{w_1 \ \phi_1 \ w_2 \ \phi_2 \ w_3 \ \phi_3 \ w_4 \ \phi_4 \ u_1 \ v_1 \ u_2 \ v_2 \ u_3 \ v_3 \ u_4 \ v_4\}^T.$$

Appendix C Matlab programs

C.1 Couple beam system

C.2 Coupled plate system

```

=====
% = Vibrations for A Coupled Beam System =
% 23-Nov-98
% Programmed by Woo Sun Park
% -----
clear all; clc;

% Boundary Condition
disp(' > The Boundary Condition of System')
disp(' (1) Clamped')
disp(' (2) Free')
bc1=input('The Boundary Condition of Beam #1? ');
bc2=input('The Boundary Condition of Beam #2? ');

% Constants of Material and Geometry of Beam
disp(' >> Properties & Geometry')
% The hysteretic damping constant (mu) (=0 No damping)
mu1=input('The hysteretic damping constant (mu) of Beam 1 = ');
mu2=input('The hysteretic damping constant (mu) of Beam 2 = ');
E1=input('Young's Modulus of beam 1 [N/m^2] = ');
E2=input('Young's Modulus of beam 2 [N/m^2] = ');
nu1=input('Poisson's ratio of beam 1 = ');
nu2=input('Poisson's ratio of beam 2 = ');
G1=E1/(2*(1+nu1)); G2=E2/(2*(1+nu2));
rho1=input('Material density of beam 1 [kg/m^3] = ');
rho2=input('Material density of beam 2 [kg/m^3] = ');
l1=input('The length of beam 1 [mm] = '); l1=l1/1000;
l2=input('The length of beam 2 [mm] = '); l2=l2/1000;

% Beam Cross-section
disp(' >>> Cross-section type of the Beams')
disp(' 1. Circular')
disp(' 2. Rectangular')
cs1=input(' Select a Beam Cross-section Type of the Beam #1? ');
cs2=input(' Select a Beam Cross-section Type of the Beam #2? ');
if cs1 == 1 & cs2 == 1;
    radius1=input('Radius of Beam #1[mm]? '); radius1=radius1/1000;
    radius2=input('Radius of Beam #2[mm]? '); radius2=radius2/1000;
    A1=pi*radius1^2; % The cross-sectional area of beam [m^2]
    I1a=pi*radius1^4/4; % The second moment of area of the cross-section [m^4]
    I1b=I1a; % The polar second moment of inertia [m^4]
    J01=pi*radius1^4/2; % Mass moment of inertia of beam1
    A2=pi*radius2^2; % Mass moment of inertia of beam2
    I2a=pi*radius2^4/4; % Mass moment of inertia of beam1
    I2b=I2a; % Mass moment of inertia of beam2
    J02=pi*radius2^4/2; % Mass moment of inertia of beam1
    m1=rho1*A1*l1; m2=rho2*A2*l2; % Mass moment of inertia of beam1
    Im1=m1*radius1^2/2; % Mass moment of inertia of beam1
    Im2=m2*radius2^2/2; % Mass moment of inertia of beam1
    k=1; % k= the shape factor for cross-section
elseif cs1 == 2 & cs2 == 2;
    bbl=input('The width of beam section #1[mm]? '); bbl=bbl/1000;
    hbl=input('The height of beam section #1[mm]? '); hbl=hbl/1000;
    A1=bbl*hbl; % The cross-sectional area of beam [m^2]
    I1a=bbl*hbl^3/12; % The second moment of area about yz plane [m^4]
    I1b=bbl*hbl^3/12; % The second moment of area about xy plane [m^4]
    J01=A1*(bbl^2+hbl^2)/12; % The polar second moment of inertia [m^4]
    b2=input('The width of beam section #2[mm]? '); b2=b2/1000;
    h2=input('The height of beam section #2[mm]? '); h2=h2/1000;
    A2=b2*h2; % The cross-sectional area of beam [m^2]
    I2a=b2*h2^3/12; % The second moment of area about yz plane [m^4]
    I2b=b2*h2^3/12; % The second moment of area about xy plane [m^4]
    J02=A2*(b2^2+h2^2)/12; % The polar second moment of inertia [m^4]
    m2=rho2*A2*l2; % Mass moment of inertia of beam2
    Im2=m2*radius2^2/2; % Mass moment of inertia of beam2
    k=1; % k= the shape factor for cross-section
end

I2b=hbl^2*bb2^3/12;
J02=A2*(bb2^2+hh2^2)/12;
m1=rho1*A1*l1; m2=rho2*A2*l2; % Mass moment of inertia of beam1
Im1=m1*(bbl^2+hh1^2)/12; % Mass moment of inertia of beam2
Im2=m2*(bb2^2+hh2^2)/12; % Mass moment of inertia of beam2
k=5/6; % k= the shape factor for cross-section
end

% An arbitrary angle of coupling of two beams
angle=input('The angle of coupling of beam 2 [clockwise] = ');
theta=angle*pi/180; % Radian

% Initializing vectors
i=0;
Psum1=0; Psub11=0; Psub12=0; Psumin1=0;
Psum2=0; Psub21=0; Psub22=0; Psumin2=0;

% Frequency Range
fmin=input('The number of minimum frequency as decade 10^(fmin) = ');
fmax=input('The number of maximum frequency as decade 10^(fmax) = ');
fnum=input('The number of frequency points between decades = ');
ff=logspace(fmin,fmax,fnum);
w=2*pi*ff;

xstep=input(' *** xstep for energy calculation [mm] = '); xstep=xstep/1000;

for f=ff
    i=i+1;

    % The Dynamic Stiffness Matrix of Beam 1
    K1=dsbeam1(E1,G1,rho1,I1a,I1b,J01,A1,l1,k,f);
    % The Dynamic Stiffness Matrix of Beam 2
    K2=dsbeam1(E2,G2,rho2,I2a,I2b,J02,A2,l2,k,f);

    % The Total Dynamic Stiffness Matrix [K=K1+K2]
    [J,T]=dsbeamasm(K1,K2,theta);

    % Clamped Beam & Free Beam connected at 90 degree
    %
    if bc1 == 1
        if bc2 == 2
            % The forced Response at node 2
            % Flexural + Extensional Vibration (Vertical)
            J11=[3,4,10,i3,i4,i7];
            J1=J(J11,J11);
            F1=[0 0 0 1 0 0]'; % Fz4=IN(unit force)
            V1=inv(J1)*F1; % Displacement vector
            K11=[3,4,10];
            F11=K1(K11,K11)*V1(1:3); F11w(i)=F11(1); F11b(i)=F11(2); F11u(i)=F11(3);
            F13=K2(K23,K23)*V1(1:3); % Force check F11 ~ F13 because K is not the same
            w2(i)=V1(1); % w2
            b2(i)=V1(2); % beta 2
            u2(i)=V1(3); % u2
            w4(i)=V1(4); % w4
            b4(i)=V1(5); % beta 4
            u4(i)=V1(6); % u4

            % Flexural + Torsional Vibration (lateral)
            J22=[7,8,12,i5,i6,i8];
            J2=J(J22,J22);
            F2=[0 0 0 1 0 0]'; % Fy4=IN(unit force)
        end
    end
end

```

```

V2=inv(J2)*F2; % Displacement vector
K22=[7,8,12];
F12=x1(K22,K22)*V2(1:3); F12v(i)=F12(1); F12g(i)=F12(2); F12a(i)=F12(3);
v2(i)=V2(1); % v2
g2(i)=V2(2); % gamma 2
a2(i)=V2(3); % alpha 2
v4(i)=V2(4); % v4
g4(i)=V2(5); % gamma 4
a4(i)=V2(6); % alpha 4

=====
% The forced response along x-axis
% 1. Vertical force (Fy4 = 1)
% 1) The vertical bending response W1 along X-axis of Beam 1
% W(x)=B1*sin(lambda*x)+B2*cos(lambda*x)+B3*sinh(lambda*x)+B4*cosh(lambda*x)
vv1=[0, 0, w2(i), b2(i)];
[r1,d2r1dx2]=resplcx2(f,vv1,rho1,A1,E1,I1a,11,xstep); z1(:,i)=r1;
% 2) The extensional response U1 along X-axis of Beam 1
% U(x)=B5*sin(w*x/c1)+B6*cos(w*x/c1)
vv2=[0, u2(i)];
[r2,dr2dx1]=resplcx2(f,vv2,rho1,E1,11,xstep); x1(:,i)=r2;
% 3) The vertical bending response W2 along X-axis of Beam 2
vv3=[w2(i)*cos(theta)+u2(i)*sin(theta), b2(i), w4(i), b4(i)];
[r3,d2r3dx2]=resplcx2(f,vv3,rho2,A2,E2,I2a,12,xstep); z2(:,i)=r3;
% 4) The extensional response U2 along X-axis of Beam 2
vv4=[-w2(i)*sin(theta)+u2(i)*cos(theta), u4(i)];
[r4,dr4dx1]=resplcx2(f,vv4,rho2,E2,12,xstep); x2(:,i)=r4;
% 5) The lateral bending response V1 along X-axis of Beam 1
vv5=[0, 0, v2(i), g2(i)];
[r5,dr5dx2]=resplcx2(f,vv5,rho1,A1,E1,I1b,11,xstep); y1(:,i)=r5;
% 6) The torsional response Alpha1 along X-axis of Beam 1
% Theta(x)=B7*sin(w*x/C2)+B8*cos(w*x/C2)
vv6=[0, a2(i)];
[r6,dr6dx1]=resplcx2(f,vv6,rho1,G1,11,k,xstep); t1(:,i)=r6;
% 7) The lateral bending response V2 along X-axis of Beam 2
vv7=[v2(i), a2(i)*sin(theta)+g2(i)*cos(theta), v4(i), g4(i)];
[r7,dr7dx2]=resplcx2(f,vv7,rho2,A2,E2,I2b,12,xstep); y2(:,i)=r7;
% 8) The torsional response Alpha2 along X-axis of Beam 2
vv8=[-g2(i)*sin(theta)+a2(i)*cos(theta), a4(i)];
[r8,dr8dx1]=resplcx2(f,vv8,rho2,G2,12,k,xstep); t2(:,i)=r8;
% Energy for Force 1 = Fx4
% SEl=(1/2)*(E*I^1/N)*SUM(abs((dw2/dx2)^2))+(E*A^1/N)*SUM(abs((du/dx)^2))
% Power1 = mul*w*(SE1)
%
x1=xstep/2:xstep:11-(xstep/2); x2=xstep/2:xstep:12-(xstep/2);
% 1. Vertical force
% Beam 1
SEBeam1=sum(abs(d2r1dx2.^2));
SEBeam11=SEBeam1*real(E1)*I1a*11/(2*length(x1));
SEBeam12=sum(abs(dr2dx.^2));
SEBeam13=SEBeam1*real(E1)*A1*11/(2*length(x1));
SE11(i)=SEBeam1+SEBeam12;
% Beam 2
SEBeam13=sum(abs(d2r3dx2.^2));
SEBeam13=SEBeam13*real(E2)*I2a*12/(2*length(x2));
SEBeam14=sum(abs(dr4dx.^2));
SEBeam14=SEBeam14*real(E2)*A2*12/(2*length(x2));
SE12(i)=SEBeam13+SEBeam14;

```

```

% Total Energy and Dissipated Power for Fx4 = 1N
Pbeam1=w(i)*mul*(SEBeam11+SEBeam12); Pd1(i)=Pbeam1;
Pbeam12=w(i)*mul2*(SEBeam13+SEBeam14); Pd12(i)=Pbeam12;
Psub11=Psub11+Pbeam11;
Psub12=Psub12+Pbeam12;
Psub1=Pbeam11+Pbeam12;
Psum1=Psum1+Psub1;
Pd1(i)=Psub1;
% Input power from Fz4=F1(4)=1N at Node 4
Powerin1=real(F1(4))*(j*w(i)*w4(i))/2; Pin1(i)=Powerin1;
Psumin1=Psumin1+Powerin1;

=====
% Energy for Force 2 = Fy4
% SE2=(1/2)*(E*I^1/N)*SUM(abs((dv2/dx2)^2))+(G*J^1/N)*SUM(abs((d theta/dx)^2))
% Power2 = mul2*w*(SE2)
% Beam 1
SEBeam1=sum(abs(d2r5dx2.^2));
SEBeam11=SEBeam1*real(E1)*I1b*11/(2*length(x1));
SEBeam22=sum(abs(dr6dx.^2));
SEBeam22=SEBeam22*real(G1)*J01*11/(2*length(x1));
SE21(i)=SEBeam1+SEBeam22;
% Beam 2
SEBeam23=sum(abs(d2r7dx2.^2));
SEBeam23=SEBeam23*real(E2)*I2b*12/(2*length(x2));
SEBeam24=sum(abs(dr8dx.^2));
SEBeam24=SEBeam24*real(G2)*J02*12/(2*length(x2));
SE22(i)=SEBeam23+SEBeam24;
% Total Energy and Dissipated Power for Fy4 = 1N
Pbeam21=w(i)*mul*(SEBeam21+SEBeam22); Pd21(i)=Pbeam21;
Pbeam22=w(i)*mul2*(SEBeam23+SEBeam24); Pd22(i)=Pbeam22;
Psub21=Psub21+Pbeam21;
Psub22=Psub22+Pbeam22;
Psub2=Pbeam21+Pbeam22;
Psum2=Psum2+Psub2;
Pd2(i)=Psub2;
% Input power from Fy4 = 1N at Node 4
Powerin2=real(F2(4))*(j*w(i)*v4(i))/2; Pin2(i)=Powerin2;
Psumin2=Psumin2+Powerin2;
% The area of energy and power
n=length(ff);
Ptot1=sum((ff(1:nf)-ff(1:nf-1))/2.*(Pd11(2:nf)+Pd11(1:nf-1)));
Ptot12=sum((ff(2:nf)-ff(1:nf-1))/2.*(Pd12(2:nf)+Pd12(1:nf-1)));
Ptotin1=sum((ff(2:nf)-ff(1:nf-1))/2.*(Pin1(2:nf)+Pin1(1:nf-1)));
Ptottr211=sum((ff(2:nf)-ff(1:nf-1))/2.*(Ptr211(2:nf)+Ptr211(1:nf-1)));
Ptot21=sum((ff(2:nf)-ff(1:nf-1))/2.*(Pd21(2:nf)+Pd21(1:nf-1)));
Ptot22=sum((ff(2:nf)-ff(1:nf-1))/2.*(Pd22(2:nf)+Pd22(1:nf-1)));
Ptotin2=sum((ff(2:nf)-ff(1:nf-1))/2.*(Pin2(2:nf)+Pin2(1:nf-1)));
Ptottr212=sum((ff(2:nf)-ff(1:nf-1))/2.*(Ptr212(2:nf)+Ptr212(1:nf-1)));
% Plot of the dissipated power and input power
figure
subplot(2,1,1); loglog(ff,Pd11,'-',ff,Pd12,'--',ff,P1,ff,Pin1,'-',') % Power
[Nm/sec]
title(' The Power of Beam System due to a unit vertical force')
xlabel('Power/Force^2 [Watt/N^2]'); ylabel('Frequency [Hz]');
legend('Pdiss1','Pdiss2','Pdiss1+Pdiss2','Pin',2);

```

```

subplot(2,1,2); loglog(ff,pd21,'-',ff,pd22,'--',ff,p2,ff,pin2,'-o') % Power
[Nm/sec]
title('The Power of Beam System due to a unit lateral force')
xlabel('Frequency [Hz]'); ylabel('Power/Force^2 [Watt/N^2]')
legend('pdiss1','pdiss2','pdiss1+pdiss2','pin',2);
%-----

```

```

function K=dsmbeam(E,G,rho,IL,I2,J0,A,1,k,f)

% Dynamic Stiffness Matrix for a Single Beam: [K]
% [f] = [K] [v]
% [f1]=[Fz1, My1, Fz2, My2, Fy1, Mz1, Fy2, Mz2, Fx1, Fx2, Mx1, Mx2]';
% [v1]=[w1, b1, w2, b2, v1, c1, v2, c2, u1, u2, a1, a2]';
% [v2]=[w3, b3, w4, b4, v3, c3, v4, c4, u3, u4, a3, a4]';
w=2*pi*f;
% Flexure xz plane - Vertical Bending
kf1=(rho*A*w^2/(E*I1))^(1/4);
thetal=kf1;
Dz1=[0,1,0,1; kf1,0,kf1,0; sin(thetal),cos(thetal),sinh(thetal),cosh(thetal);
      kf1*cos(thetal),-kf1*sin(thetal),kf1*cosh(thetal),kf1*sinh(thetal)];
Dz2=E*I1*kf1^2*[-kf1,0,kf1,0; 0,1,0,-1;
               kf1*cos(thetal),-kf1*sin(thetal),-kf1*cosh(thetal),-kf1*sinh(thetal);
               -sin(thetal),-cos(thetal),sinh(thetal),cosh(thetal)];
Kfz=Dz2*inv(Dz1);

% Flexure xy plane - Lateral Bending
kf2=(rho*A*w^2/(E*I2))^(1/4);
thetal=kf2;
Dy1=[0,1,0,1; kf2,0,kf2,0; sin(thetal),cos(thetal),sinh(thetal),cosh(thetal);
      kf2*cos(thetal),-kf2*sin(thetal),kf2*cosh(thetal),kf2*sinh(thetal)];
Dy2=E*I2*kf2^2*[-kf2,0,kf2,0; 0,1,0,-1;
               kf2*cos(thetal),-kf2*sin(thetal),-kf2*cosh(thetal),-kf2*sinh(thetal);
               -sin(thetal),-cos(thetal),sinh(thetal),cosh(thetal)];
Kfy=Dy2*inv(Dy1);

% Extension
c1=sqrt(E/rho); ke=w/c1;
thetal3=ke;
D3=[0,1; sin(thetal3),cos(thetal3)];
D4=E*A*ke*[-1,0; cos(thetal3),-sin(thetal3)];
Ke=D4*inv(D3);

% Torsion
c2=sqrt(k*g/rho); kt=w/c2;
thetal4=kt;
D5=[0,1; sin(thetal4),cos(thetal4)];
D6=G*J0*kt*[-1,0; cos(thetal4),-sin(thetal4)];
Kt=D6*inv(D5);

M4=zeros(4);
Kf={kfz N4; Kfy};
K={kf zeros(8,4);
  zeros(2,8) Ke zeros(2);
  zeros(2,10) Kt};

```

```

function [J,T]=dsbeamasm(K1,K2,theta)
%=====
% Assembling the Dynamic Stiffness Matrix of Euler-Bernoulli Beam Systems =
%=====
%=====
% Dynamic Stiffness Matrix: [K] for a single Beam
%=====
% [f] = [K] [v]
% [f1]=[Fz1, My1, Fz2, My2, Fy1, Mz1, Fy2, Mz2, Fx1, Fx2, Mx1, Mx2]';
% [v1]=[w1, b1, w2, b2, v1, c1, v2, c2, u1, u2, a1, a2]';
% [f2]=[Fz3, My3, Fz4, My4, Fy3, Mz3, Fy4, Mz4, Fx3, Fx4, Mx3, Mx4]';
% [v2]=[w3, b3, w4, b4, v3, c3, v4, c4, u3, u4, a3, a4]';
%=====
% Dynamic Stiffness Matrix: [J] (18 x 18) for a Coupled Beam System
%=====
% [f] = [J] [v] = ([T1]*([K1]+[K2])*[T]) [v]
%=====
A=zeros(12);
K12=[K1,A; A,K2]; % Total Dynamic Stiffness Matrix for Beam 1 and 2 {24x24}
%=====
% TRANSFORMATION MATRIX [Tb]
%=====
% Coupled with arbitrary angle (theta; +clockwise) in Global X-Z Plane
c=cos(theta); s=sin(theta);
T=[1 2 3 4 5 6 7 8 9 0 1 2 3 4 5 6 7 8
   0 1 0 0 0 0 0 0 0 0 0 0 0 0 0 0 0 0; % 1
   0 0 1 0 0 0 0 0 0 0 0 0 0 0 0 0 0 0; % 2
   0 0 0 1 0 0 0 0 0 0 0 0 0 0 0 0 0 0; % 3
   0 0 0 0 1 0 0 0 0 0 0 0 0 0 0 0 0 0; % 4
   0 0 0 0 0 1 0 0 0 0 0 0 0 0 0 0 0 0; % 5
   0 0 0 0 0 0 1 0 0 0 0 0 0 0 0 0 0 0; % 6
   0 0 0 0 0 0 0 1 0 0 0 0 0 0 0 0 0 0; % 7
   0 0 0 0 0 0 0 0 1 0 0 0 0 0 0 0 0 0; % 8
   0 0 0 0 0 0 0 0 0 1 0 0 0 0 0 0 0 0; % 9
   0 0 0 0 0 0 0 0 0 0 1 0 0 0 0 0 0 0; % 10
   0 0 0 0 0 0 0 0 0 0 0 1 0 0 0 0 0 0; % 11
   0 0 0 0 0 0 0 0 0 0 0 0 1 0 0 0 0 0; % 12
   0 0 c 0 0 0 0 0 0 0 0 s 0 0 0 0 0 0; % 13
   0 0 0 1 0 0 0 0 0 0 0 0 0 0 0 0 0 0; % 14
   0 0 0 0 0 0 0 0 0 0 0 0 0 0 0 0 0 0; % 15
   0 0 0 0 0 0 0 0 0 0 0 0 0 0 0 0 0 0; % 16
   0 0 0 0 0 0 0 0 0 0 0 0 0 0 0 0 0 0; % 17
   0 0 0 0 0 0 0 0 0 0 0 0 0 0 0 0 0 0; % 18
   0 0 0 0 0 0 0 0 0 0 0 0 0 0 0 0 0 0; % 19
   0 0 0 0 0 0 0 0 0 0 0 0 0 0 0 0 0 0; % 20
   0 0 -s 0 0 0 0 0 0 0 0 c 0 0 0 0 0 0; % 21
   0 0 0 0 0 0 0 0 0 0 0 0 0 0 0 0 0 0; % 22
   0 0 0 0 0 0 0 0 -s 0 0 0 0 c 0 0 0 0; % 23
   0 0 0 0 0 0 0 0 0 0 0 0 0 0 0 0 0 0; % 24
];
J=T'*K12*T; % Assembled Dynamic Stiffness Matrix for Beam 1 and 2
%

```

```

%=====
% Build the Dynamic Stiffness Matrix: [Kd]
%=====
% The Flexural Wavenumber
k1=(w^2*rho1/D1)^(1/4); %Plate free bending wavenumber (kb)
k2=(w^2*rho2/D2)^(1/4);

kn11=(kn1^2+k1^2)^(1/2); kf11(i)=kn11; kn12=-(kn1^2+k1^2)^(1/2); kf12(i)=kn12;
kn13=(kn1^2-k1^2)^(1/2); kf13(i)=kn13; kn14=-(kn1^2-k1^2)^(1/2); kf14(i)=kn14;
kn21=(kn2^2+k2^2)^(1/2); kf21(i)=kn21; kn22=-(kn2^2+k2^2)^(1/2); kf22(i)=kn22;
kn23=(kn2^2-k2^2)^(1/2); kf23(i)=kn23; kn24=-(kn2^2-k2^2)^(1/2); kf24(i)=kn24;

if inplane == 1
% The In-plane Wavenumber
% Plate 1
kL1=sqrt(2*rho01*w^2*(1-nu1^2)/E1); %Longitudinal
kT1=sqrt(2*rho01*w^2*(1+nu1)/E1); %Transverse
lambda11=(kn1^2-kL1^2)^(1/2); ki11(i)=lambda11;
lambda12=-(kn1^2-kL1^2)^(1/2); ki12(i)=lambda12;
lambda13=(kn1^2-kT1^2)^(1/2); ki13(i)=lambda13;
lambda14=-(kn1^2-kT1^2)^(1/2); ki14(i)=lambda14;
% Plate 2
kL2=sqrt(2*rho02*w^2*(1-nu2^2)/E2); %Longitudinal
kT2=sqrt(2*rho02*w^2*(1+nu2)/E2); %Transverse
lambda21=(kn2^2-kL2^2)^(1/2); ki21(i)=lambda21;
lambda22=-(kn2^2-kL2^2)^(1/2); ki22(i)=lambda22;
lambda23=(kn2^2-kT2^2)^(1/2); ki23(i)=lambda23;
lambda24=-(kn2^2-kT2^2)^(1/2); ki24(i)=lambda24;
end

% Matrix [pLn]
% Plate 1
pLn1=[
    1      kn1      1      1      1      1;
    exp(kn1*iL1) exp(kn12*L1) exp(kn13*L1) exp(kn14*L1);
% Plate 2
    kn11*exp(kn11*L1) kn12*exp(kn12*L1) kn13*exp(kn13*L1) kn14*exp(kn14*L1)];
pLn2=[
    kn21      kn22      kn23      kn24;
    exp(kn21*L2) exp(kn22*L2) exp(kn23*L2) exp(kn24*L2);
    kn21*exp(kn21*L2) kn22*exp(kn22*L2) kn23*exp(kn23*L2) kn24*exp(kn24*L2)];

% Matrix [p2n]
% Plate 1
p2111=kn11^3-(2-nu1)*kn1^2*kn11; p2121=kn12^3-(2-nu1)*kn1^2*kn12;
p2131=kn13^3-(2-nu1)*kn1^2*kn13; p2141=kn14^3-(2-nu1)*kn1^2*kn14;
p2211=-kn11^2*nu1*kn1^2; p2221=-kn12^2*nu1*kn1^2;
p2231=-kn13^2*nu1*kn1^2; p2241=-kn14^2*nu1*kn1^2;
p2311=-kn11^3*exp(kn11*L1)+(2-nu1)*kn1^2*kn11*exp(kn11*L1);
p2321=-kn12^3*exp(kn12*L1)+(2-nu1)*kn1^2*kn12*exp(kn12*L1);
p2331=-kn13^3*exp(kn13*L1)+(2-nu1)*kn1^2*kn13*exp(kn13*L1);
p2341=-kn14^3*exp(kn14*L1)+(2-nu1)*kn1^2*kn14*exp(kn14*L1);
p2411=kn11^2*exp(kn11*L1)-nu1*kn1^2*exp(kn11*L1);
p2421=kn12^2*exp(kn12*L1)-nu1*kn1^2*exp(kn12*L1);
p2431=kn13^2*exp(kn13*L1)-nu1*kn1^2*exp(kn13*L1);
p2441=kn14^2*exp(kn14*L1)-nu1*kn1^2*exp(kn14*L1);
p2n1=D1*[ p2111, p2121, p2131, p2141;
           p2211, p2221, p2231, p2241;
           p2311, p2321, p2331, p2341;
           p2411, p2421, p2431, p2441 ];

```

```

%=====
% Vibrations for A Coupled Plate System =
%=====
% 30-Sep-99
% Programmed by Woo Sun Park
%=====
clear all; clc;
% Constants of Material and Geometry of Plate
disp(' >> Properties & Geometry ')
angle=input('The angle of assembling of Plate 2 [clockwise+]= '); %angle=90;
theta=angle*pi/180; % degree -> radian
% Material Property
% Plate 1
mu1=input('The hysteretic damping constant(mu) of Plate 1 = ');
EI=input('Young's Modulus (N/m^2) = ');
nu1=input('Poisson's ratio = ');
L1=input('The length of plate 1 [m] = ');
b1=input('The width of plate 1 [m] = ');
A1=L1*b1; %the surface area [m^2]
h1=input('The thickness of plate [m] = ');
rho01=input('The Material density [kg/m^3] = ');
rho1=rho01*h1 % the mass of the plate per unit surface area [kg/m^2]
% Plate 2
L2=input('The length of plate 2 [m] = ');
mu2=mu1; E2=E1; nu2=nu1; b2=b1; A2=L2*b2; h2=h1; rho02=rho01; rho2=rho02*h2;
D1=E1*h1^3/(12*(1-nu1^2)); D2=E2*h2^3/(12*(1-nu2^2)); %D=the flexural rigidity
G1=E1/(2*(1+nu1)); G2=E2/(2*(1+nu2)); %G=Shear Modulus
gamma1=(1+nu1)/(1-nu1); gamma2=(1+nu2)/(1-nu2);
% Frequency Range
fmin=input('The number of minimum frequency as decade 10^(fmin) = ');
fmax=input('The number of maximum frequency as decade 10^(fmax) = ');
fnum=input('The number of frequency points between decades = ');
ff=logspace(fmin,fmax,fnum);

inplane=input('Include In-plane Vibration ? [No=0, Yes=1] ');
% Applying Input Force(N) Vector (Global)
if inplane == 1
    F0=[1, zeros(1,11)]'; % Vertical Force at the left-hand edge
else
    if angle == 0
        F0=[1, zeros(1,5)]'; % Vertical Force at the left-hand edge only
    else
        F0=[1, zeros(1,4)]'; % Vertical Force at the left-hand edge only
    end
end

m=input('The number of Fourier components [m] = ');
% Displacement step
xstep=input(' *** xstep [mm]= '); xstep=xstep/1000; %increment of x
ystep=input(' *** ystep [mm]= '); ystep=ystep/1000; %increment of y

i=0;
for f=ff
    i=i+1;
    w=2*pi*f;
    SEf1tot=0; SEf2tot=0; SEi1tot=0; SEi2tot=0; Pinsumf=0; Pinsumi=0;
    for n=1:2:m; % The number of half-range Fourier components
        kn1=n*pi/b1; kn2=n*pi/b2;

```

```

if L1 <= L2
    cor1=[exp(-kn11*L1) 0 0 0; 0 1 0 0; 0 0 exp(-kn13*L1) 0; 0 0 0 1];
    if inplane == 1
        cor2=[exp(-lambda11*L1) 0 0 0; 0 1 0 0; 0 0 exp(-lambda13*L1) 0; 0 0 0 1];
    else
        L1 > L2
        cor1=[exp(-kn21*L2) 0 0 0; 0 1 0 0; 0 0 exp(-kn23*L2) 0; 0 0 0 1];
        if inplane == 1
            cor2=[exp(-lambda21*L2) 0 0 0; 0 1 0 0; 0 0 exp(-lambda23*L2) 0; 0 0 0 1];
        else
            p1n1=p1n1*cor1; p1n2=p1n2*cor1;
            p2n1=p2n1*cor1; p2n2=p2n2*cor1;
            if inplane == 1
                r1n1=r1n1*cor2; r1n2=r1n2*cor2;
                r2n1=r2n1*cor2; r2n2=r2n2*cor2;
            end
        end
    end

% Dynamic Stiffness Matrix [Kd] for each plate
if inplane == 1
    Kdfl=p2n1*inv(p1n1); Kdf2=p2n2*inv(p1n2); % Flexural
    Kdli=r2n1*inv(r1n1); Kdi2=r2n2*inv(r1n2); % In-plane
else
    Kdfl=p2n1*inv(p1n1); Kdf2=p2n2*inv(p1n2); % Flexural only
end

N4=zeros(4); N8=zeros(8); c=cos(theta); s=sin(theta);

% Transformation Matrix T2 [16x12]
T2=[ 1 0 0 0 0 0 0 0 0 0 0 0;
     0 1 0 0 0 0 0 0 0 0 0 0;
     0 0 1 0 0 0 0 0 0 0 0 0;
     0 0 0 1 0 0 0 0 0 0 0 0;
     0 0 0 0 1 0 0 0 0 0 0 0;
     0 0 0 0 0 1 0 0 0 0 0 0;
     0 0 0 0 0 0 1 0 0 0 0 0;
     0 0 0 0 0 0 0 1 0 0 0 0;
     0 0 -s 0 0 0 0 0 0 c 0 0 0;
     0 0 0 0 0 0 0 0 0 0 1 0;
     0 0 0 0 0 0 0 0 0 0 0 1;
     0 0 0 0 0 0 0 0 0 0 0 0];

if angle == 0
    % Transformation Matrix T1 [8 x 6]
    T1=[ 1 0 0 0 0 0;
         0 1 0 0 0 0;
         0 0 1 0 0 0;
         0 0 0 1 0 0;
         0 0 0 0 1 0;
         0 0 0 0 0 1];
else
    % Transformation Matrix T1 [8 x 5] - Considering Constraint
    T1=[ 1 0 0 0 0;
         0 1 0 0 0;
         0 0 1 0 0;
         0 0 0 1 0;
         0 0 0 0 1;
         0 0 0 0 0];
end

% Remove the singularity in Matrix Inversion
if L1 >= b1 | L2 >= b2

```

```

T1=[ 1 0 0 0 0 0 ; % w1
0 1 0 0 0 0 ; % theta 1
0 0 0 0 0 0 ; % w2
0 0 0 1 0 0 ; % theta 2
0 0 0 0 0 0 ; % w3
0 0 0 1 0 0 ; % theta 3
0 0 0 0 1 0 ; % w4
0 0 0 0 0 1 ; % theta 4
end

% Inclusion of In-plane Vibration
if inplane == 1
    Kdf12=[Kdf1, N4; N4, Kdf2]; % Dynamic Stiffness Matrix for Flexure
    Kdf12=[Kdf1, N4; N4, Kdf2]; % Dynamic Stiffness Matrix for In-plane
    Kdf12=[Kdf12, N8; N8, Kdf12]; % Total Dynamic Stiffness Matrix
    Kd=T2.*Kdf12*T2; % Reduced Dynamic Stiffness Matrix
else
    % Flexural only
    Kdf12=[Kdf1, N4; N4, Kdf2]; % Dynamic Stiffness Matrix for Flexure
    Kdf12=[Kdf12, N8; N8, Kdf12]; % Total Dynamic Stiffness Matrix
    Kd=T1.*Kdf12*T1; % Reduced Dynamic Stiffness Matrix
end

% Natural Frequency
DK=det(inv(Kd)); mag(l)=abs(DK);
phase=atan2(imag(DK), real(DK))*180/pi; % radian => degree
phi(l)=phase;

% === Forced Response ===
F=2*F0/b1*sin(n*pi/2); % Concentrated Force at the centre of left-hand side edge
if inplane == 1
    W=T2*(inv(Kd)*F); % Displacement vector [Flexural + In-plane]
    if L1 >= b1 | L2 >= b2
        Ann1=cor1*inv(p1n1)*W(1:4); Ann2=cor1*inv(p1n2)*W(5:8);
        Cnn1=cor2*inv(r1n1)*W(9:12); Cnn2=cor2*inv(r1n2)*W(13:16);
    else
        Ann1=inv(p1n1)*W(1:4); Ann2=inv(p1n2)*W(5:8);
        Cnn1=inv(r1n1)*W(9:12); Cnn2=inv(r1n2)*W(13:16);
    end

    Xn0=Ann1.*[1 1 1 1]';
    Un0=Cnn1.*[lambda11 lambda12 kn1 kn1]';
    Vn0=Cnn1.*[kn1 kn1 lambda13 lambda14]';
else
    W=T1*(inv(Kd)*F); % Displacement vector [Flexural only]
    if L1 >= b1 | L2 >= b2
        Ann1=cor1*inv(p1n1)*W(1:4); Ann2=cor1*inv(p1n2)*W(5:8);
    else
        Ann1=inv(p1n1)*W(1:4); Ann2=inv(p1n2)*W(5:8);
    end

    Xn0=Ann1.*[1 1 1 1]';
end

% Integrate over x
x1=xstep/2:xstep:L1-xstep/2;
Xn1=Ann1(1)*exp(kn1*x1)+Ann1(2)*exp(kn12*x1)+Ann1(3)*exp(kn13*x1)+exp(k
n14*x1);
dXdX1=Ann1(1)*kn1*exp(kn1*x1)+Ann1(2)*kn12*exp(kn12*x1)+Ann1(3)*kn13*exp(kn13*
x1)+Ann1(4)*kn14*exp(kn14*x1); %Xn1
d2XdX1=Ann1(1)*kn1^2*exp(kn1*x1)+Ann1(2)*kn12^2*exp(kn12*x1)+Ann1(3)*kn13^2*ex
p(kn13*x1)+Ann1(4)*kn14^2*exp(kn14*x1); %Xn1

```

```

dXdX12=dXdX1.^2; d2XdX12=d2XdX1.^2;

x2=xstep/2:xstep:L2-xstep/2;
Xn2=Ann2(1)*exp(kn21*x2)+Ann2(2)*exp(kn22*x2)+Ann2(3)*exp(kn23*x2)+exp(k
n24*x2);
dXdX2=Ann2(1)*kn21*exp(kn21*x2)+Ann2(2)*kn22*exp(kn22*x2)+Ann2(3)*kn23*exp(kn23*
x2)+Ann2(4)*kn24*exp(kn24*x2); %Xn2
d2XdX2=Ann2(1)*kn21^2*exp(kn21*x2)+Ann2(2)*kn22^2*exp(kn22*x2)+Ann2(3)*kn23^2*ex
p(kn23*x2)+Ann2(4)*kn24^2*exp(kn24*x2); %Xn2
dXdX22=dXdX2.^2; d2XdX22=d2XdX2.^2;

if inplane == 1
    Ux1=lambda11*Cnn1(1)*exp(lambda11*x1)+lambda12*Cnn1(2)*exp(lambda12*x1)+kn1*Cnn
    1(3)*exp(lambda13*x1)+Cnn1(4)*exp(lambda14*x1);
    Vx1=kn1*(Cnn1(1)*exp(lambda11*x1)+Cnn1(2)*exp(lambda12*x1)+lambda13*Cnn1(3)*exp
    (lambda13*x1)+lambda14*Cnn1(4)*exp(lambda14*x1);
    dUdx1=lambda11^2*Cnn1(1)*exp(lambda11*x1)+lambda12^2*Cnn1(2)*exp(lambda12*x1)+kn
    1*(lambda13*Cnn1(3)*exp(lambda13*x1)+lambda14*Cnn1(4)*exp(lambda14*x1));
    dVdx1=kn1*(lambda11*Cnn1(1)*exp(lambda11*x1)+lambda12*Cnn1(2)*exp(lambda12*x1)+
    lambda13^2*Cnn1(3)*exp(lambda13*x1)+lambda14^2*Cnn1(4)*exp(lambda14*x1);
    Ux2=lambda21*Cnn2(1)*exp(lambda21*x2)+lambda22*Cnn2(2)*exp(lambda22*x2)+kn2*Cnn
    2(3)*exp(lambda23*x2)+Cnn2(4)*exp(lambda24*x2);
    Vx2=kn2*(Cnn2(1)*exp(lambda21*x2)+Cnn2(2)*exp(lambda22*x2)+lambda23*Cnn2(3)*exp
    (lambda23*x2)+lambda24*Cnn2(4)*exp(lambda24*x2);
    dUdx2=lambda21^2*Cnn2(1)*exp(lambda21*x2)+lambda22^2*Cnn2(2)*exp(lambda22*x2)+kn
    2*(lambda23*Cnn2(3)*exp(lambda23*x2)+lambda24*Cnn2(4)*exp(lambda24*x2));
    dVdx2=kn2*(lambda21*Cnn2(1)*exp(lambda21*x2)+lambda22*Cnn2(2)*exp(lambda22*x2)+
    lambda23^2*Cnn2(3)*exp(lambda23*x2)+lambda24^2*Cnn2(4)*exp(lambda24*x2);
end

% Integrate over y
k=0;
for y=ystep/2:ystep:b1-ystep/2
    k=k+1;
    Wy0(k)=Xn0*sin(kn1*y);
    Wxy1(k)=Xn1*sin(kn1*y); Wxy2(k)=Xn2*sin(kn2*y);
    if inplane == 1
        Uy0(k)=Un0*sin(kn1*y); Vy0(k)=Vn0*cos(kn1*y);
        Uxy1(k)=Ux1*sin(kn1*y); Uxy2(k)=Ux2*cos(kn2*y);
        Vxy1(k)=Vx1*cos(kn1*y); Vxy2(k)=Vx2*cos(kn2*y);
    end

    % Strain Energy of Plate 1
    d2Wdx1(k,:)=d2XdX1*sin(kn1*y); d2Wdx12(k,:)=d2Wdx1(k,:).^2;
    d2Wdy1(k,:)=kn1^2*Wxy1(k,:); d2Wdy12(k,:)=d2Wdy1(k,:).^2;
    d2Wdxy1(k,:)=dXdX1*kn1*cos(kn1*y);
    if inplane == 1
        dUxydx1(k,:)=dUdx1*sin(kn1*y); dVxydy1(k,:)=dVdx1*cos(kn1*y);
        dUxydy1(k,:)=kn1*Ux1*cos(kn1*y); dVxydy1(k,:)=kn1*Vx1*sin(kn1*y);
    end

    SPf1(k,:)=abs(d2Wdx12(k,:))+abs(d2Wdy12(k,:))+2*nu1*real(d2Wdx1(k,:)).*conj(d2Wdy
    1(k,:))+2*(1-nu1)*abs(d2Wdxy1(k,:)).^2;
    if inplane == 1
        SPf1(k,:)=abs(dUxydx1(k,:).^2)+abs(dVxydy1(k,:).^2)+2*nu1*real(dUxydx1(k,:)).*con
        j(dVxydy1(k,:))+2*(1-nu1)*abs(dUxydy1(k,:)).^2;
    end
end

```

```

% Strain Energy of Plate 2
d2Wdx2(k,:) = d2xdk2*sin(kn2*y);
d2Wdy2(k,:) = -kn2*2*Wxy2(k,:).^2;
d2Wdy2(k,:) = d2Wdy2(k,:).^2;
d2Wdy2(k,:) = dXdx2*kn2*cos(kn2*y);

if inplane == 1
    dUxydx2(k,:) = dUdx2*sin(kn2*y);
    dUxydy2(k,:) = kn2*Ux2*cos(kn2*y);
    dVxydx2(k,:) = dVdx2*cos(kn2*y);
    dVxydy2(k,:) = -kn2*Vx2*sin(kn2*y);
end
% Power Input
if inplane == 1
    PSEf2(k,:) = abs(d2Wdx2(k,:)) + abs(d2Wdy2(k,:)) + abs(d2Wdy2(k,:)).^2;
    PSEf2(k,:) = abs(dUxydx2(k,:)).^2 + abs(dUxydy2(k,:)).^2 + 2*nu2*real(dUxydx2(k,:)).*conj(d2Wdy2(k,:)).*conj(d2Wdy2(k,:)).^2;
    PSEf2(k,:) = abs(dVxydx2(k,:)).^2 + abs(dVxydy2(k,:)).^2 + 2*nu2*real(dVxydx2(k,:)).*conj(d2Wdy2(k,:)).^2;
end
% Power Input for Flexural vibrations
if inplane == 1
    Pini(k) = real(F(1)*sin(kn1*y)*(j*w*Wy0(k))/2); % Re(Fv)/2
    Pini(k) = real(F(7)*sin(kn1*y)*(j*w*Wy0(k))/2); % Re(Fv)/2
else
    Pini(k) = real(F(1)*sin(kn1*y)*(j*w*Wy0(k))/2); % Re(Fv)/2
    Pini(k) = real(F(7)*sin(kn1*y)*(j*w*Wy0(k))/2); % Re(Fv)/2
end
end % y-loop end(k)

% Sum up Strain Energy for m
SEf1tot = SEf1tot + sum(sum(SEf1)).*ystep.*xstep;
SEf2tot = SEf2tot + sum(sum(SEf2)).*ystep.*xstep;
if inplane == 1
    SEf1tot = SEf1tot + sum(sum(SEf1)).*ystep.*xstep;
    SEf2tot = SEf2tot + sum(sum(SEf2)).*ystep.*xstep;
end
% Sum up Power Input for all m
Pinsumf = Pinsumf + sum(Pinfi).*ystep;
if inplane == 1
    Pinsumi = Pinsumi + sum(Pinfi).*ystep;
end
end % The number of half-sine wave loop(n)

if inplane == 1
    Pdisssf1(i) = mu1*w*real(D1)/2*SEf1tot; % Power Dissipated for Flexure of Plate 1
    Pdisssf2(i) = mu2*w*real(D2)/2*SEf2tot; % Power Dissipated for Flexure of Plate 2
    Pdisssf1(i) = mu1*w*real(E1*h1/(2*(1-nu1^2)))*SEf1tot; % Power Dissipated for In-plane of Plate 1
    Pdisssf2(i) = mu2*w*real(E2*h2/(2*(1-nu2^2)))*SEf2tot; % Power Dissipated for In-plane of Plate 1
    Pdisssf1(i) = Pdisssf1(i) + Pdisssf2(i) + Pdisssf1(i) + Pdisssf2(i);
else
    Pdisssf1(i) = mu1*w*real(D1)/2*SEf1tot; Pdisssf2(i) = mu2*w*real(D2)/2*SEf2tot;
    Pdisssf1(i) = Pdisssf1(i) + Pdisssf2(i);
end
end

if inplane == 1
    Pinfi(i) = Pinsumf;
    Pinfi(i) = Pinsumi;
    Pinfi(i) = Pinfi(i) + Pinfi(i);
else
    Pinfi(i) = Pinsumf;
    Pinfi(i) = Pinfi(i);
end
end % Frequency-loop end(i)
end % Frequency-loop end(i)

```